THE COMPLEX FUNCTIONS OF THE RECEPTOR-LIKE CYTOPLASMIC KINASE BIK1 IN PLANT IMMUNITY AND DEVELOPMENT

A Dissertation

by

WENWEI LIN

Submitted to the Office of Graduate and Professional Studies of
Texas A&M University
in partial fulfillment of the requirements for the degree of

DOCTOR OF PHILOSOPHY

Chair of Committee,	Libo Shan
Committee Members,	Ping He
	Daniel J. Ebbole
	Elizabeth (Betsy) Pierson
Head of Department,	Leland S. Pierson III

December 2015

Major Subject: Plant Pathology

ABSTRACT

The sessile plants have evolved a large number of receptor-like kinases (RLKs) and receptor-like cytoplasmic kinases (RLCKs) to modulate diverse biological processes, including plant innate immunity, growth and development. Phosphorylation of RLK/RLCK complex constitutes an essential step to initiate the immune signaling. Two Arabidopsis plasma membrane-resident RLKs FLS2 and BAK1 interact with RLCK BIK1 to initiate plant immune responses to bacterial flagellin. Classically defined as a serine/threonine kinase, BIK1 is shown here to possess tyrosine kinase activity with mass spectrometry, immunoblot and genetic analyses. BIK1 is auto-phosphorylated and trans-phosphorylated by BAK1 at multiple tyrosine (Y) residues in addition to serine/threonine residues. BIK1Y150 is likely catalytic important, whereas Y243 and Y250 are more specifically involved in tyrosine phosphorylation. Importantly, the BIK1 tyrosine phosphorylation plays a crucial role in BIK1-mediated plant innate immunity as the transgenic plants carrying BIK1Y150F, Y243F or Y250F (the mutation of tyrosine to phenylalanine) failed to complement the *bik1* mutant deficiency in immunity. Together with previous finding of BAK1 as a tyrosine kinase, these results unveiled tyrosine phosphorylation as a common regulatory mechanism that controls membrane-resident receptor signaling in plants and metazoans.

BAK1 complexes with the receptor kinase FLS2 in bacterial flagellin-triggered immunity and BRI1 in brassinosteroid (BR)-mediated growth. In contrast to its positive role in plant immunity, we report here that BIK1 acts as a negative regulator in BR

signaling. The *bik1* mutants display various BR hypersensitive phenotypes accompanied with increased accumulation of de-phosphorylated BES1 proteins and regulation of BZR1 and BES1 target genes. BIK1 associates with BRI1, and is released from BRI1 receptor upon BR treatment, which is reminiscent of FLS2-BIK1 complex dynamics in flagellin signaling. The ligand-induced release of BIK1 from receptor complexes is associated with BIK1 phosphorylation. However, in contrast to BAK1-dependent FLS2-BIK1 dissociation, BAK1 is dispensable for BRI1-BIK1 dissociation. Consequently, unlike FLS2 signaling which depends on BAK1 to phosphorylate BIK1, BRI1 directly phosphorylates BIK1 to transduce BR signaling.

Rapid activation of two branches of Mitogen-activated protein kinase (MAPK) cascades consisting of MEKK1-MKK1/2-MPK4 and MEKK1/?-MKK4/5-MPK3/6 is associated with perception of flagellin. There is limited understanding of how the signal transmits from the FLS2-BAK1 receptor complex to MAPK cascades. I have performed a series of genetic studies on the mutants of *bik1* and its related family members. Various combinations of higher order of mutants indicate that flagellin-mediated MAPK activation functions downstream of BIK1. I found that the *mekk1/2/3* deletion mutant largely restored various growth defects of *bik1*, and further genetic assays revealed that the alleviated growth defects can mainly be attributed to the *mekk1* mutation, but not *mekk2*. I also demonstrated that BIK1 likely associates with MEKK1 on the plasma membrane, indicating that BIK1 bridges PRR complexes and MAPK cascades to relay immune signaling.

ACKNOWLEDGEMENTS

I would like to express my deepest gratitude to my committee chair Dr. Libo Shan and my committee members, Dr. Ping He for all the support and excellent guidance they have provided me throughout my Ph.D. period at Texas A&M.

Thanks to Dr. Daniel J. Ebbole and Dr. Elizabeth (Betsy) Pierson for accepting to be members of my Ph.D. examining committee and for their guidance and support throughout the course of this research.

Thanks also go to my friends and colleagues of Dr. Shan and Dr. He lab, past and present, for helping me to get started and providing me with an excellent atmosphere for doing research. I would also like to thank my project collaborators Dr. Patrick Krysan at University of Wisconsin-Madison and Dr. Sixue Chen at University of Florida. I appreciate the great support provided by them.

Thanks for the faculty and staff in the Plant Pathology & Microbiology Department for making my time at Texas A&M University a great experience.

Finally, I would like to thank all my family for their encouragement and to Xiaomin for her patience and love. I always know I can truly count on them, because they believe in me and because they are always close to me despite the physical distance.

This Ph.D. dissertation is dedicated to them.

TABLE OF CONTENTS

Page

LIST OF FIGURES

Page

CHAPTER I

INTRODUCTION

Pattern-triggered immunity

Lacking an adaptive immune system and specialized immune cells, sessile plants largely rely on the innate immune system to fend off potential infections (Chisholm et al., 2006b; Jones and Dangl, 2006b). The first layer of innate immunity is activated by sensing of the conserved microbial signatures, termed as pathogen- or microbe-associated molecular patterns (PAMPs or MAMPs) by plasma membrane (PM)-resident pattern recognition receptors (PRRs) (Boller and Felix, 2009; Schwessinger and Ronald, 2012). PRRs also detect the endogenous molecules derived from damaged cells, termed as damage-associated molecular patterns (DAMPs) (Boller and Felix, 2009). Collectively, PRR-triggered immunity (PTI) attributes partly to host resistance against a broad spectrum of microbial infections (Antolin-Llovera et al., 2012; Monaghan and Zipfel, 2012).

PRRs are often receptor-like kinases (RLKs) or receptor-like proteins (RLPs) in plants. PRR-mediated signaling often involves receptor-like cytoplasmic kinases (RLCKs) that modulate growth, development and innate immunity (Shiu and Bleecker, 2001, 2003). Precise recognition of PAMPs by RLKs initiate confirmation changes, which often leads to homo-dimerization or hetero-dimerization of other RLKs. Intriguingly, plants have evolved a large number of RLKs, RLPs and RLCKs that form the largest family of plant membrane receptors. There are more than 610 RLKs in Arabidopsis and more than 1,100 in rice.

Arabidopsis FLS2 (flagellin sensing 2), one of the best-characterized PRRs in plants, encodes a leucine-rich repeat (LRR) that recognizes bacterial flagellin or its active peptide derivative flg22 (Gomez-Gomez and Boller, 2000b). Upon flg22 perception, FLS2 complexes with the LRR-RLK BAK1 (brassinosteroid insensitive 1-associated kinase 1) (Chinchilla et al., 2007b; Heese et al., 2007b). BIK1 (*Botrytis*-induced kinase 1), a PM-localized RLCK, is rapidly phosphorylated upon flg22 perception in an FLS2- and BAK1-dependent manner (Lu et al., 2010; Zhang et al., 2010). BIK1 functions as a kinase substrate of BAK1 and forms a complex with FLS2 and BAK1 in transducing flagellin signaling (Lu et al., 2010). BSK1 (BR-signaling kinase 1), another RLCK and originally identified as a substrate of the brassinosteroid receptor BRI1 (BR insensitive 1), associates with FLS2 and positively regulates PTI signaling (Shi et al., 2013). SCD1 (stomatal cytokinesis-defective 1), an FLS2-associated protein identified from proteomics analysis, is required for certain aspects of flg22-mediated responses yet its mechanistic involvement in PTI signaling remains elusive (Korasick et al., 2010). Activation of MAP kinases (MAPKs) and calcium-dependent protein kinases (CDPKs), two intracellular signaling pathways, functions independently or synergistically downstream of FLS2 and BAK1 receptor complex to activate the expression of flg22-responsive genes (Asai et al., 2002; Boudsocq et al., 2010b). In addition, flg22 perception leads to Ca^{2+} ion fluxes, production of reactive oxygen species (ROS) and ethylene, deposition of callose and stomatal closure to prevent pathogen entry (Boller and Felix, 2009; Schwessinger and Ronald, 2012).

BAK1 is also functionally required for responses triggered by multiple MAMPs, including flg22, EF-Tu (elongation factor-Tu), PGN (peptidoglycan), LPS (lipopolysaccharide), cold-shock protein and oomycete elicitor INF1 (*Phytophthora infestans* elicitin 1) in Arabidopsis and tobacco (Chinchilla et al., 2007b; Heese et al., 2007b; Shan et al., 2008b). In addition, BAK1 plays important roles in mediating plant growth hormone BR signaling (Li et al., 2002b; Nam and Li, 2002). BAK1 heterodimerizes with several RLKs including BRI1, EFR (EF-Tu receptor) and AtPEPR1 (Arabidopsis DAMP peptide 1 receptor) (Chinchilla et al., 2007b; Heese et al., 2007b; Li et al., 2002b; Nam and Li, 2002; Postel et al., 2010; Roux et al., 2011b). BAK1 positively regulates plant immunity and BR signaling likely through its transphosphorylation with corresponding RLK receptors. The function of BAK1 was controlled by a protein Ser/Thr phosphatase type 2A (PP2A) during plant innate immunity (Segonzac et al., 2014). Consistent with BIK1 as a kinase substrate of BAK1, BIK1 also complexes with various RLKs, including FLS2, EFR, and AtPEPRs (Lin et al., 2013a; Liu et al., 2013; Lu et al., 2010; Zhang et al., 2010). The PUB E3 ligases have been shown to be involved in regulating FLS2, and its defense signaling (Lu et al., 2011). PUB13 and its closest homolog PUB12 were shown to interact with BAK1 *in vivo* and *in vitro* and to be phosphorylated by BAK1. This phosphorylation was enhanced by flagellin perception or in the presence of BIK1. The phosphorylation of PUB12/PUB13 led to the association of FLS2-PUB12/PUB13. PUB12/PUB13 polyubiquitinate FLS2 to initiate 26S proteasome mediated degradation of FLS2 *in vivo* in response to flagellin, thus resulting in attenuation of FLS2-mediated defense signaling (Lu et al., 2011).

Upon the perception of flg22 or elf18, the activated PRRs complex phosphorylates BIK1, and the phosphorylated BIK1 directly interact with and phosphorylate the NADPH oxidase RbohD at specific sites in a calcium independent manner to mediate ROS production (Kadota et al., 2014; Li et al., 2014b). MAPK signaling cascades and CDPK (Ca^{2+}-dependent protein kinases) signaling networks play specific and overlapping roles in activating the defense response genes downstream PRRs complexes upon the recognition of PAMPs (Boudsocq et al., 2010a). The activated MAPK cascade phosphorylates and activates the cyclin-dependent kinase C (CDKC) by MPK3, which in turn phosphorylates the Arabidopsis RNA polymerase II C-terminal domain (CTD) to regulate immune gene expression. A CTD phosphatase-like 3 (CPL3) directly dephosphorylated CTD to counteract MAPK-mediated CDKC regulation (Li et al., 2014a). Arabidopsis SH4-related 3 (ASR3) functions as a transcriptional repressor regulated by PAMP-activated MPK4 to fine-turn plant immune gene expression via its ERF-associated amphiphilic repression motifs (Li et al., 2015) (Figure 1.1). However, it remains unclear as to how signals are transduced from the PRR complexes to downstream MAPK cascades.

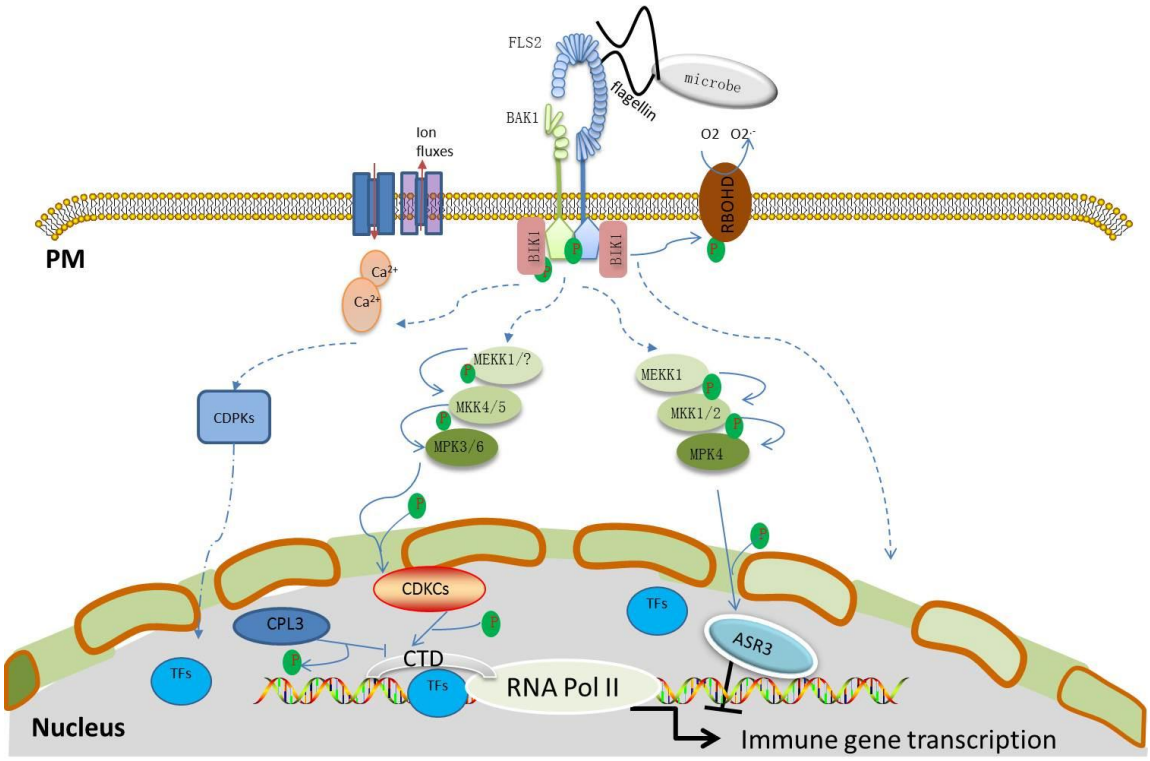

Figure 1. 1 Flagellin-triggered signaling in Arabidopsis.
Upon flagellin perception, FLS2 complexes with BAK1 and BIK1. Rapid phosphorylation in the receptor complex further activates the signaling via the MAPK and CDPK cascades or other unknown pathway. Activation of BIK1 also phosphorylates RbohD to trigger the ROS bust. Activated MPK3 phosphorylates and activates CDKCs, which further phosphorylate the tail of RNAPII CTD hetapeptide to mediate the expression of specific immune genes. The phosphorylated CTD is counterregulated by CPL3 directly through dephosphorylation. The activated MPK4 phosphorylates the transcriptional repressor ASR3 to suppress the transcription of immune genes.

Effector-triggered immunity

To circumvent PTI, adapted pathogens secrete virulence effector molecules directly into the plant cells. To confine pathogens, plants have evolved disease resistance (R) genes which initiate effector-triggered immunity (ETI). ETI is often accompanied with a hypersensitive response, which is typically associated with program cell death (PCD) of the infected cells and the production of antimicrobial molecules in the surrounding tissue that collectively contribute to the restriction of pathogen spreading

(Chisholm et al., 2006a; Collier and Moffett, 2009; Dodds and Rathjen, 2010; Jones and Dangl, 2006a). A local HR also confers a form of resistance to plants against future infections by inducing systemic acquired resistance (Lee et al.) (Spoel and Dong, 2012).

In contrast to highly diverse pathogen effectors, the cognate R proteins in plants are structurally conserved. The most common R proteins are intracellular nucleotide-binding site leucine-rich repeat protein (NLR) consisting of a variable amino (N)-terminus followed by a nucleotide-binding site (NBS) domain in the center and an LRR domain at the carboxyl (C)-terminus. NBS-LRR proteins are further divided into two subclasses according to the presence of an N-terminal Toll and human interleukin receptor or Coiled-Coil domains (Collier and Moffett, 2009; DeYoung and Innes, 2006; Eitas and Dangl, 2010; Elmore et al., 2011; Maekawa et al., 2011).With few exceptions, most of the plant NLR proteins do not interact with cognate effectors directly but instead they "recognize" the host proteins that are perturbed or modified by pathogen effectors. For instance, Arabidopsis *thaliana* protein RPM1-INTERACTING PROTEIN 4 (RIN4) interacts with CC-NLR proteins RPM1 and RPS2, while being targeted and modified by three distinct *P. syringae* effectors, AvrRpm1, AvrB and AvrRpt2. AvrRpm1 and AvrB trigger phosphorylations of RIN4 by a cytoplasmic kinase family member RIPK, which further leads to a prolyl-peptidyl isomerase (PPIase), ROC1-mediated RIN4 isomerization. It was hypothesized that the conformational change of RIN4 was detected by RPM1 and activates immune responses (Li et al., 2014c). In contrast, RIN4 was directly cleaved by the bacterial cysteine protease AvrRpt2, resulting in RPS2 activation (Kim et al., 2005). In the absence of RPM1 and RPS2, AvrRpt2, AvrB and AvrRpm1

targeted RIN4 to suppress PTI, therefore promoting infection, demonstrating that RIN4 plays an important role in plant defense. In addition, plant R proteins monitor additional host protein, which do not have direct measurable role in resistance but serve as decoys to trap pathogen effectors. For example, the tomato R protein Prf (*Pseudomonas* resistance and fenthion sensitivity) mediates the resistance to *P. syringae* AvrPto (Ntoukakis et al., 2014). The direct interaction between Prf and the protein kinase Pto results in an inactive Prf (Ntoukakis et al., 2014). A role for Pto in basal immunity has not been established, but its kinase domain resembles that of the PRRs FLS2, EFR and BAK1, which are also targeted by AvrPto during infection (Shan et al., 2008a).

Apparently, different NLR proteins launch distinct mechanisms to activate complex downstream immune signaling in multiple subcellular compartments. Various components have been identified to be important regulators in ETI, including NDR1 (Non-race-specific 1), lipase-like proteins EDS1 (Enhanced Disease Susceptibility 1), PAD4 (Phytoalexin Deficient 4) and SAG101 (Senescence-associated gene 101). Genetically, NDR1 is required for multiple CC-NLRs for ETI activation, whereas EDS1 is indispensable for TIR-NLR-mediated ETI. EDS1 couples with PAD4 or SAG101 to launch downstream ETI signaling. Furthermore, MAP kinases (MAPKs), WRKY transcription factors, CDPK, as well as salicylic acid (Ntoukakis et al.) and other plant hormones play pivotal roles in mediating convergent immune responses downstream of NLR immune sensors (Chisholm et al., 2006a; Rushton et al., 2010; Spoel and Dong, 2012).

CHAPTER Ⅱ

TYROSINE PHOSPHORYLATION OF BAK1/BIK1 MEDIATES ARABIDOPSIS INNATE IMMUNITY*

Summary

The innate immune response is initiated by the recognition of conserved microbial signatures via membrane-resident receptor complex. The dimerization and phosphorylation of Arabidopsis FLS2/BAK1/BIK1 receptor kinase complex are essential to initiate and transduce immune signaling to bacterial flagellin. BIK1, a classic serine/threonine kinase, was found here to be autophosphorylated and transphosphorylated by BAK1 at multiple tyrosine residues to relay plant immune signaling. Importantly, the BIK1 tyrosine phosphorylation plays a crucial role in BIK1-mediated plant innate immunity as the transgenic plants carrying BIK1Y150F, Y243F or Y250F (the mutation of tyrosine to phenylalanine) failed to complement the bik1 mutant deficiency in immunity. The essential function of tyrosine kinase activity of BIK1 in plants echoes the function of non-receptor tyrosine kinases that transduce receptor tyrosine kinase signaling via dimerization and phosphorylation in metazoans. Thus, despite lack of classical tyrosine kinases, tyrosine phosphorylation is also an important regulatory mechanism to control membrane-resident receptor signaling in plants.

---

* Reprinted with permission from "Tyrosine phosphorylation of protein kinase complex BAK1/BIK1 mediates Arabidopsis innate immunity" by Lin, W., Li, B., Lu, D., Chen, S., Zhu, N., He, P., and Shan, L. *Proceedings of the National Academy of Sciences of the United States of America* 111, 3632-3637. 2014, Wenwei Lin.

Introduction

In contrast to animals, plants do not possess the adaptive immune system but predominantly rely on the innate immune system to protect themselves from potential microorganisms damages (Chisholm et al., 2006b; Jones and Dangl, 2006b). The first layer of innate immunity is activated by sensing of the conserved microbial signatures, termed as pathogen- or microbe-associated molecular patterns (PAMPs or MAMPs) by plasma membrane-resident pattern recognition receptors (PRRs) (Boller and Felix, 2009; Schwessinger and Ronald, 2012).

Arabidopsis FLS2 signaling is one of the best-characterized PTI signaling pathways in plants. (Gomez-Gomez and Boller, 2000b). Upon flg22 perception, FLS2 rapidly complexes with its co-receptor BAK1 (Chinchilla et al., 2007b; Heese et al., 2007b). BIK1 is rapidly phosphorylated upon flg22 perception in an FLS2- and BAK1-dependent manner (Lu et al., 2010; Zhang et al., 2010). BIK1 functions as a kinase substrate of BAK1 and forms a complex with FLS2 and BAK1 in transducing flagellin signaling (Lu et al., 2010).

Autophosphorylation and transphosphorylation have been demonstrated in many RLKs and RLCKs to regulate diverse signaling pathways. Sequential transphosphorylation between BRI1 and BAK1 is essential to fully activate BR signaling (Wang et al., 2008b). Both BRI1 and BAK1 phosphorylate BIK1 *in vitro* and *in vivo*, whereas BIK1 is also able to transphosphorylate BAK1 and FLS2 (Lin et al., 2013a; Lu et al., 2010). In general, plant RLKs and RLCKs are classified as serine/threonine kinases, and many serine/threonine phosphorylation sites have been identified and

demonstrated for their function importance (Shiu and Bleecker, 2001). It has been shown recently that BRI1 and BAK1 possess tyrosine kinase activity in addition to serine/threonine kinase activity by α-phosphotyrosine antibody and mutational analyses (Oh et al., 2009; Oh et al., 2010). In this study, extensive mass spectrometry (MS) analysis of BIK1 autophosphorylation and transphosphorylation by BAK1 was performed. Consistent with previous mutational analyses (Laluk et al., 2011; Lu et al., 2010), several genetically defined serine/threonine residues that are important for BIK1 functions were identified from my MS assay. In particular, T237 is an essential site for BIK1 autophosphorylation and transphosphorylation by BAK1. Surprisingly, MS analysis identified three BIK1 tyrosine phosphorylation sites Y23, Y234 and Y250. Moreover, Y250 was revealed as a transphosphorylation site by BAK1. Mutational analysis suggested that BIK1Y150 is likely catalytic important, whereas Y243 and Y250 are more specifically involved in tyrosine phosphorylation. Transgenic complementation assays indicate that Y150, Y243 and Y250 are crucial for BIK1 functions in plant defense. Thus, plant RLCK BIK1 is a kinase with dual-specificity, and both tyrosine and serine/threonine kinase activities are essential for its function in *Arabidopsis* innate immunity. These studies further suggest the complexity of phosphorylation events in plant RLK/RLCK-mediated signaling.

Method and materials

Plant growth condition and generation of transgenic plant

Arabidopsis plants were grown in soil (Metro Mix 366) in a growth room at 23 ℃, 65% relative humidity and 75 μE m^{-2} s^{-1} light with a 12-hr photoperiod for approximate 4 weeks before protoplast isolation or bacterial inoculation. To grow Arabidopsis seedlings, the seeds were surface sterilized with 50% bleach for 10 min, and then placed on the plates with half-strength Murashige and Skoog medium (½ MS) containing 0.5% sucrose, 0.8% agar and 2.5 mM MES at pH 5.7. The *bik1* mutant plants, WT Col-0 plants, *pCB302* empty vector (EV) transgenic plants (in Col-0 background) and *pBIK1::BIK1-HA* transgenic plants in *bik1* mutant background were described previously. The *pBAK1::BAK1-GFP* transgenic plants in Col-0 background were obtained from Dr. J. Li. The *Agrobacterium*-mediated transformation was used to introduce *pCB302-pBIK1::BIK1-HA* into *pBAK1::BAK1-GFP* transgenic plants, and the double transgenic plants were selected with Basta resistance and immunoblot using α-HA (Andreasson et al.) and α-GFP (Andreasson et al.) antibodies. To generate *pBIK1::BIK1*^{Y150F}*-HA, pBIK1::BIK1*^{Y243F}*-HA* or *pBIK1::BIK1*^{Y250F}*-HA* transgenic plants in the *bik1* mutant background, individual point mutations were introduced into *pCB302-pBIK1::BIK1-HA* by site-directed mutagenesis kit. The *BIK1* coding region for each derivative was fully sequenced to confirm the proper mutation. The transformants were selected with Basta resistance, screened for α-HA by immunoblot analysis, and the lines with comparable protein expression level with *pBIK1::BIK1-HA* transgenic plants were used to produce homozygous plants for further analysis. The *BIK1km* transgenic plants

were generated with *35S::BIK1-HA* construct. At least two homozygous lines for each transgenic line were analyzed.

Plasmid constructs, protoplast transfection and BiFC assay

Arabidopsis BIK1 full length, BAK1 cytosolic domain (BAK1CD), BAK1 kinase domain (BAK1K), FLS2 cytosolic domain (FLS2CD) constructs were reported previously (Lu et al., 2010). The BIK1 and BAK1 mutants were generated with site-directed mutagenesis kits. *BAK1* and *BIK1* were sub-cloned into the modified BiFC vectors from *pHBT-BAK1-HA* or *pHBT-BIK1-HA* vector with BamHI and StuI digestion. The protoplast isolation and transfection were reported previously (Lu et al., 2010). Briefly, 100 μL of protoplasts at a density of 2×10^5/mL were transfected with *pBIK1::BIK1-HA* or its mutants for flg22-induced BIK1 phosphorylation assay, and 50 μL of protoplasts were transfected with *pBIK1::BIK1-HA* or its mutants and *pFRK1::LUC/UBQ-GUS* for *FRK1* promoter activity assay. For BiFC assay, 200 μL of protoplasts were transfected with various BiFC constructs as indicated in the figures. Fluorescent signals in the protoplasts were examined with confocal microscope (Olympus FV1000 Confocal Microscope) 12 hr after transfection. The filter sets used for excitation (Ex) and emission (Em) are as follows: YFP was excited at 515 nm, and the emission was collected between 520 and 550 nm; chlorophyll was excited at 488 nm, and the emission was collected between 560 and 650 nm; bright field at 633 nm. Images were captured in multichannel mode, and analyzed and processed with OLYMPUS FLUOVIEW Ver.3.0 Viewer.

BIK1* in vivo *tyrosine phosphorylation

500 μL of protoplasts were transfected with *pBIK1::BIK1-GFP*, and treated with 1μM flg22 for 10 min 8 hr after transfection. The cells were lysed with 500μL of immunoprecipitation (IP) extraction buffer (10 mM Hepes, pH 7.5, 100 mM NaCl, 1 mM EDTA, 10% glycerol, 0.5% Triton X-100, and 1x protease inhibitor mixture from Roche). After vortex vigorously for 30 s, the samples were centrifuged at 12,470×g for 10 min at 4℃. The 10 % supernatant was added with 4XSDS loading buffer for Western blot with an α-GFP antibody for input control, and the left supernatant was incubated with 2 μL of α-GFP antibody for 2 hr and then with 8 μL of protein-G-agarose beads (Andreasson et al.) for another 2 hr at 4℃ with gentle shaking. The beads were collected and washed three times with IP washing buffer (10 mM Hepes, pH 7.5, 100 mM NaCl, 1 mM EDTA, 10% glycerol, and 0.1% Triton X-100) and once with 50 mM Tris-HCl, pH 7.5. The immunoprecipitated proteins were analyzed by Western blot with an α-phosphotyrosine (pY20) antibody (Invitrogen).

Seedling co-immunoprecipitation (co-IP) assay

Approximate 10 g of 10-day old transgenic seedlings grown from ½ MS agar plates were ground in liquid N_2, and further with 10 mL of ice-cold extraction buffer. After vortexing vigorously for 30 s, the samples were centrifuged at 12,470 ×g for 10 min at 4℃. The 10% of supernatant was used for Western input control (α-HA and α-GFP) assay, and the remaining portion was incubated with 10μL of α-GFP antibody for

2 hr and then with 20 μL of protein-G-agarose for another 2 hr at 4℃ with gentle shaking. The beads were collected and washed three times with IP washing buffer and once with 50 mM Tris-HCl, pH 7.5. The immunoprecipitated proteins were analyzed by Western blot with an α-HA or α-GFP antibody.

In vitro *pull-down assay*

For GST glutathione agarose pull-down assay, GST and GST-BIK1 were individually expressed in *E. coli* BL21 strain and purified as the form of fusion proteins immobilized with glutathione agarose following the standard protocol. 5 μg of MBP or MBP-BAK1CD (tagged with HA) fusion proteins were pre-incubated with 5 μL of prewashed glutathione agarose beads in 150 μL of incubation buffer (10 mM Hepes at pH 7.5, 100 mM NaCl, 1 mM EDTA, 10% glycerol, and 0.5% Triton X-100) at 4 ℃ for 1 hr with gentle shaking. After centrifuging at 16,162 x g for 5 min, the supernatant was transferred and incubated with prewashed GST or GST-BIK1 glutathione agarose beads at 4 ℃ for another 1h. The beads were collected and washed four times with IP washing buffer and once with 50 mM Tris-HCl at pH 7.5. The immunoprecipitated proteins were analyzed by Western blot with an α-HA antibody.

For MBP amylose agarose pull-down assay, MBP and MBP-BAK1CD amylose agarose beads were used as bait against GST or GST-BIK1 fusion proteins for immunoprecipitation assay following a similar protocol as above. The immunoprecipitated proteins were analyzed by Western blot with an α-GST antibody.

In vitro *phosphorylation Assay*

Expression and affinity purification of the GST and MBP fusion proteins were performed as the standard protocol. The protein concentration was determined with the BioRad Quick Start Bradford Dye Reagent and confirmed by the Nano Drop ND-1000 Spectrophotometer. For *in vitro* kinase assay, kinase reactions were performed in 30 μL of kinase buffer (20 mM Tris-HCl, pH 7.5, 10 mM $MgCl_2$, 5mM EGTA, 100 mM NaCl, and 1 mM DTT) containing 10 μg of fusion proteins with 0.1 mM cold ATP and 5 μCi of [^{32}P]-γ-ATP at room temperature for 3 hr with gentle shaking. The reactions were stopped by adding 4× SDS loading buffer. The phosphorylation of fusion proteins was analyzed by autoradiography after separation with 10% SDS/PAGE.

MS analysis

The *in vitro* phosphorylation assay for MS analysis was performed in a 10 μL reaction containing 20 mM Tris-HCl, pH 7.5, 10 mM $MgCl_2$, 100 mM NaCl, 3 mM $CaCl_2$, 1 mM DTT and 0.1 mM ATP. 1 μg of MBP-BAK1CD fusion proteins were used as a kinase to phosphorylate 10 μg of GST-BIK1Km fusion proteins and 10 μg of GST-BIK1 fusion proteins were used in BIK1 auto-phosphorylation assay. The reaction was performed for 3 hr at room temperature with gentle shaking, and stopped by adding 4 × SDS loading buffer. Six individual reactions were combined and separated by 10% SDS-PAGE gel. The gel was stained with Thermo GelCode Blue Safe Protein Stain and destained with dH_2O. The corresponding bands were excised for MS analysis, which was performed according to Gao et al. (Gao et al., 2013). Briefly, gel bands were

digested in-gel with trypsin overnight, and phosphopeptides were enriched for liquid chromatography-MS/MS analysis with a LTQ Orbitrap XL mass spectrometer (Thermo Scientific). The MS/MS spectra were analyzed with Mascot (Matrix Science; version 2.2.2), and the identified phosphorylated peptides sequences were manually annotated to ensure confidence in phosphorylation site assignment.

Pathogen infection assay

P. syringae tomato DC3000 (*Pst*) and *P. syringae maculicola* ES4326 (*Psm*) strains were grown overnight at 28°C in King's B medium with 50μg/mL rifampicin or streptomycin respectively. Bacteria were collected, washed, and diluted to the desired density with ddH_2O adjusted by spectrometer. For flg22-mediated protection assay, leaves from 4-week old soil grown plants were pre-inoculated with 100 nM flg22 or H_2O and 24 hr later, the same leaves were infiltrated with *Pst* at the concentration of 5×10^5 cfu/mL using a needleless syringe. For *Psm* infection assay, the leaves were directly infiltrated with *Psm* at the concentration of 5×10^5 cfu/mL. Bacterial counting was performed from six different plants with six leaves and combined two leaves as a set to be three repeats at 2 and 3 dpi. Two leaf discs were ground in 100 μl ddH_2O and serial dilutions were plated on KB medium with appropriate antibiotic selection. Bacterial colony forming units (cfu) were counted 2 days after incubation at 28°C. Each data point is shown as the mean of triplicates. The disease symptoms from the representative were recorded infected leaves at the indicated time points.

For *Botrytis cinerea* infection assay, *B. cinerea* strain BO5-10 was cultured on Potato Dextrose Agar (Difco) and incubated at room temperature. Conidia were collected and re-suspended in 1/4 PDA with 0.5% Knox Gelatine. The suspension was passed through Mirocloth. The conidia density was adjusted to $2.5x10^5$ spores/mL, and 10 µL of spore suspension was dropped on 5-week old soil-grown detached leaves. The infected leaves were covered with a dome and at least 30 leaves from 15 plants for each line were assayed.

ROS production assay

Four to five leaves from each five-week old plant were excised into leaf discs of 0.25 cm^2, following an overnight incubation in 96-well plate with 100 µL of ddH_2O to eliminate the wounding effect. H_2O was replaced by 100 µL of reaction solution containing 50 µM of luminol and 10 µg/mL of horseradish peroxidase (Sigma) supplemented with 100 nM of flg22. Measurements with a luminometer (Perkin Elmer, 2030 Multilabel Reader, Victor X3), were made immediately after adding the luminol solution with a 1 min interval reading time for a period of 30 min. The measured value for ROS production from 36 leaf discs per treatment was indicated as means of RLU (Relative Light Units).

Result

BIK1 directly interacts with BAK1 in vivo *and* in vitro

BIK1 associates with multiple MAMP/DAMP receptors, including FLS2, EFR and AtPEPR1/2, and plays important roles in PTI signaling (Liu et al., 2013; Lu et al., 2010; Zhang et al., 2010). In previous studies, it was reported that flg22-induced BIK1 phosphorylation depends on FLS2 and BAK1 (Lu et al., 2010). Furthermore, I found that BIK1 associated with BAK1 when transiently co-expressed in *Arabidopsis* protoplasts (Lu et al., 2010). To further investigate the role of BIK1 in FLS2/BAK1 receptor complex, I determined the association of BIK1 and BAK1 both *in vivo* and *in vitro* (Fig 2.1). The HA epitope-tagged *BIK1* under the control of its native promoter (*pBIK1::BIK1-HA*) was transformed into the *pBAK1::BAK1-GFP* transgenic plants, and *in vivo* co-immunoprecipitation (Co-IP) assays were performed in intact plants. BAK1-GFP immunoprecipitated BIK1-HA was detected by Western blot with an α-HA antibody upon α-GFP antibody immunoprecipitation (Fig 2.1A). Consistently, bimolecular fluorescence complementation (BiFC) assay indicated that BIK1 associates with BAK1 as indicated by the yellow fluorescence protein (YFP) signal primarily on the plasma membrane when co-expressing *BIK1* fused to the carboxyl-terminal half of *YFP* (*BIK1-cYFP*) and *BAK1* fused to the amino-terminal half of *YFP* (*BAK1-nYFP*) in protoplasts (Fig 2.1B). Neither of the individual constructs emitted YFP signal in protoplasts (Fig 2.1B). To test whether BAK1 directly interacts with BIK1 through the cytosolic kinase domain, I performed *in vitro* pull-down assay with the glutathione-S-transferase (GST)-BIK1 fusion proteins (GST-BIK1) immobilized on glutathione

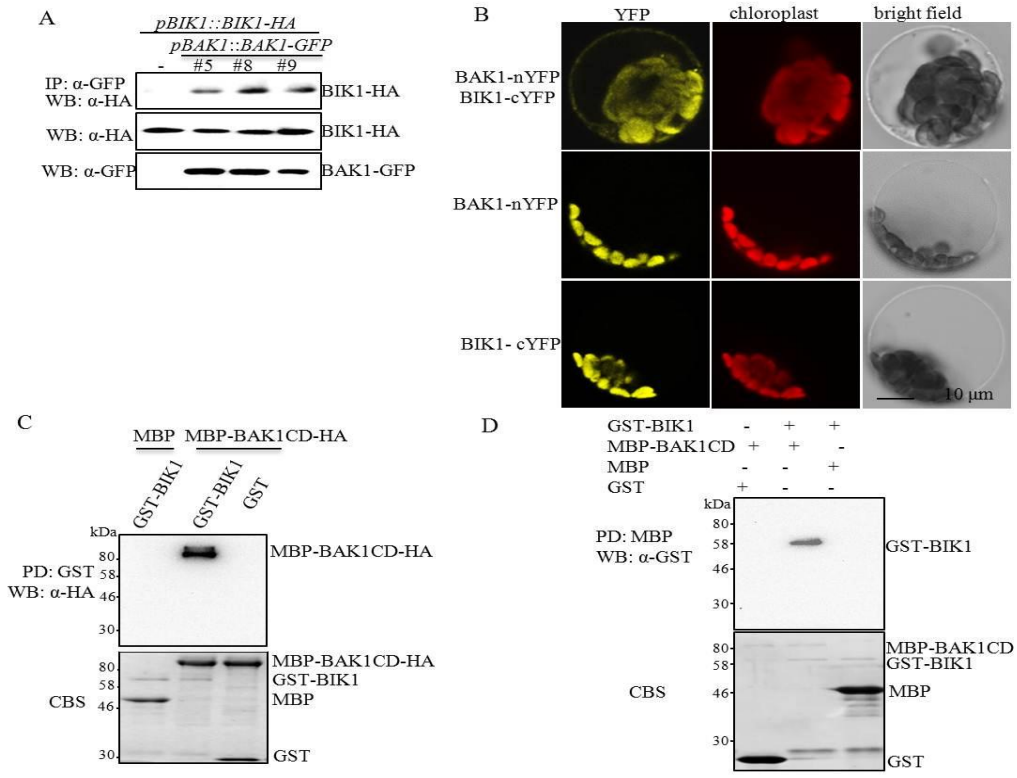

Figure 2. 1 BIK1 interacts with BAK1 *in vivo* and *in vitro*.
(**A**) BIK1 associates with BAK1 in transgenic plants. Total proteins from seedlings carrying *pBIK1::BIK1-HA/pBAK1::BAK1-GFP* (line #5, #8 and #9) or *pBIK1::BIK1-HA* were immunoprecipitated with an α-GFP antibody (IP: α-GFP) and analyzed with Western blot using an α-HA-HRP antibody (WB: α-HA) shown in the top panel. The expression of BIK1-HA and BAK1-GFP in transgenic plants is shown in the middle and bottom panels, respectively. (**B**) BIK1 interacts with BAK1 in BiFC assay. The various BiFC constructs were transfected into *Arabidopsis* protoplasts and the cells were observed under a confocal microscope with different filters. (**C**) BIK1 interacts with the BAK1 cytosolic domain (BAK1CD) with *in vitro* pull-down assay. MBP was the control for MBP-BAK1CD tagged with HA epitope. GST was the control for GST-BIK1. GST or GST-BIK1 immobilized on glutathione sepharose beads was incubated with MBP or MBP-BAK1CD proteins. The beads were collected and washed for Western blot of immunoprecipitated proteins with an α-HA-HRP antibody. (**D**) BIK1 interacts with BAK1 cytosolic domain *in vitro*. MBP was the control for MBP-BAK1 protein with a HA tag. GST was the control for GST-BIK1 protein. MBP and MBP-BAK1CD were incubated with MBP beads, and then incubated with GST or GST –BIK1. The beads were collected and washed for Western blot of immunoprecipitated proteins with an α-GST antibody. The above experiments were repeated three times with similar results.

sepharose beads as bait against BAK1 cytosolic domain (BAK1CD) fused to maltose binding protein (MBP) with an HA epitope tag. As shown in Fig 2.1C, MBP-BAK1CD could be pulled down by GST-BIK1, but not GST, sepharose beads. Similarly, GST-

BIK1 could be pulled down by MBP-BAK1CD amylose-agarose beads (Fig 2.1D). Taken together, the data demonstrate that BIK1 forms a complex with BAK1 by direct interaction with BAK1 cytosolic kinase domain.

Trans-phosphorylation in FLS2/BAK1/BIK1 complex

BIK1 is predicted to encode a serine/threonine-protein kinase with a typical kinase domain containing 11 motifs (I~XI), relatively short amino-terminal (NT) and carboxyl-terminal (CT) domains (Fig. 2.2A) (Veronese et al., 2006). Site-directed mutagenesis has suggested that several serine/threonine residues are important for its kinase activity and biological functions (Laluk et al., 2011; Lu et al., 2010). However, the biochemical evidence of these phosphorylation sites is still lacking. Consistent with BIK1 interaction with BAK1, it was shown previously that BAK1 directly phosphorylates BIK1 and BIK1 is able to transphosphorylate BAK1 and FLS2 (Lu et al., 2010). Phosphorylation sites of BIK1 by BAK1 have not been demonstrated. To systemically examine BIK1 autophosphorylation and transphosphorylation mediated by BAK1, I performed a series of analyses of recombinant GST-BIK1 tryptic peptides by liquid chromatography-tandem mass spectrometry (LC/MS/MS) after *in vitro* BIK1 autophosphorylation or BAK1 transphosphorylation reactions. Fourteen serine (S) residues and 10 threonine (T) residues were identified in BIK1 protein after autophosphorylation reaction (Fig 2.2A). Among these 24 residues, 12 (S19, S20, S26, S28, S32, S33, T35, T42, S48, S49, S54 and T56) are in the N terminus, 7 (S206, S233, S236, T237, T242, S252 and S253) are in the kinase domain, and five (T362, T368, T375, T378 and T386) are in the C terminus. I

did not identify any phosphorylation residues with GST-BIK1 kinase inactive mutant (Km) protein, which carries a mutation in the putative ATP binding site. I further identified the BIK1 phosphorylation sites mediated by BAK1 with GST-BIK1Km as a substrate and MBP-BAK1CD as a kinase. Five serine or threonine sites (S26, S206, T237, T368 and T386) in BIK1 were phosphorylated by BAK1 (Fig 2.2A). Notably, all these five serine/threonine sites were also BIK1 autophosphorylation sites.

In agreement with previous mutagenesis studies that T237 is an important phosphorylation site of BIK1 in response to flg22 treatment (Lu et al., 2010), MS analyses revealed that T237 was phosphorylated by both autophosphorylation and by transphosphorylation by BAK1 (Fig 2.2A and 2.2B). To further confirm the importance of T237 of BIK1, I mutagenized T237 to Alanine (T237A) in GST-BIK1Km protein and tested its ability to be phosphorylated by MBP-BAK1CD with an *in vitro* kinase assay. As shown in Fig. 2.2C, BAK1CD directly phosphorylated BIK1Km *in vitro* in the presence of [^{32}P]-γ-ATP whereas the phosphorylation level of BIK1Km^{T237A} by BAK1CD was largely reduced, suggesting that T237 is a major phosphorylation site for BAK1-mediated transphosphorylation of BIK1. In contrast, mutation of the adjacent S236 residue (S236A) in BIK1Km or BIK1Km^{T237A} had little effect on its phosphorylation by BAK1CD (Fig 2.2C). This is consistent with a previous report that S236A mutation did not affect the flg22-induced BIK1 mobility shift (Lu et al., 2010). Taken together, the data suggest that BIK1T237 residue is an important and major phosphorylation site in flg22-mediated signaling.

Notably, T237 of BIK1 is equivalent to T450 of BAK1 based on the amino acid sequence alignment between the kinase domains of BIK1 and BAK1 (Supplemental Fig. 1). MS analyses identified both T450 and T455 of BAK1 as major phosphorylation sites for autophosphorylation and transphosphorylation by BRI1 (Wang et al., 2008b). T455 is also a highly conserved site in RLK/RLCK family members (Supplemental Fig. 1) (Wang et al., 2008b). To investigate whether these two sites are required for BAK1 to transphosphorylate BIK1, I generated MBP fusion proteins of BAK1CDT450A and BAK1CDT455N. As shown in Fig. 2.2D, compared with WT BAK1CD, the kinase activity and transphosphorylation of BAK1CDT450A or BAK1CDT455N to BIK1Km was significantly reduced or completely eliminated with an *in vitro* kinase assay. The similar result was obtained for BAK1CDT450A/T455N double mutant. It was previously reported that BIK1 was able to transphosphorylate BAK1 with BAK1 kinase domain (BAK1K) as a substrate, which does not possess autophosphorylation activity due to the lack of jutax-membrane domain (Lu et al., 2010). Interestingly, BAK1KT455N, but not BAK1KT450A, dramatically reduced the ability to be phosphorylated by BIK1 (Fig 2.2E), suggesting that T455 of BAK1 is an important phosphorylation site by BIK1. I also found that MBP-BAK1CD is able to phosphorylate GST-FLS2K with an *in vitro* kinase assay (Fig 2.2F). The data suggest the transphosphorylation events in FLS2/BAK1/BIK1-mediated signaling are more complicated than anticipated.

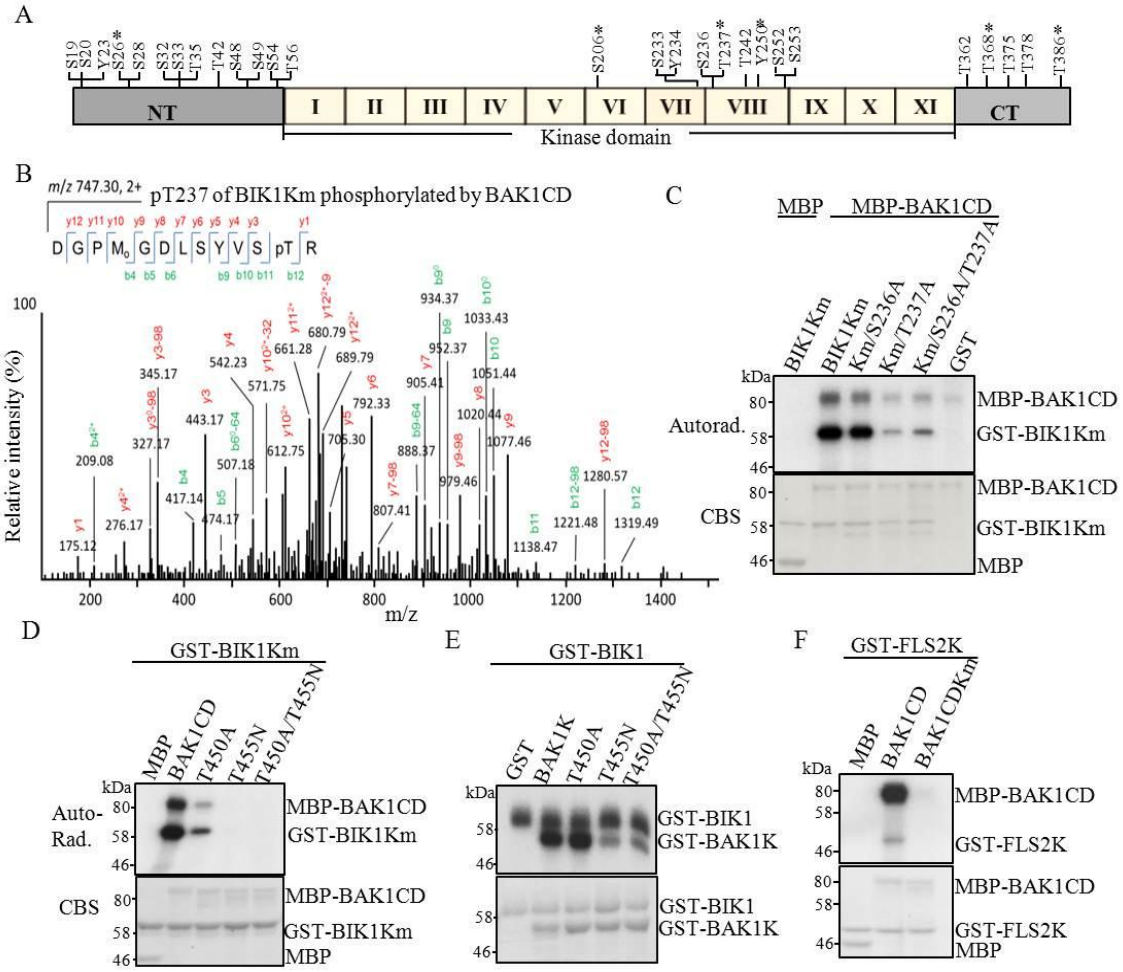

Figure 2. 2 Transphosphorylation in FLS2/BAK1/BIK1 complex.

(**A**) Schematic structure of BIK1. The position of phosphorylated amid acid detected from MS analysis of BIK1 autophosphorylation is labeled. * indicates the residues identified from both BIK1 autophosphorylation and transphosphorylation by BAK1. NT, N-terminal domain; I~XI, eleven kinase sub-domains; CT, C-terminal domain. (**B**) BIK1 T237 is phosphorylated by BAK1 with MS analysis. Sequence of a doubly charged peptide ion at m/z 747.30 matches to DGPMGDLSYVSpTR of BIK1. (**C**) BIK1 T237 is an essential phosphorylation site by BAK1 *in vitro*. MBP is the control for MBP-BAK1CD and GST is the control for GST-BIK1Km. The *in vitro* kinase assay was performed using MBP-BAK1CD as a kinase and BIK1Km variants as the substrates. Phosphorylation was analyzed by autoradiography (top panel), and the protein loading was shown by Coomassie blue staining (CBS) (bottom panel). (**D**) BAK1 T450 and T455 are required for auto-phosphorylation and trans-phosphorylation of BIK1 *in vitro*. BIK1Km fusion proteins were used as the substrates for BAK1CD variants in an *in vitro* kinase assay. (**E**) T455 is one of phosphorylation site of BAK1 by BIK1 *in vitro*. BAK1K variants were used as the substrates for BIK1 in an *in vitro* kinase assay. (**F**) BAK1 phosphorylates FLS2 *in vitro*. GST-FLS2K fusion proteins were used as the substrates for BAK1CD variants in an *in vitro* kinase assay.

The above kinase assays were repeated four times with similar results. The MS analysis was repeated twice.

Specific tyrosine phosphorylation of BIK1

During the course of analyzing my comprehensive MS data, I repetitively identified three tyrosine phosphorylation sites (Y23, Y234 and Y250) in BIK1 autophosphorylation reactions (Fig 2.2A, 2.3A, 2.3B and Supplemental Fig. 2A). This is a rather surprising finding as plant RLCKs have been classified as serine/threonine-protein kinases (Shiu and Bleecker, 2001). To further confirm my MS data, I performed *in vitro* BIK1 phosphorylation assays and detected tyrosine phosphorylation with a specific α-phosphotyrosine antibody (α-pY20), which has been used to characterize tyrosine phosphorylation of BRI1 and BAK1 (Oh et al., 2009; Oh et al., 2010). As shown in Fig. 2.3C, when expressed *in vitro* BIK1, but not BIK1Km, cross-react strongly with α-pY20, indicating that BIK1 possesses tyrosine kinase activity. Thus, BIK1 is a dual-specificity kinase with both serine/threonine and tyrosine activities. To further test their involvement in BIK1 tyrosine phosphorylation, I individually substituted three Tyr residues identified by MS analysis (Y23, Y234 and Y250) and two other Tyr residues (Y243 and Y245) in the BIK1 activation domain with Phenylalanine (F). I also aligned the BIK1 kinase domain with several *Arabidopsis* RLKs/RLCKs and human IRAK1 (Interleukin-1 receptor-associated kinase 1), and found that Y150 and Y250 of BIK1 are highly conserved in all of these RLKs/RLCKs (Fig S2). These two corresponding residues in BRI1 (BRI^{Y956} and BRI^{Y1057}) are essential for BRI1 kinase activity (Oh et al., 2009). In addition, BIK1Y316 is conserved in PBL1 and BAK1 (Fig S2). Thus, I also created BIK1Y150F and BIK1Y316F for tyrosine activity assays. Compared to the WT BIK1, the $BIK1^{Y150F}$, $BIK1^{Y243F}$ and $BIK1^{Y250F}$ mutant proteins

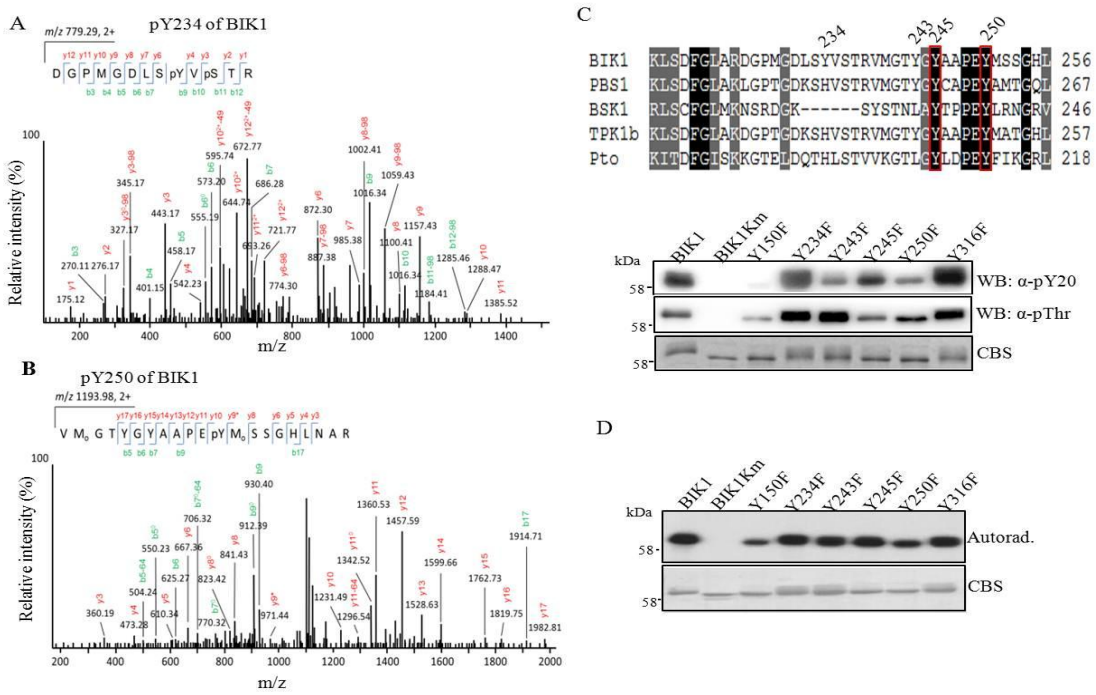

Figure 2. 3 Specific tyrosine phosphorylation of BIK1.
(A) BIK1 Y234 is auto-phosphorylated with MS analysis. (**B**) BIK1 Y250 is auto-phosphorylated with MS analysis. (**C**) BIK1 is auto-phosphorylated on tyrosine residues *in vitro*. The fusion proteins of GST-BIK1 and its variants were used in the *in vitro* phosphorylation assay and BIK1 tyrosine phosphorylation was detected by immunoblotting with anα- pY20 antibody (top panel), and an α-phosphotheronine (pThr) antibody was used to detect threonine phosphorylation (middle panel). The protein loading was shown by CBS (bottom panel). Amino acid sequence alignment of the kinase activation loop of BIK1, PBS1, BSK1, TPK1b and Pto is shown. The number indicates the position of amino acid in BIK1. (**D**) *In vitro* BIK1 auto-phosphorylation detected by [^{32}P]-γ-ATP (Top panel). The protein loading was shown by CBS (bottom panel).

exhibited dramatically less or compromised cross-reactivity to α-pY20 antibody, whereas the BIK1^{Y234F}, BIK1^{Y245F} and BIK1^{Y316F} retained wild-type tyrosine kinase activity (Fig 2.3C). Notably, the BIK1^{Y150F} mutant also dramatically reduced threonineand/or serine kinase activity as detected with α-phosphothreonine antibody (α-pThr) (Fig 2.3C) or autoradiograph with [^{32}P]-γ-ATP (Fig 2.3D). Thus, Y150 is essential for BIK1 catalytic activity. Significantly, the BIK1^{Y243F} and BIK1^{Y250F} had little or no effect on threonine and/or serine kinase activity (Fig 2.3C, 2.3D). Apparently, Y243 and Y250 are important tyrosine phosphorylation sties of BIK1.

BAK1-mediated BIK1 tyrosine phosphorylation

BIK1 is a substrate of BAK1 and BAK1 possesses tyrosine kinase activity (Lu et al., 2010; Oh et al., 2010). Thus, I examined whether BIK1 serves as a tyrosine kinase substrate of BAK1 with α-pY20 antibody in an *in vitro* kinase assay. As shown in Fig. 2.4A, BIK1Km is phosphorylated at tyrosine residues by MBP-BAK1CD as indicated by cross-reactivity with α-pY20 antibody. Consistent with previous report (Oh et al., 2010), BAK1CD exhibited strong tyrosine autophosphorylation activity (Fig 2.4A). The tyrosine phosphorylation of BIK1 by BAK1 was confirmed with MS analyses, which identified Y243 and Y250 as BAK1-mediated phosphorylation sites of BIK1 (Fig 2.4B). The data further revealed the importance of $BIK1^{Y243}$ and $BIK1^{Y250}$ autophosphorylation and BAK1 transphosphorylation (Fig 2.3). Consistently, the tyrosine phosphorylation of $BIK1Km^{Y250F}$ by BAK1CD was reduced compared to that of BIK1Km (Fig 2.4A). In addition, $BIK1Km^{Y243F}$ was significantly compromised in phosphorylation by BAK1CD, suggesting its important role in mediating tyrosine phosphorylation by BAK1. The overall phosphorylation of $BIK1Km^{Y243F}$ and $BIK1Km^{Y250F}$ by BAK1 as detected by autoradiograph of $[^{32}P]$-γ-ATP remained comparable to that of BIK1Km (Fig 2.4C). Thus, I have demonstrated that BIK1 is a tyrosine kinase substrate of BAK1, and Y243 and Y250 are two important BIK1 sites that are phosphorylated by BAK1.

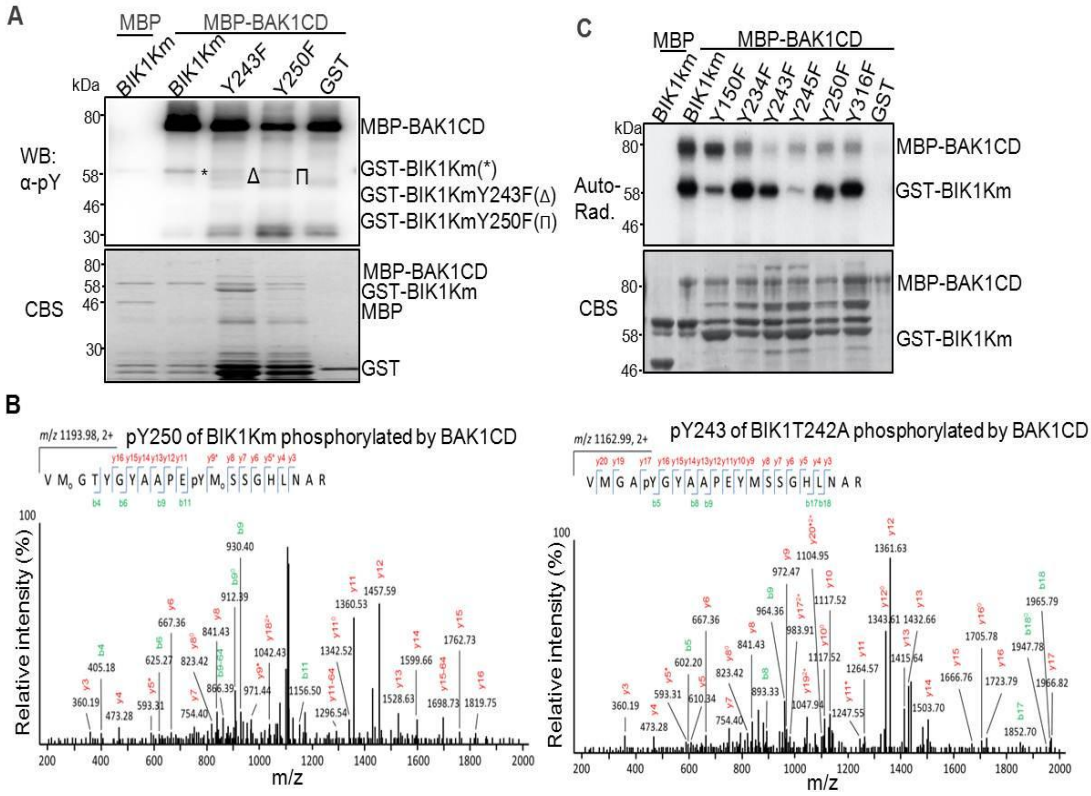

Figure 2. 4 BAK1-mediated tyrosine phosphorylation on BIK1.
(**A**) BAK1 phosphorylates BIK1 on tyrosine residues *in vitro.* The *in vitro* kinase assay was performed using MBP-BAK1CD as a kinase and BIK1Km variants as the substrates. The α-pY20 antibody was used for Western blot to detect tyrosine phosphorylation (*Upper*) and the protein loading was shown by CBS (*Lower*). (**B**) BIK1 Y250 (*Left*) and Y243 (*Right*) are phosphorylated by BAK1 with MS analysis. (**C**) *In vitro* phosphorylation of BIK1Km variants by BAK1. The *in vitro* kinase assay was performed using MBP-BAK1CD as a kinase and BIK1Km variants as the substrates in the presence of [^{32}P]-γ-ATP. The phosphorylation was shown by autoradiography (top panel) and the protein loading was shown by CBS (*Lower*).
The above experiments were repeated three times with similar results. MS analysis was repeated twice.

Tyrosine residues are involved in flg22-induced BIK1 phosphorylation

BIK1 is quickly phosphorylated upon flg22 perception as shown with a mobility shift by Western blot (Lu et al., 2010). I examined flg22-mediated BIK1 tyrosine phosphorylation *in vivo* with α-pY20 antibody after immunoprecipitation of protoplast expressed BIK1-GFP (Fig 2.5A). The mobility shift of BIK1-GFP detected by α-GFP

antibody indicates flg22-induced BIK1 phosphorylation (Fig 2.5A). Importantly, the α-pY20 antibody showed cross-reactivity to the immunoprecipitated BIK1 either with or without flg22 treatment, providing the evidence that BIK1 tyrosine phosphorylation occurs *in vivo* (Fig 2.5A). Notably, both the shifted and un-shifted BIK1 bands could be detected by α-pY20 antibody, suggesting that BIK1 has basal level of tyrosine phosphorylation in the absence of flg22 treatment.

To investigate the role of specific tyrosine residues of BIK1 *in vivo*, I created the above described tyrosine mutants in protoplast expression vectors and tested their effect on flg22-induced BIK1 phosphorylation. Consistent with its requirement in catalytic activity, $BIK1^{Y150F}$ dramatically reduced the ratio of shifted band versus un-shifted band upon flg22 treatment (Fig 2.5B). Significantly, $BIK1^{Y250F}$ also lost the flg22-induced mobility shift compared with WT BIK1 (Fig 2.5B). In addition, the mobility shift of $BIK1^{Y245F}$ was also partially compromised upon flg22 treatment (Fig 2.5B). However, $BIK1^{Y234}$, $BIK1^{Y243}$ and $BIK1^{Y316}$ seem to be dispensable for flg22-induced BIK1 mobility shift (Fig 2.5B). This result reconciles my MS and biochemical analysis in which Y250 is an important BIK1 auto-phosphorylation and BAK1-mediated transphosphorylation site, suggesting its essential role in flg22-mediated signaling. Overexpression of *BIK1* in protoplasts constitutively activated PTI reporter, *pFRK1::LUC* (Lu et al., 2010). Consistently with this notion, expression of $BIK1^{Y150F}$ or $BIK1^{Y250F}$ in protoplasts was no longer able to activate *pFRK1::LUC*, whereas $BIK1^{Y234F}$, $BIK1^{Y243F}$, $BIK1^{Y245F}$ or $BIK1^{Y316F}$ only partially compromised the activation of *pFRK1::LUC* (Fig 2.5C). These results establish that Y150 and Y250 are two

important sites of BIK1 in flg22-triggered phosphorylation and signaling. However, the BIK1Y23F mutant retained WT tyrosine kinase activity (Supplemental Fig 2B) and did not impair flg22-induced BIK1 mobility shift (Supplemental Fig. 2C) or the activation of *pFRK1::LUC* (Supplemental Fig 2D), suggesting that mutation of Y23 does not affect its function in flg22 signaling.

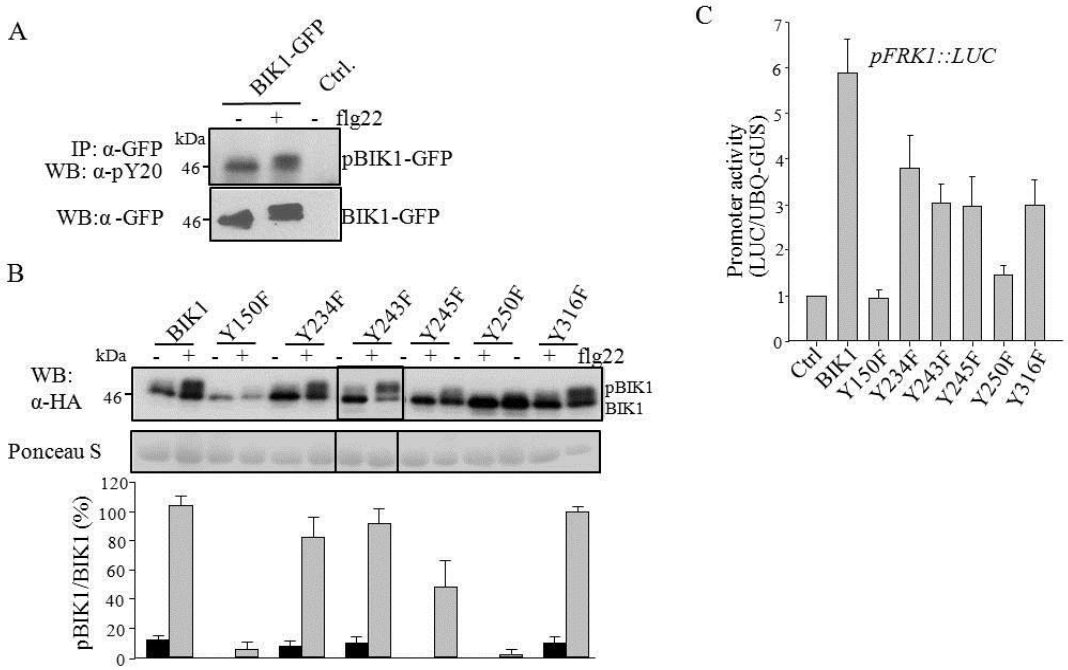

Figure 2. 5 BIK1 tyrosine phosphorylation in flg22 signaling.
(**A**) *In vivo* tyrosine phosphorylation of BIK1. BIK1-GFP or the empty vector control (Ctrl) was expressed in WT protoplasts for 8 hr followed by 1μM flg22 treatment for 10 min. BIK1 tyrosine phosphorylation was detected by immunoblotting with an α-pY20 antibody (top panel). The expression of BIK1 was detected by immunoblotting with an α-GFP antibody (bottom panel). (**B**) Requirement of specific tyrosine residues in flg22-induced BIK1 phosphorylation. BIK1 or BIK1 variants were expressed in WT protoplasts for 8 hr followed by 1μM flg22 treatment for 10 min, and subjected with immunoblotting with an α-HA antibody. The flg22-mediated BIK1 phosphorylation is indicated by the mobility shift (top panel) and the protein loading is shown by Ponceau S staining of the membrane (middle panel). The intensity of the shifted and un-shifted bands was quantified by ImageJ software and % of their ratio is shown (bottom bar graph). (**C**) Activation of *pFRK1::LUC* by BIK1 or BIK1 variants. The *pFRK1::LUC* was co-transfected with *BIK1, BIK1* variants or a vector control in protoplasts for 6 hr. *UBQ10-GUS* was included as a transfection control and the luciferase activity was normalized with GUS activity.
The above experiments were repeated three to four times with similar results.

Multiple tyrosine residues are required for BIK1-mediated plant immunity

To further elucidate the functional significance of specific tyrosine residues of BIK1, I complemented the *bik1* mutant plants with HA epitope-tagged WT BIK1 or various mutants, including BIK1Km, Y150F, Y243F and Y250F under the control of its native promoter, and examined their immune responses. Multiple lines of each construct were obtained and two lines with comparable protein expression level as WT BIK1 for each construct were chosen for further assays. The *bik1* mutant compromises various flg22-triggered immune responses including flg22-induced ROS production, and resistance to *Pseudomonas syringae pv. tomato* DC3000 (*Pst*) infection (Lu et al., 2010; Veronese et al., 2006; Zhang et al., 2010). I first examined the flg22-induced ROS production in these transgenic lines. The WT *BIK1* construct was completely restored whereas *BIK1Km*, $BIK1^{Y150F}$, $BIK1^{Y243F}$ or $BIK1^{Y250F}$ still retained the compromised flg22-induced ROS production in the *bik1* mutant compared to Col-0 WT or empty vector transgenic plants in Col-0 background (Fig 2.6A and Supplemental Fig 3A). The *bik1* mutant is more resistant to *Pst* infection, but is unable to mediate flg22-induced resistance. As shown in Fig 2.6B and 2.6C, the expression of WT *BIK1*, but not *BIK1Km*, $BIK1^{Y150F}$, $BIK1^{Y243F}$ or $BIK1^{Y250F}$ in the *bik1* mutant plant was able to restore WT level resistance to *Pst* infection and flg22-mediated resistance to *Pst* infection (Fig 2.6B and 2.6C). Correspondingly in plants with enhanced resistance to *Pst* infection, the *bik1* mutant is more resistant to *P. syringae maculicola* (*Psm*) infection compared to WT Col-0 plants, indicated by *in planta* bacterial multiplication 2- and 3-day after inoculation (dpi) (Fig 2.6D) and disease symptom development (Fig 2.6E). The susceptibility to *Psm*

infection of *bik1* mutant plants expressing WT *BIK1* was similar to WT Col-0 plants, whereas the *bik1* mutant plants expressing *BIK1Km*, *BIK1*^{Y150F}, *BIK1*^{Y243F} or *BIK1*^{Y250F} showed the similar level of resistance with the *bik1* mutant 2 and 3 dpi (Fig 2.6D, 2.6E and Supplemental Fig 3B). The *BIK1* gene was originally identified as a *Botrytis*–induced gene and the *bik1* mutant is more susceptible to *B. cinerea* infection than WT plants (Veronese et al., 2006). The *bik1* transgenic plants with *BIK1Km* or tyrosine substitution mutants were as susceptible as the *bik1* mutant compared to Col-0 WT plants as measured by symptom development (Fig 2.6F and Supplemental Fig 3C) and lesion diameter (Fig 2.6G and Supplemental Fig 3C) after *B. cinerea* infection. Taken together, the genetic analyses indicate that Y150, Y243 and Y250 are important for BIK1 functions in plant innate immunity and BIK1 tyrosine phosphorylation constitutes an essential step in PTI signaling. In addition to compromised immune responses, the *bik1* mutant exhibits certain growth defects in particular at the later development stage, including early flowering, and twisted and curling rosette leaves (Veronese et al., 2006). The WT BIK1 complementation plants rescued these growth defects in the *bik1* mutants (Fig S5). However, the transgenic plants carrying either *BIK1Km*, *BIK1*^{Y150F}, *BIK1*^{Y243F} or *BIK1*^{Y250F} resembled the *bik1* mutant having curling rosette leaves at later development stage and early flowering phenotypes (Fig Supplemental Fig. 4). These observations indicated that the kinase activity and the tyrosine residues (Y150, Y243 and Y250) are also required for BIK1 functions in growth and development.

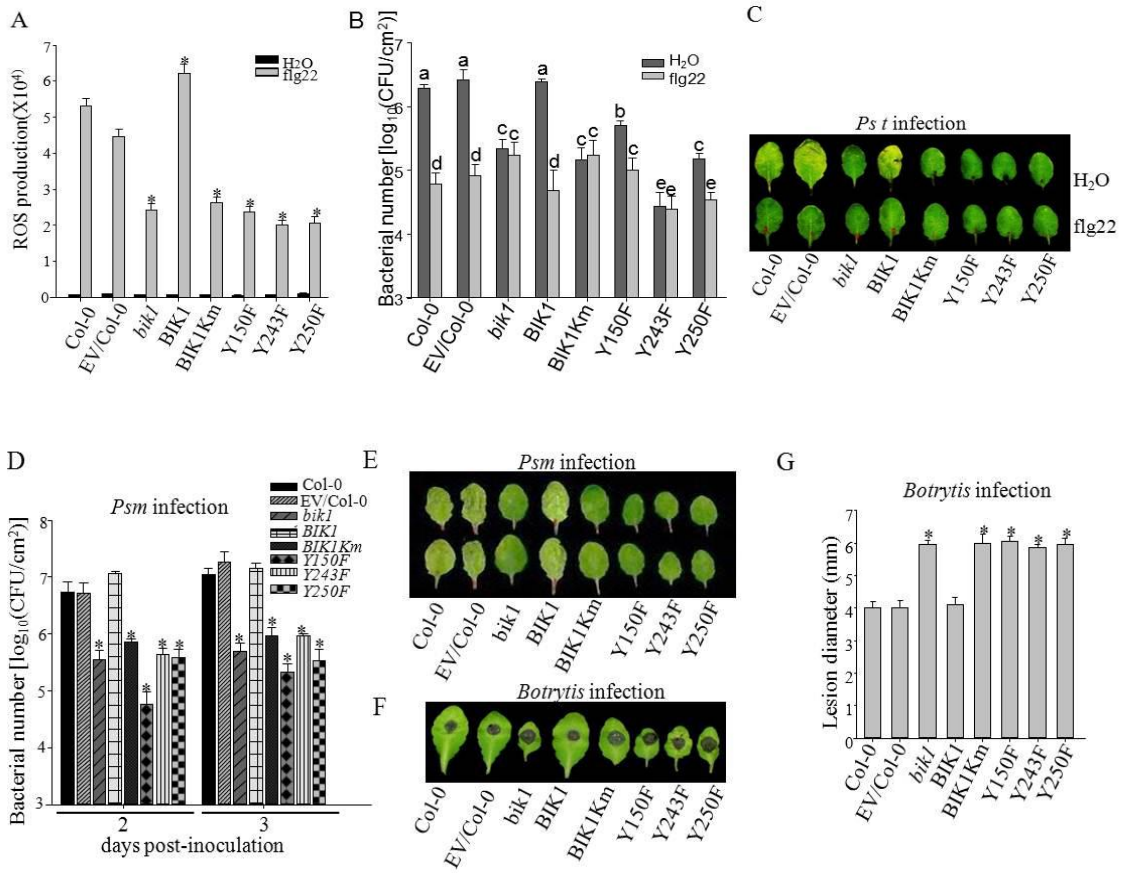

Figure 2. 6 Y150, Y243 and Y250 are required for BIK1 functions in plant immunity.
(**A**) flg22-triggered oxidative burst in WT Col-0, *bik1* mutant and different BIK1 complementation transgenic plants. ROS production in response to 100 nM flg22 from leaf discs of 5-week old plants was measured and presented as total photon counts during 30 min of treatment. Values presented are mean ± SE (n=36). (**B**) flg22-mediated restriction of bacterial growth. Four-week old plants were pretreated with H_2O or 100 nM flg22 for 24 hr and followed by hand-inoculation of *Pst* at 5 x 10^5 cfu/ml. *B*acterial growth was measured at 2 dpi. The data are shown as mean ±SE of three repeats and the different letters indicate a significant difference with $p<0.05$ established by a one-way ANOVA when compare with data from WT Col-0 plants. (**C**) The disease symptom of *Pst* infection. The similar experiments were performed as in (**C**) and the picture was taken at 3 dpi. (**D**) Bacterial growth of *Psm* infection. Leaves from 4-week old plants were hand-inoculated with *Psm* at 5 x 10^5 cfu/ml and the bacterial growth was measured at 2 and 3 dpi. The data are shown as mean ± SE of three repeats and * indicates a significant difference with $p<0.05$ established by a one-way ANOVA when compare with data from WT plants. (**E**) Disease symptom of *Psm* infection. The similar experiments were performed as in (D) and the picture was taken at 3 dpi. (**F**) Disease symptom of *B. cinerea* infection. Leaves from 5-week old plants were deposited with 10 μL of *B. cinerea* strain BO5 at a concentration of 2.5 x 10^5 spores/mL. Disease symptom was recorded 2 dpi. (**G**) Lesion development of *B. cinerea* infection. Similar assays were performed as in (F) and the lesion diameter was measured at 2 dpi. The data are shown as mean ± SE (n=30) of at least 30 leaves and * indicates a significant difference with $p<0.05$ when compare with data from WT plants.
The above experiments were repeated two times with similar results. The BIK1 complementation transgenic plants were *pBIK1::BIK1*^{Y150F}-HA #2-1, *pBIK1::BIK1*^{Y243F}-HA # 1-3, *pBIK1::BIK1*^{Y250F}-HA # A-7.

Discussion

Plant RLKs are architecturally related to metazoan receptor tyrosine kinases (RTKs). However, unlike RTKs that are generally tyrosine protein kinases, plant RLKs/RLCKs belong to RLK/Pelle/IRAK protein kinase family that is classified as serine/threonine kinase (Shiu and Bleecker, 2001). Recently, two *Arabidopsis* LRR-RLKs BRI1 and BAK1 have been shown to possess tyrosine kinase activity (Oh et al., 2009; Oh et al., 2010). Tyrosine phosphorylation of BKI1 (BRI1 kinase inhibitor 1) by BRI1 upon BR perception releases BKI1 into the cytosol and allows the recruitment of BAK1 to BRI1 (Jaillais et al., 2011). BAK1 is auto-phosphorylated at Y610 that is important for BR signaling and some aspects of plant defense (Oh et al., 2010). The cellular roles of BAK1 tyrosine phosphorylation in plant innate immunity remain unclear. Here I show that BIK1, an important component in plant PTI signaling, is auto-phosphorylated and trans-phosphorylated by BAK1 at several tyrosine residues in addition to serine/threonine residues. BAK1 physically interacts with BIK1 *in vitro* and *in vivo*, and directly phosphorylates BIK1 at multiple serine/threonine/tyrosine residues. $BIK1^{T237}$ is essential for its autophosphorylation and phosphorylation by BAK1. BIK1 also is able to reciprocally phosphorylate BAK1, and $BAK1^{T455}$ is likely a phosphorylation site by BIK1. BIK1 Y23, Y234 and Y250 were identified as autophosphorylation sites with comprehensive MS analysis. $BIK1^{Y250}$ also was phosphorylated by BAK1. Mutational and transgenic analyses indicate the importance of Y150, Y243 and Y250 in BIK1 tyrosine phosphorylation and functions in plant innate immunity. The BIK1 Y150F, Y243F or Y250F mutant was no longer able to

complement the *bik1* mutant-associated compromised PTI responses, including flg22-induced ROS burst and resistance to *Pst* infection, and disease resistance to fungal pathogen *B. cinerea*. The data revealed that plant RLCK BIK1 functions as a dual-specificity protein kinase in plant innate immunity and supported the notion that tyrosine phosphorylation is likely a common regulatory mechanism that controls plasma membrane-resident receptor signaling in plants and metazoans.

Extensive mutagenesis analyses have identified many serine/threonine sites important for BIK1 functions (Laluk et al., 2011). Several serine and threonine residues, including S33, T35, T42 in the BIK1 N-terminus, are important for BIK1 autophosphorylation and phosphorylation of an artificial substrate MBP (Laluk et al., 2011). These several sites were also identified as BIK1 autophosphorylation sites in MS analysis. In addition, I also identified 9 other serine/threonine residues in the N-terminus from MS analyses of BIK1 autophosphorylation, suggesting the important regulatory role of N-terminus in BIK1 kinase activity. In supporting of the this, S33 is important for BIK1-mediated flg22-induced resistance to *B. cinerea* and *Pst* infection (Laluk et al., 2011). In addition, the four sites identified by MS analyses, S233, S236, T237 and T242, lie within the activation loop of BIK1 kinase domain. T237A mutation blocks flg22-induced BIK1 mobility shift and BIK1-mediated *FRK1* promoter induction (Lu et al., 2010). The *bik1* mutant plants carrying S236A, T237A or T242A could not restore the compromised flg22-induced resistance to *B. cinerea* and *Pst* infection (Laluk et al., 2011). Significantly, the MS analysis also revealed T237 as a BIK1 transphosphorylation site by BAK1, which further reconciles the importance of this site in transducing BAK1

and BIK1-mediated signaling. Apparently, S233 may not be important for BIK1 functions since S233A mutation complemented *bik1* mutant to WT level of plant disease resistance (Laluk et al., 2011). I also identified 5 threonine sites (T362, T368, T375, T378 and T386) in the C-terminus as BIK1 autophosphorylation and/or BAK1 transphosphorylation sites. The importance of these sites for BIK1 biological functions awaits to be determined.

BIK1 was originally identified as a *Botrytis*-induced kinase (Veronese et al., 2006). It was shown later that BIK1 is rapidly phosphorylated upon bacterial flagellin perception and associates with flagellin receptor FLS2 and BAK1 complex in plant PTI signaling (Lu et al., 2010; Zhang et al., 2010). BIK1 is also phosphorylated upon ethylene (ET) treatment and required for responses to ethylene (Laluk et al., 2011). A recent study indicates that BIK1 regulates ethylene signaling through interaction with PEPR1, a LRR-RLK perceiving *Arabidopsis* endogenous peptide Pep1 (Liu et al., 2013). Apparently, Pep/PEPR/BIK1 ligand-receptor complex acts downstream of the canonical ET signaling cascade to regulate ET responses (Liu et al., 2013). In contrast to its positive roles in plant immunity and ET signaling, BIK1 is a negative regulator in plant hormone BR signaling. BIK1 complexes with BRI1 and is directly phosphorylated by BRI1 in transducing BR signaling (Lin et al., 2013a). BRI1 also possesses tyrosine phosphorylation activity (Oh et al., 2009). It will be interesting to test whether BRI1 phosphorylates BIK1 at certain tyrosine residues, such as Y250. I showed that $BIK1^{Y250}$ plays critical roles in plant immunity and development. It is of importance to determine whether $BIK1^{Y250}$ is also required for its function in BR and ET signaling. Notably,

BAK1^{Y610} is indispensable for plant resistance to nonpathogenic *Pst hrpA* mutant, but is dispensable for flg22-mediated seedling growth inhibition (Oh et al., 2010), suggesting that BAK1 Y610 is required for some but not all aspects of BAK1 functions. The similar scenario could exist in BIK1 tyrosine phosphorylation.

In metazoans, cell-surface RTK-mediated signaling controls multiple cellular processes and progression of different types of cancer (Lemmon and Schlessinger, 2010). Ligand binding will typically induce RTK dimerization and autophosphorylation, which often creates binding sites for certain non-receptor tyrosine kinases, such as Src, to relay RTK signaling (Yeatman, 2004). The identification of both BAK1 and BIK1 as tyrosine kinases in plants resembles metazoan RTK signaling. Tyrosine kinase activity is also involved in Toll-like receptor (TLR)-mediated innate immunity in animals (Chaudhary et al., 2007). Signaling via all TLRs (except TLR3) leads to the recruitment of the adaptor protein MyD88 (myeloid differentiation factor 88), and the serine/threonine-specific protein kinases IRAK1 and IRAK4. Upon association with MyD88, IRAK1 is phosphorylated by the activated IRAK4, and subsequently released from MyD88 to propagate the signaling by association with an E3 ubiquitin ligase TRAF6 (tumor necrosis factor receptor–associated factor 6) (Takeuchi and Akira, 2010). Spleen tyrosine kinase (SYK), a non-receptor tyrosine kinase involved in animal innate and adaptive immunity, is activated by multiple MAMPs, and directly associates with certain TLRs (TLR3, TLR4, and TLR9) and various downstream molecules, such as MyD88, TRAF6 and TRAF3 (Lin et al., 2013b). SYK negatively regulates TLR4 cytosolic signaling by inhibiting TRAF6 ubiquitination activity, whereas positively regulates

ligand-induced TLR4 endocytosis via activating TRAF3, suggesting the dual roles of SYK in TLR4 signaling (Lin et al., 2013b). Thus, both serine/threonine kinases and tyrosine kinases are involved in TLR-mediated innate immunity. Despite the apparent lack of classical tyrosine kinases, dual-specificity protein kinases, such as BIK1, may exhibit the functions of both serine/threonine and tyrosine non-receptor kinases in transducing signaling from membrane-bound receptors.

CHAPTER III

INVERSE MODULATION OF PLANT IMMUNE AND BRASSINOSTEROID SIGNALING PATHWAYS BY A RECEPTOR-LIKE CYTOPLASMIC KINASE BIK1*

Summary

In this study, the comprehensive phenotypic, genetic and biochemical examination of *bik1* mutants revealed that in contrast to its positive roles in plant immune, BIK1 negatively regulates brassinosteroid (BR)-mediated responses and signaling. The *bik1* mutants confer hypersensitivity to brassinolide (BL) treatment and insensitivity to BR synthesis inhibitor brassinazole (BRZ) treatment. BIK1 associates with BRI1 and dissociates from BRI1 complex upon the recognition of BL in a BAK1 independent manner. BIK1 is phosphorylated by BRI1, and the phosphorylation was enhanced by BL treatment. Genetic evidence revealed that BIK1 functions downstream of BRI1 and negatively regulates BR signaling in growth and development. These studies indicated that BIK1 mediates distinct functions in plant immunity and development via differential phosphorylation and dynamic association with specific receptor complexes.

---

* Reprinted with permission from "Inverse modulation of plant immune and brassinosteroid signaling pathways by the receptor-like cytoplasmic kinase BIK1" by Lin, W., Lu, D., Gao, X., Jiang, S., Ma, X., Wang, Z., Mengiste, T., He, P., and Shan, L. *Proceedings of the National Academy of Sciences of the United States of America* 110, 12114-12119. 2013, Wenwei Lin.

Introduction

Metazoans and plants have evolved complex mechanisms to cope with the constant challenges of environmental stresses while maintaining their growth and development. Being sessile and lacking sophisticated adaptive immune system, plants possess a large number of receptor-like kinases (RLKs) and receptor-like cytoplasmic kinases (RLCKs) that modulate growth, development and innate immunity (Shiu and Bleecker, 2001, 2003). RLKs sense different extrinsic and intrinsic cues through the extracellular domain and mediate diverse signaling events via the kinase domain. Arabidopsis Brassinosteroid Insensitive 1 (BRI1), a leucine-rich repeat-receptor kinase (LRR-RK) perceives polyhydroxylated growth hormone brassinosteroid (BR) to regulate plant growth and development (Li and Chory, 1997). ERECTA families LRR-RKs possess overlapping and distinct functions in the control of stomatal patterning by recognizing peptide ligands EPIDERMAL PATTERNING FACTOR 1 (EPF1) and EPF2 (Lee et al., 2012). Despite structural similarity with BRI1, Flagellin Sensing 2 (FLS2) and EF-Tu Receptor (EFR) recognize microbe-associated molecular pattern (MAMP) flagellin and elongation factor Tu (EF-Tu) respectively, and initiate innate immune signaling to defend pathogen attacks (Gomez-Gomez and Boller, 2000a; Zipfel et al., 2006). Apparently, signaling specificity is achieved by specific receptor-ligand interaction. Instead of ligand perception, RLCKs without an apparent extracellular domain often complex with RLKs and relay the signaling via phosphorylation.

In BR signaling, BRI1 receptor directly binds to brassinolide (BL), the most active form of BRs via a surface pocket embedded in a 70-amino-acid island of LRR

ectodomain (Hothorn et al., 2011; She et al., 2011). Subsequent heterodimerization, reciprocal and sequential phosphorylation of BRI1 and BAK1 (BRI1-associated kinase 1) accompanied with release of C-terminal tail and BRI1 Kinase Inhibitor protein (BKI1) have been proposed to be necessary to fully activate BRI1 (Wang and Chory, 2006; Wang et al., 2008a; Wang et al., 2005b). The activated BRI1 phosphorylates downstream RLCKs BR-Signaling Kinases (BSKs) and Constitutive Differential Growth 1 (CDG1), which further interacts with and phosphorylates the phosphotase bri1 Suppressor 1 (BSU1) (Kim et al., 2011; Kim et al., 2009; Tang et al., 2008). The phosphorylated BSU1 induces de-phosphorylation and inactivation of Brassinosteroid Insensitive 2 (BIN2), a GSK3-like kinase, leading to the nuclear accumulation of two de-phosphorylated transcription factors Brassinazole-Resistant 1 (BRZ1) and bri1-Ems-Suppressor 1(BES1) for the regulation of BR-responsive genes (Kim et al., 2011; Kim et al., 2009; Li and Nam, 2002; Wang et al., 2002; Yin et al., 2002).

In flagellin signaling, FLS2 receptor instantaneously forms a ligand-induced complex with BAK1 and concomitant trans-phosphorylation events likely constitute key initial steps in signal transduction (Schulze et al., 2010). The plasma membrane-associated RLCK Botrytis-Induced Kinase 1 (BIK1) associates with FLS2 and BAK1 and is directly phosphorylated by BAK1 (Lu et al., 2010; Zhang et al., 2010). BIK1 dissociates from FLS2 in a BAK1-dependent manner upon flagellin perception. BIK1 positively regulates plant innate immunity and the bik1 mutants were compromised in diverse flagellin-mediated responses and immunity to nonpathogenic bacterial infection. Activation of MAP kinases (MAPKs) and calcium-dependent protein kinases (CDPKs),

two independent intracellular signaling pathways downstream of FLS2/BAK1 receptor complex, governs the expression of MAMP-responsive genes (Boudsocq et al., 2010a). In addition, MAMP perception leads to ion fluxes, production of reactive oxygen species (ROS), deposition of callose and stomatal closure to prevent pathogen entry (Boller and Felix, 2009; Schwessinger and Ronald, 2012). Once activated, immune signaling is subjected for down-regulation to prevent excessive or prolonged activation of immune responses. Two plant U-box E3 ubiquitin ligases PUB12 and PUB13 associate with FLS2 upon flagellin perception in a BAK1-dependent manner. PUB12 and PUB13 directly ubiquitinate FLS2 and promote flagellin-induced FLS2 degradation, which in turn attenuates FLS2 signaling (Lu et al., 2011).

Despite distinct signaling outcomes, BAK1 is a shared component in flagellin and BR signaling via heterodimerization with corresponding receptors FLS2 and BRI1 (Chinchilla et al., 2007a; Heese et al., 2007a; Li et al., 2002a; Nam and Li, 2002). With a relatively short extracellular LRR domain, BAK1 does not directly bind to ligands but instead functions as a regulatory partner to positively modulate FLS2 and BRI1 signaling via trans-phosphorylation. BAK1 is also known as somatic embryogenesis receptor kinase 3 (SERK3), belonging to a subfamily of RLKs with 5 members, SERK1 to SERK5 (Chinchilla et al., 2009). In addition to BAK1/SERK3, BRI1 also associates with SERK1 and SERK4/BKK1 (BAK1-like 1) that play partially redundant roles with BAK1 in BR signaling (He et al., 2007; Karlova et al., 2006). The functional redundancy of SERK family in BR signaling was further revealed with serk1bak1serk4 triple mutants, which displayed an extreme de-etiolated phenotype reminiscent of a null bri1

mutant (Gou et al., 2012). Similarly, BAK1 and SERK4 also exhibit redundant functions in plant innate immunity via association with multiple MAMP receptors (Roux et al., 2011a). Recent studies have shown that BR homeostasis and signaling unidirectionally modulate FLS2-mediated immune responses (Albrecht et al., 2012; Belkhadir et al., 2012). The essential role of BAK1 in both BR and flagellin signaling pathways suggests that it may function as a rate-limiting factor to make a trade-off between growth and immunity. Interestingly, BR antagonizes FLS2 signaling in both BAK1-dependent and -independent manners. To date, signaling components downstream of BAK1 appear to be divergent in FLS2 and BRI1 pathways. Here, I found that BIK1, a positive regulator in plant immunity, acts as a negative regulator in BR signaling. In contrast to its compromised immune responses, the bik1 mutants display various BR hypersensitive phenotypes, including enhanced hypocotyl length of dark-grown seedlings and root growth inhibition upon BL treatment. The bik1 mutants also exhibit increased accumulation of de-phosphorylated BES1 and expression of BZR1 and BES1 target genes. BIK1 interacts with BRI1 at low BR concentration and releases from BRI1 upon exogenous BL treatment in a kinase-dependent manner. Unlike BIK1-FLS2 dissociation, which is BAK1 dependent, the BIK1-BRI1 dissociation is independent of BAK1. Apparently, release of BIK1 from receptor complexes is a result of BIK1 phosphorylation upon signal perception. In FLS2 signaling, BAK1 is crucial for flagellin-mediated BIK1 phosphorylation and complex dissociation. However, in BR signaling, BRI1 is able to phosphorylate BIK1 directly and the phosphorylation event was further enhanced upon BL treatment.

Method and materials

Plant materials and growth conditions

The *bik1, sid2, bak1-4 and bik1sid2* mutants were reported previously (Laluk et al., 2011; Lu et al., 2010). The *bri1-119* (*bri1-6,* ABRC stock CS399) and *det2-1* (ABRC stock CS6159) were obtained from the Arabidopsis Biological Resource Center (ABRC). The *bri1-5* mutants were obtained from Dr. Y. Yin. The *bik1bri1-5, bik1bri1-119, bik1det2-1* double mutants were generated by genetic crosses and confirmed by genotyping. *Arabidopsis* plants were grown in soil (Metro Mix 360) in a growth room at 23°C, 60% relative humidity and 75 μE m^{-2} s^{-1} light with a 12 hr photoperiod for approximately 4 weeks before protoplast isolation or RNA isolations. To grow *Arabidopsis* seedlings, the seeds were surface sterilized with 50% bleach for 10 min, and then placed on the plates with half-strength Murashige and Skoog medium (½ MS) containing 0.5% sucrose, 0.8% agar and 2.5 mm MES at pH 5.7. For various BR response assays, 100 nM BL (Chemiclones Inc.) or 2 μM BRZ (TCI AMERICA) were added in the medium. The plates were first stored at 4℃ for 3 days in the dark for seed stratification, and then incubated in the growth room with constant light or wrapped with foil paper for dark growth assay. At least 25 seedlings were measured for each genotype and each treatment. All experiments were repeated three to four times and the representative data were shown in the figures.

Plasmid construction and generation of transgenic plant

Arabidopsis FLS2, BAK1, BAK1km, BIK1, BIK1km constructs in plant expression vector or protein expression vector were reported previously (Lu et al., 2010). Full-length *BRI1* was amplified by PCR from Col-0 cDNA library and cloned into a plant expression vector with an HA epitope-tag at the C terminus with BamHI and StuI digestion. Cytosolic domain (MacDonald et al.) of BRI1 was cloned into the modified GST fusion protein expression vector pGEX4T-1 (Pharmacia) or pMAL-c2 (New England Biolabs) with BamHI and StuI digestion. The full-length BRI1 or BIK1 was sub-cloned into the modified BiFC vectors (a kind gift from Dr. F. Rolland) with BamHI and StuI digestion. Point mutations of *BRI1Km* were generated using the site-specific mutagenesis kit (Stratagene). The *BIK1* promoter up to 2.5Kb was amplified by PCR from Col-0 genomic DNA and introduced into *pCR2.1-TOPO* vector (Invitrogen). The *BIK1* gene tagged with double HA epitope from protoplast expression vector was subcloned into the BamHI and EcoRI sites of pCB302 binary vector to generate *pCB302-BIK1-HA*. The *BIK1* promoter from *pCR2.1-TOPO* vector was further subcloned into *pCB302-BIK1-HA* by SacI and BamHI to create *pCB302-pBIK1::BIK1-HA*. All the constructs were fully sequenced to verify absence of any mutations in the protein coding region and promoter region. Stable transgenic lines were generated using the standard *Agrobacterium tumefaciens*-mediated transformation in the *pBRI1::BRI1-GFP* (kindly provided by Dr. J. Li) transgenic plants or the *bik1* mutant plants. The expression of BIK1 and BRI1 proteins was confirmed by Western blot with an α-HA or

α-GFP antibody. The primer sequences of constructs and point mutations are listed in the Supplemental Data.

Protein extraction, Western blot and co-immunoprecipitation assay

To detect BES1 proteins, 10-day-old seedlings grown on ½ MS agar plate were transferred to 6-well cell culture plates containing 1 ml of H_2O per well (10 seedlings/well). After overnight incubation, the seedlings were submerged with 1 ml of 2 μM BL solution for indicated times, and ground to fine powder in liquid N2. The total proteins were extracted with 2 x sample buffer and subjected for Western blot with an α-BES1 antibody (a kind gift from Dr. Y. Yin) to detect the phosphorylation status of BES1.

Protoplasts isolation and transfection were performed as described (Lu et al., 2010). For Co-IP assay, 2 x 10^5 protoplasts transfected with indicated plasmids were lysed with 0.5 ml of extraction buffer (10 mM Hepes, pH7.5, 100 mM NaCl, 1mM EDTA, 10% glycerol, 0.5% Triton X-100, and protease inhibitor cocktail from Roche). After vortexing vigorously for 30 s, the samples were centrifuged at 16,162 x g for 10 min at 4 ℃. The supernatant was incubated with α-HA or α-FLAG antibody for 2 hr and then with protein-G-agarose beads (Andreasson et al.) for another 2 hr at 4 ℃ with gentle shaking. The beads were collected and washed three times with washing buffer (10 mM Hepes, pH7.5, 100 mM NaCl, 1 mM EDTA, 10% glycerol, and 0.1% Triton X-100) and once with 50 mM Tris-HCl, pH7.5. The immunoprecipitated proteins were analyzed by Western blot with an α-HA or α-FLAG antibody. For seedling Co-IP, approximate 15 g

of leaf samples from 4-week-old soil-grown plants were ground in liquid N2, and further ground in 10 ml of ice-cold extraction buffer 1 (20 mM Tris-HCl at pH 8.5, 150 mM NaCl, 1 mM EDTA, 20% glycerol, 1mM PMSF, 20 mM NaF, 50 nM microcystin, and protease inhibitor cocktail). Samples were centrifuged at 7000g for 15 min at 4°C. The resulting supernatants were further centrifuged at 100,000g for 2 hr at 4°C to precipitate the total membrane fraction. The pellet was re-suspended in 1 ml buffer 2 (10 mM Tris-HCl at pH 7.5, 150 mM NaCl, 1 mM EDTA, 10% glycerol, 1% Triton X-100, 1 mM PMSF, 20 mM NaF and protease inhibitor cocktail). The resulting fraction was used to perform Co-IP assay with the same procedures as protoplast Co-IP assay.

In vitro phosphorylation and immunocomplex kinase assays

Expression of GST and MBP fusion proteins and affinity purification were performed as standard protocol. The protein concentration was determined with Nano Drop ND-1000 spectrophotometer and confirmed by the BIORAD Quick Start Bradford Dye Reagent. For *in vitro* kinase assay, kinase reactions were performed in 30 μl of kinase buffer (20 mM Tris-HCl, pH 7.5, 10 mM MgCl2, 5 mM EGTA, 100 mM NaCl, and 1 mM DTT) containing 10 μg of fusion proteins with 0.1 mM cold ATP and 5 μCi of [^{32}P]-γ-ATP at room temperature for 3 hr with gentle shaking. The reactions were stopped by adding 4 × SDS loading buffer. The phosphorylation of fusion proteins was analyzed by autoradiography after separation with 10% SDS-PAGE. For immunocomplex kinase assays, 0.8 ml protoplasts at a density of 2 × 10^5/ml were transfected with 120 μg of plasmid DNA. The protoplasts were lysed with 0.5 ml of IP

buffer (50 mM Tris-HCl, pH 7.5, 150 mM NaCl, 5 mM EDTA, 1 mM DTT, 2 mM NaF, 2 mM Na_3VO_3, 1% Triton, and protease inhibitor cocktail). After centrifugation at 16,162 X g for 10 min at 4℃, the supernatant was incubated with an α-HA antibody for 2 hr and then protein-G–agarose beads for another 2 hr at 4℃ with gentle shaking. The beads were collected and washed once with IP buffer and once with kinase buffer. The kinase reactions were performed in 20 μl of kinase buffer with 2 μg of GST fusion proteins, 0.1 mM cold ATP, and 5 μCi of [^{32}P]-γ-ATP at room temperature for 1 hr with gentle shaking. The phosphorylation of GST and MBP fusion proteins was analyzed by 10% SDS-PAGE.

In vitro pull-down assay

5 μg of GST fusion proteins were pre-incubated with 5 μl of pre-washed amylose agrose beads (New England Biolabs) in 150 μl incubation buffer (10 mM Hepes, pH7.5, 100 mM NaCl, 1 mM EDTA, 10% glycerol, and 0.5% Triton X-100) at 4℃ for 1 hr with gentle shaking. After centrifuging at 16,162 x g for 5 min, the supernatant was transferred and incubated with pre-washed MBP fusion proteins immobilized on amylose-agarose beads at 4℃ for another 1 hr. The beads were collected and washed four times with washing buffer and once with 50 mM Tris-HCl, pH7.5. The immunoprecipitated proteins were analyzed by Western blot with an α-GST antibody.

Real-time RT-PCR Analysis

Total RNA was isolated from leaves or seedlings with TRIzol Reagent (Invitrogen). First strand cDNA was synthesized from 1 μg of total RNA with reverse transcriptase. Real-time RT-PCR analysis was carried out using iTaq SYBR green Supermix (Bio-Rad) supplemented with ROX in an ABI GeneAmp PCR System 9700. *UBQ10* was used as a control gene, and the expression of individual genes was normalized to the expression of UBQ10. The RT-PCR primer sequences are listed in the Supplemental Data.

BiFC assay

200 ul of protoplasts at a density of 2 x 105/ml were transfected with 40 μg of total DNA constructs. Fluorescent signals in the protoplasts were examined with confocal microscope (Leica Microsystems CMS GmbH) 18 hr after transfection. The filter sets used for excitation (Ex) and emission (Em) are as follows: GFP, 488 nm (Ex)/BP505 to 530 nm (Em); chlorophyll, 543 nm (Ex)/LP650 nm (Em); bright field, 633 nm. Signals were captured in multichannel mode, and images were analyzed and processed with Leica LAS AF Life and Adobe Photoshop (Adobe Systems).

Results

The bik1 mutant confers hypersensitivity to brassinolide

Given the observation that the *bik1* mutant plants exhibit slightly reduced primary root elongation, early flowering and reduced fertility (Veronese et al., 2006), it is likely

that BIK1 is involved in plant growth and development. In addition, the *bik1* mutant plants have moderately elongated and curling petioles, which were often observed in *BRI1* overexpressing plants (Supplemental Fig 5 A and B) or mutants with constitutive activation of BR signaling (Yan et al., 2009). BIK1 is a direct phosphorylation target of BAK1, an important component in BR signaling and BIK1 trans-phosphorylates BAK1 to enhance BAK1 kinase activity (Lu et al., 2010). These observations promoted me to examine the potential involvement of BIK1 in BR signaling.

BAK1 positively regulates BR signaling by transphosphorylation of BRI1 receptor (Li et al., 2002a; Nam and Li, 2002; Wang et al., 2008a). Surprisingly, in contrast to *bak1-4* mutants, which are partially insensitive to BL treatment, *bik1* mutants display constitutive BR responses and are hypersensitive to BL treatment. When grown in the dark, the hypocotyls of *bik1* mutants elongated slightly, but significantly longer than those of wild type (WT) plants, whereas *bak1-4* mutants exhibited relatively short hypocotyls (Fig 3.1A and 3.1B, bottom panels). In the presence of brassinazole (BRZ), an inhibitor of BR biosynthesis, the *bik1* mutants displayed much more pronounced hypocotyl elongation than WT plants (Fig 3.1A and 3.1B, top panels), suggesting that the *bik1* mutants were less sensitive to BRZ treatment. Treatment with BL increased hypocotyl elongation and inhibited root growth of WT seedlings grown under the light. Consistent with its positive role in BR signaling, *bak1-4* mutants were partially insensitive to BL treatment (Fig 3.1C and 3.1D). However, the *bik1* mutants were hypersensitive to BL treatment and root growth inhibition and hypocotyl elongation was greater compared to WT seedlings (Fig 3.1C and 3.1D).

To confirm that the phenotypes observed in the *bik1* mutants were attributed to the mutation in *BIK1*, I complemented the *bik1* mutants with *BIK1* cDNA under the control of its native promoter (2.5 Kb upstream of start codon). The *BIK1* transgene rescued *bik1* mutant phenotypes in response to BRZ treatment (Fig 3.1E). Interestingly, I observed that the *bik1* mutants exhibited twisted hypocotyls when grown in the dark (Supplemental Fig 6). This phenotype is likely due to the constitutive activation of BR signaling in the *bik1* mutants since the treatment of BL induced *bik1*-like hypocotyl twisting in the WT, but not *bri1-5* seedlings (Supplemental Fig 6) (Wolf et al., 2012). The BL treatment further accelerated the hypocotyl twisting in the *bik1* mutants, consistent with the observation that the *bik1* mutants were hypersensitive to BL treatment. As expected, the BR biosynthesis mutant *det2* still responded to BL treatment to induce hypocotyl twisting (Supplemental Fig 6). In addition, the exogenously prolonged application of BR biosynthesis inhibitor BRZ in the growth medium retarded the seedling growth and development likely as a result of reduced BR biosynthesis (Supplemental Fig 7). Compared to WT plants, the *bik1* mutants substantially ameliorated the BRZ-mediated growth inhibition (Supplemental Fig 7). Together, the data suggest that the mutation in *BIK1* activated BR signaling.

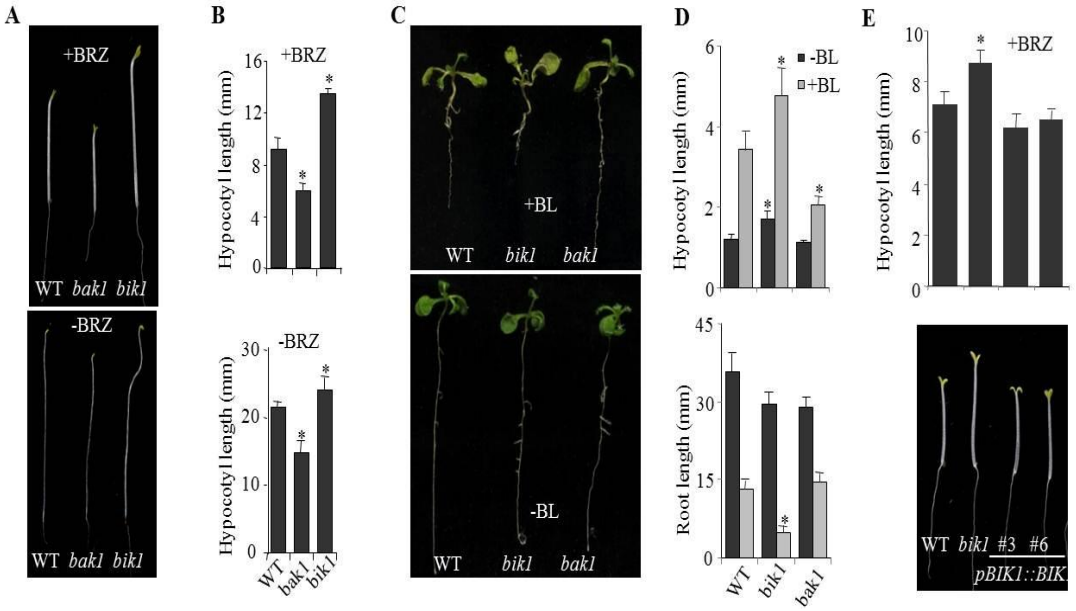

Figure 3. 1 Elevated BR responses in the *bik1* mutant plants.
(**A**) The *bik1* mutants are partially insensitive to BRZ treatment. The seedlings of WT (Col-0), *bak1-4* and *bik1* mutants were grown in the dark for 8 days on ½ MS plates with or without 2μM BRZ. (**B**) Quantification of hypocotyl length shown in (A). The data are shown as mean ± SE from at least 25 seedlings. Asterisk indicates a significant difference with $P<0.05$ when compared with data from WT seedlings. (**C**) The *bik1* mutants are hypersensitive to BL treatment. The seedlings were grown on ½ MS plates with or without 100 nM BL under the constant light for 14 days. (**D**) Quantification of root and hypocotyl length shown in (C). The data are shown as mean ± SE from at least 25 seedlings. Asterisk indicates a significant difference with $P<0.05$ when compared with data from WT seedlings. (**E**) *BIK1* complementation lines restore the BRZ insensitivity of the *bik1* mutants. Representative seedlings and hypocotyl length of WT, *bik1* mutants and two complementation lines of *pBIK1::BIK1-HA* in *bik1* mutants (#3 and #6) grown on ½ MS plates with 2μM BRZ in the dark for 8 days are shown.
The above experiments were repeated three to four times with similar results.

SA-independent BR hypersensitivity in the bik1 mutants

The *bik1* mutants have elevated salicylic acid (SA) accumulation compared to WT plants (Veronese et al., 2006). To investigate whether the high level of SA attributes to the observed BR phenotypes in the *bik1* mutants, I examined the BR responses in the *bik1sid2* double mutants, in which the high SA level is diminished by a SA biosynthesis mutant *sid2* (Laluk et al., 2011). Similar to the *bik1* mutants, the *bik1sid2* mutants exhibited elongated hypocotyls in the absence or presence of BRZ when grown in the

dark, and displayed hypersensitivity to BL treatment with elevated hypocotyl elongation and root inhibition when grown under the light (Fig 3.2 A and B). The dark grown *bik1sid2* double mutants also showed twisted hypocotyls in the absence of BL treatment and the BL treatment exacerbated the phenotype (Fig 3.2 C, D). The data suggest that BR hypersensitivity in the *bik1* mutants probably not caused by the high level of SA. This result is consistent with the previous observation that BIK1-mediated plant growth is SA-independent (Veronese et al., 2006).

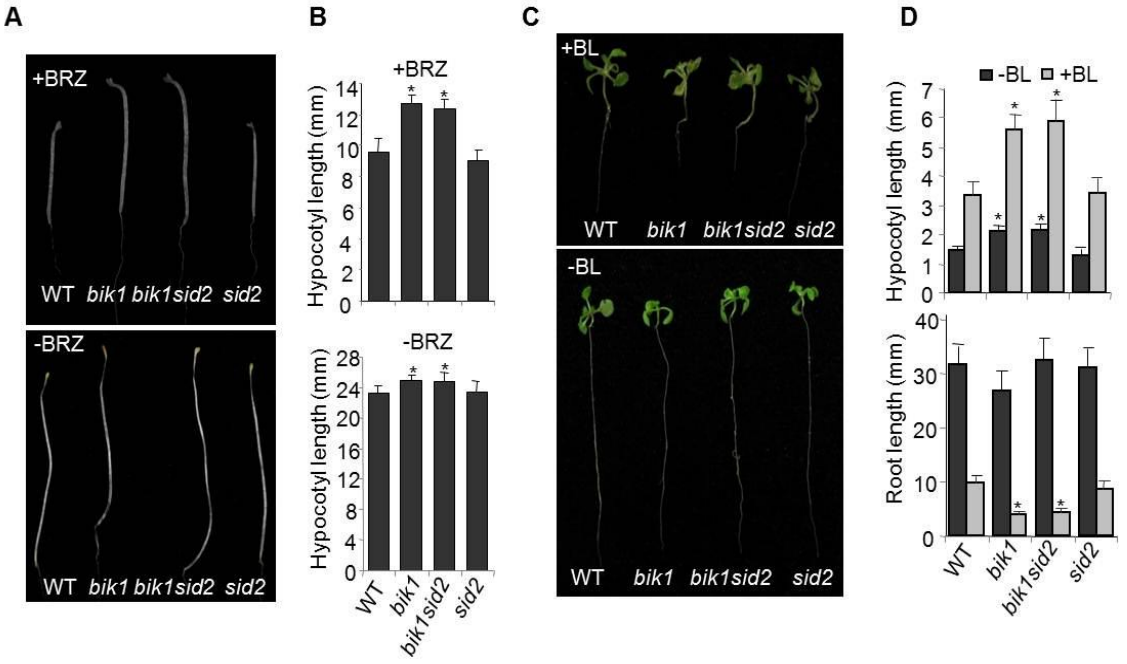

Figure 3. 2 The BR hypersensitivity of *bik1* mutant is SA independent.
(**A**) Eight-day-old dark-grown seedlings of WT, *bik1*, *bik1sid2* and *sid2* plants in the absence or presence of 2 μM BRZ. (**B**) The average hypocotyl length of WT, *bik1*, *bik1sid2* and *sid2* seedlings. (**C**) Fourteen-day-old seedlings of WT, *bik1*, *bik1sid2* and *sid2* plants in the absence or presence of 100 nM BL under the constant light. (**D**) The average hypocotyl and root length of WT, *bik1* ,*bik1sid2*,and *sid2* seedlings. The data are the mean±SE from at least 20 seedlings. Asterisk indicates a significant difference with $P<0.05$ when compared with data from WT seedlings.

BIK1 negatively regulates BR signaling

The elicitation of BR signaling induces de-phosphorylation of two closely related transcription factors, BES1 and BZR1, which in turn regulate the expression of BR target genes including *BR6OX*, *CPD* and *DWF4* (Sun et al., 2010; Yu et al., 2011). I examined the phosphorylation status of endogenous BES1 proteins with a specific α-BES1 antibody in WT and *bik1* mutant seedlings treated with or without BL. In WT seedlings, the BL treatment induced BES1 de-phosphorylation as indicated with the mobility shift of BES1 proteins from high molecular weight to low molecular weight in Western blot. Compared to WT plants, the *bik1* mutants exhibited elevated amount of de-phosphorylated BES1 proteins either with or without BL treatment (Fig 3.3A), consistent with the observation that the *bik1* mutants confer constitutively active and enhanced BR sensitivity (Fig 3.1 and Supplemental Fig 5, 6, 7). Apparently, both phosphorylated and de-phosphorylated forms of BES1 proteins accumulated more in the bik1 mutants than those in WT plants (Fig 3.3A).

Down-regulation of BR biosynthesis genes BR6OX, CPD and DWF4 constitutes a negative feedback regulation mechanism in response to BR treatment or situations of enhanced BR signaling. Consistently, the expression of BR6OX, CPD and DWF4 was significantly lower in the bik1 seedlings than that in WT before BL treatment, and the expression was further reduced in the bik1 mutants upon BL treatment compared to WT plants (Fig 3.3B). I also investigated whether the activation of BR signaling in the bik1 mutants was plant developmental stage specific. The similar reduction of BR6OX, CPD and DWF4 gene expression was observed in the 4-week-old bik1 mutant plants

compared to WT plants (Fig 3.3C). Thus, BIK1 negatively regulates BR signaling upstream of BES1 phosphorylation.

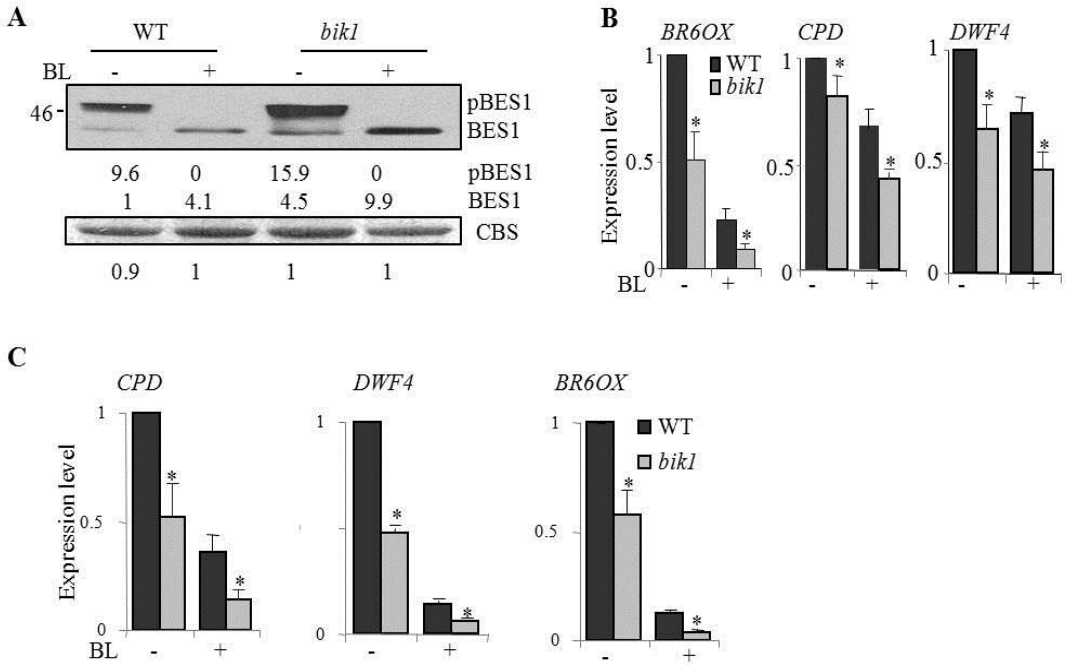

Figure 3. 3 BIK1 negatively regulates BR signaling.
(**A**) BES1 phosphorylation in WT and *bik1* mutant plants. The phosphorylated (pBES1) and dephosphorylated BES1 proteins were detected with an α-BES1 antibody (upper panel). Equal loading was ensured by total protein quantification before loading and by Coomassie brilliant blue staining (CBS) of the membrane (bottom panel). (**B**) Expression of BR responsive genes with qRT-PCR analysis. Ten-day-old seedlings were treated with 2μM BL or H_2O for 2 hr. The expression of *BR6OX, CPD or DWF4* was normalized to the expression of *UBQ10*. (**C**) BR-regulated gene expression in WT and *bik1* adult plants. The leaves of 4-week-old plants were treated with 2 μM BL or H_2O control for 3 hr, and the samples were collected for qRT-PCR analysis. The expression of *CPD, DWF4* and *BR6OX* was normalized to the expression of *UBQ10*. The data are shown as mean ± SE (n=3) from three independent biology repeats. Asterisk indicates a significant difference with $P<0.05$ when compared with data from WT seedlings or adult plants.
Experiments were repeated three times with similar results.

BIK1 associates with BRI1

BIK1 is a plasma membrane localized protein with a putative myristoylation motif (Veronese et al., 2006). In flagellin signaling, BIK1 associates with both FLS2 and

BAK1 (Lu et al., 2010; Zhang et al., 2010). To examine whether BIK1 forms a complex with BRI1, I performed co-immunoprecipitation (Co-IP) assay with co-expressing FLAG epitope-tagged BIK1 and HA epitope-tagged BRI1 in protoplasts. As shown in Fig. 3.4A, BIK1 co-immunoprecipitated BRI1 *in vivo* (Fig 3.4A). Interestingly, the association of BIK1 with BRI1 appears to be reduced upon BL treatment (Fig 3.4A), suggesting that BIK1 might be released from the receptor complex upon BL perception. BIK1-BRI1 association and BL-induced dissociation were also confirmed with *Nicotiana benthamiana* transient assay (Supplemental Fig 8A) To further investigate the *in vivo* association of BIK1 and BRI1 in intact plants, I transformed the HA-tagged *BIK1* under the control of its native promoter (*pBIK1::BIK1-HA*) into the *pBRI1::BRI1-GFP* transgenic plants. As shown in Fig. 3.4B, BIK1-HA co-immunoprecipitated BRI1-GFP as detected with α-GFP antibody upon α-HA antibody immunoprecipitation. Consistently, bimolecular fluorescence complementation (BiFC) assay also indicated that BRI1 associates with BIK1 with co-transfection of *BIK1* fused to carboxy-terminal half of YFP (yellow fluorescence protein) (BIK1-cYFP) and *BRI1* fused to the amino-terminal half of YFP (BRI1-nYFP) in protoplasts (Fig 3.4C). Neither of the individual constructs emitted YFP signals in protoplasts. To test whether BRI1 directly interacts with BIK1 through the cytosolic kinase domain, I performed an *in vitro* pull-down assay with a BRI1 cytosolic domain (BRI1CD) fused to maltose binding protein (MBP) immobilized on amylose-agarose beads as bait against glutathione-S-transferase (GST)-BIK1 fusion proteins. As shown in Fig. 3.4D, GST-BIK1 could be pulled down by MBP-BRI1CD, not MBP itself. Similarly, GST-BRI1CD could be pulled down by

MBP-BIK1 (Supplemental Fig. 8B). Taken together, the data demonstrate that BIK1 functions in BR signaling by direct interaction with BRI1 cytosolic kinase domain.

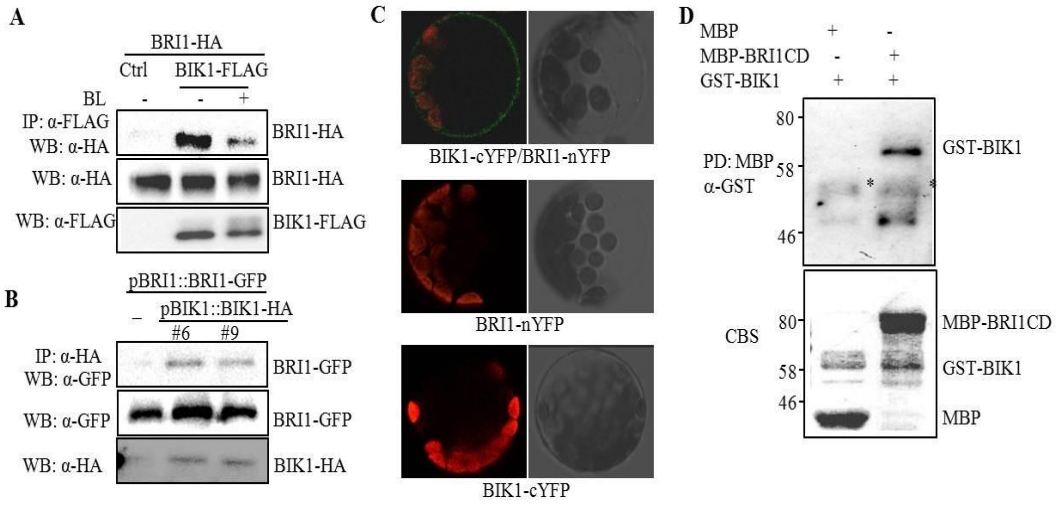

Figure 3. 4 BIK1 associates with BRI1.
(**A**) BIK1 associates with BRI1 in protoplasts. The protoplasts were co-expressed with BIK1-FLAG and BRI1-HA. Co-IP was carried out with an α-FLAG antibody (IP: α-FLAG), and the proteins were analyzed using Western blot with α-HA antibody. The top panel shows that BIK1-FLAG co-immunoprecipitated with BRI1-HA. The middle and bottom panels show the expression of BRI1-HA and BIK1-FLAG proteins. Protoplasts were treated with 2μM BL for 2 hr. (**B**) BIK1 associates with BRI1 in transgenic plants. The membrane proteins from 4-week-old soil-grown plants of two independent *pBIK1::BIK1-HA* transgenic plants in *pBRI1::BRI1-GFP* background (#6 and #9) or *pBRI1::BRI1-GFP* plants as a control were immunoprecipitated with α-HA antibody and analyzed with Western blot using α-GFP antibody (top panel). The expressions of BRI1-GFP and BIK1-HA in transgenic plants are shown (middle and bottom panels). (**C**) BIK1 interacts with BRI1 with BiFC assay in *Arabidopsis* protoplasts. The various BiFC constructs were transfected into protoplasts and the cells were observed under a confocal microscope. (**D**) BIK1 interacts with BRI1 cytosolic domain *in vitro*. GST-BIK1 proteins were incubated with MBP or MBP-BRI1CD beads (PD:MBP), and the beads were collected and washed for Western blot of immunoprecipitated proteins with an α-GST antibody. Asterisk indicates non-specific bands.
The above experiments were repeated three times with similar results.

BL-induced BRI1 phosphorylation on BIK1

BIK1 interacts with BRI1 *in vivo* and *in vitro*. I tested whether BRI1 could directly phosphorylate BIK1 to transduce BR signaling. An *in vitro* kinase assay with GST-

BIK1Km as a substrate indicates that MBP-BRI1CD directly phosphorylated GST-BIK1Km *in vitro* in the presence of [^{32}P]-γ-ATP (Fig 3.5A). Interestingly, it appears that MBP-BRI1CD exhibited stronger kinase activity towards BIK1 than BAK1 (Fig 3.5A). BRI1 phosphorylation on BIK1 was also observed with an immunocomplex kinase assay in which HA epitope-tagged full length BRI1 was expressed in protoplasts, and BRI1 was pulled down with an α-HA antibody for an *in vitro* kinase assay using GST-BIK1Km or GST-BAK1Km as a substrate. The immunoprecipitated BRI1 phosphorylated BIK1Km (Fig 3.5B). Importantly, BIK1 phosphorylation by BRI1 was enhanced upon BRI1 activation by BL treatment (Fig 3.5B). The BL treatment also enhanced BRI1 phosphorylation on BAK1Km (Fig 3.5B). BL treatment did not induce BIK1 phosphorylation by BRI1Km (Supplemental Fig 9A). BL-induced BIK1 phosphorylation by BRI1 was further detected by an α-pThr antibody with coexpressing BRI1 and BIK1 in protoplasts (Supplemental Fig 9B).The data indicate that BIK1 is a direct substrate of BRI1 and BL induces BRI1 phosphorylation on BIK1.

The flg22 treatment induces rapid BIK1 phosphorylation as indicated with protein mobility shift with SDS-PAGE (Supplemental Fig 10) (Lu et al., 2010; Zhang et al., 2010). I did not observe the clear and reproducible mobility shift of BIK1 upon BL treatment although I modified SDS-PAGE with various ratio of bisacrylamide to acrylamide concentration for a better separation of different phosphorylation statuses of phosphorylated proteins (Supplemental Fig 10) (Demmel et al., 2008). The data suggest that the phosphorylation change of BIK1 mediated by BR might be distinct from that triggered by flagellin. However, when co-expressed BIK1 with BRI1, a mobility shift of

BIK1 was observed upon BL treatment (Fig 3.5C), suggesting BRI1 phosphorylates BIK1 *in vivo* in BR signaling.

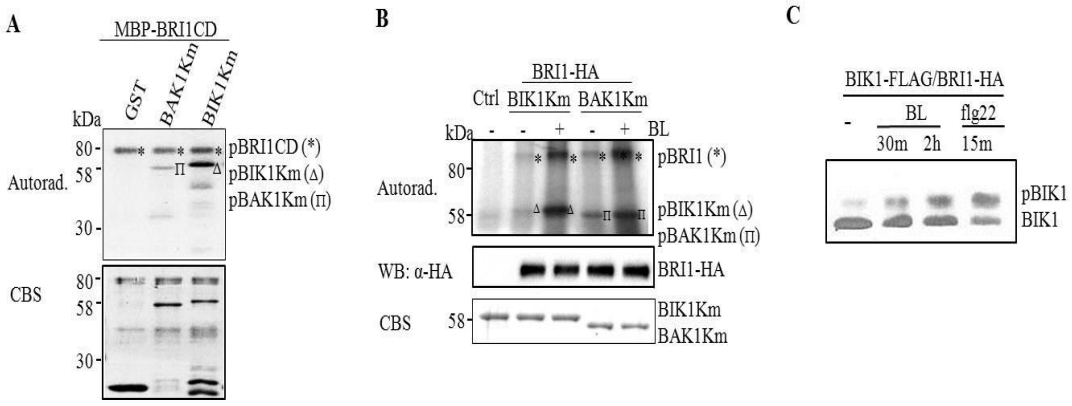

Figure 3. 5 BL-induced BRI1 phosphorylation on BIK1.
(**A)** BRI1 phosphorylates BIK1 *in vitro*. An *in vitro* kinase assay was performed by incubating MBP-BRI1CD with GST, GST-BIK1Km or GST-BAK1Km proteins. Proteins were separated by 10% SDS-PAGE and analyzed by autoradiography (top panel), and the protein loading control was shown by CBS (bottom panel). (**B**) BL treatment enhances BRI1 phosphorylation on BIK1. BRI1-HA was expressed in WT protoplasts for 10 hr followed by 2 μM BL treatment for 2 hr. BRI1-HA proteins were immunoprecipitated with an α-HA antibody and subjected to an *in vitro* kinase assay with GST-BIK1Km or GST-BAK1Km proteins as substrates (top panel). The middle panel shows the BRI1-HA expression and the bottom panel shows GST-BIK1Km and GST-BAK1Km proteins. (**C**) Overexpression BRI1 promotes BL-induced BIK1 phosphorylation. The protoplasts were co-transfected with BIK1-FLAG and BRI-HA, and incubated for 6 hr before 2 μM BL treatment for 30 min or 2 hr, or 1 μM flg22 treatment for 15 min. The samples were collected for SDS-PAGE with 10% acrylamide at a ratio of 1:37.5 for bisacrylamide to acrylamide.
The above experiments were repeated three times with similar results.

Differential requirement of BAK1 for BIK1-FLS2 and BIK1-BRI1 dissociation

BRI1 interacts with and phosphorylates BIK1. I tested whether the kinase activity of BIK1 and BRI1 is required for the BIK1-BRI1 interaction. I co-expressed GFP-tagged kinase-dead BIK1 (BIK1Km-GFP) with HA-tagged BRI1 in protoplasts for Co-IP assay. As shown in Fig 3.6A, BIK1Km-GFP co-immunoprecipitated BRI1-HA *in vivo*. However, the BL-induced BIK1-BRI1 dissociation (Fig 3.4A) was no longer observed

with BIK1Km (Fig 3.6A). In addition, BIK1 still interacts with kinase-dead BRI1 (BRI1Km), and this interaction was not reduced upon BL treatment (Fig 3.6B). Thus, the kinase activity of BIK1 and BRI1 is not required for BIK1-BRI1 interaction, whereas it is indispensable for BL-induced BIK1-BRI1 dissociation. Apparently, release of BIK1 from BRI1 receptor complex upon BL-induced phosphorylation is one of early steps in transducing BR signaling.

BL-induced BIK1-BRI1 dissociation is strikingly similar with the dynamics of BIK1-FLS2 complex formation upon flagellin perception (Lu et al., 2010; Zhang et al., 2010). BIK1 constitutively interacts with FLS2 in the absence of flagellin, whereas the interaction was reduced upon treatment by flg22, a 22-amino acid peptide of flagellin (Supplemental Fig 11A). In FLS2 signaling, BAK1 is essential for flg22-induced BIK1 phosphorylation and BAK1 directly phosphorylates BIK1 *in vitro*, whereas FLS2 has little kinase activity (Lu et al., 2010; Zhang et al., 2010). Consistently, BAK1 is indispensable for flg22-induced BIK1-FLS2 dissociation (Fig 3.6C). These results support that phosphorylation of BIK1 by BAK1 upon flg22 perception leads to its dissociation from FLS2 receptor complex, and thereby transducing intracellular FLS2 signaling. In contrast, BL-induced BIK1-BRI1 dissociation still occurred in the *bak1-4* mutants (Fig 3.6D), indicating that BAK1 is not essential for BIK1 release from BRI1 receptor in BR signaling. Consistent with the direct phosphorylation of BIK1 by BRI1, the BRI1 immunoprecipitated from *bak1-4* mutants was still able to phosphorylate BIK1 *in vitro* (Supplemental Fig 11B). Considering that BIK1-BRI1 dissociation is a result of BIK1 phosphorylation and BRI1 phosphorylates BIK1, it is likely that BAK1 plays little

role on BIK1 phosphorylation in BR signaling. Thus, BRI1 directly phosphorylates BIK1 to transduce BR signaling, whereas BAK1 is essential to phosphorylate BIK1 in transducing flg22 signaling.

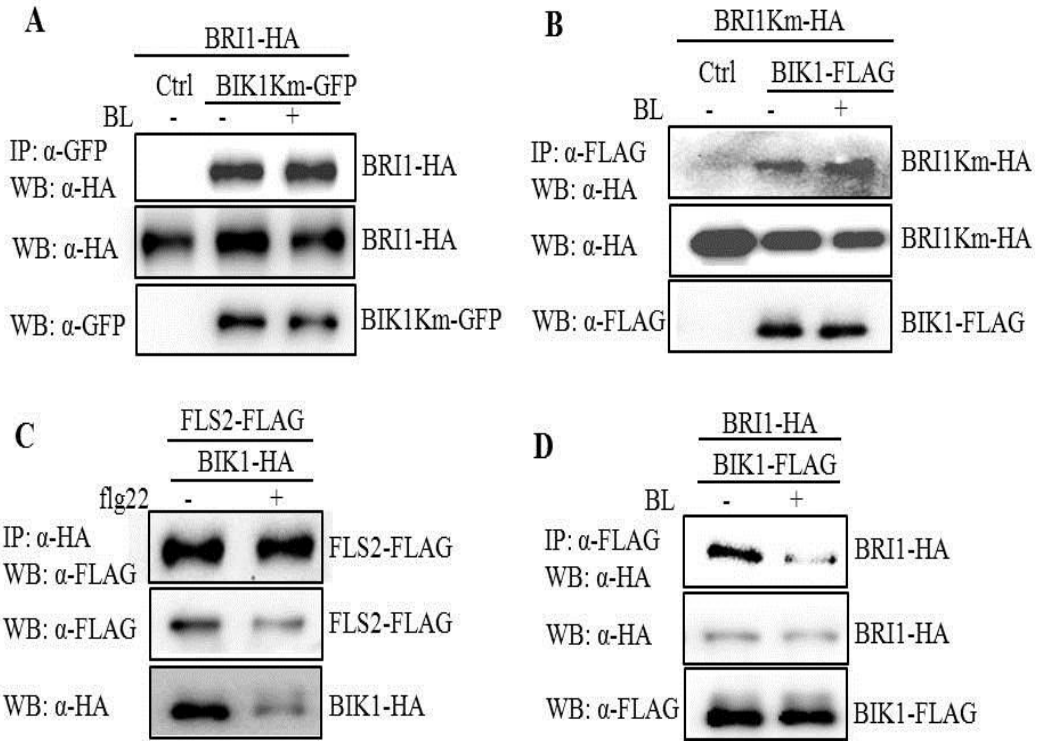

Figure 3. 6 The dissociation of BIK1-BRI1.

(**A**) The kinase activity of BIK1 is not required for its association with BRI1 but essential for its release from BRI1. The protoplasts from WT were co-expressed with BRI1-HA and BIK1Km-GFP or a control vector. Co-IP was carried out with an α-GFP antibody (IP: α-GFP), and the proteins were analyzed using Western blot with α-HA antibody. Protoplasts were treated with 2 μM BL for 2 hr. (**B**) The kinase activity of BRI1 is essential for its dissociation with BIK1. (**C**) BAK1 is required for flg22-induced BIK1-FLS2 dissociation. The BIK1-FLS2 interaction was performed with *bak1-4* protoplasts. Protoplasts were treated with 1 μM flg22 for 15 min. (**D**) BAK1 is not required for BL-induced BIK1-BRI1 dissociation. The BIK1-BRI1 interaction was performed with *bak1-4* protoplasts. Protoplasts were treated with 2 μM BL for 2 hr.

The above experiments were repeated three times with similar results.

BIK1 acts downstream of BRI1 in BR signaling

My phenotypic, molecular and biochemical data suggested that BIK1 negatively regulates BR signaling via association and phosphorylation by BRI1. I further investigated whether BRI1 functions genetically upstream of BIK1 by crossing the *bik1* mutants with *bri1-5* or *bri1-119* mutants to generate the *bik1bri1-5* and *bik1bri1-119* double mutants. As shown in Fig 3.7A, the *bik1bri1-5* and *bik1bri1-119* double mutants partially rescued the growth deficiency in the *bri1* mutants. The double mutants displayed reduced growth dwarfism, enlarged leave size, and elongated inflorescence stems and branches compared to the *bri1-5* or *bri1-119* single mutants (Fig 3.7A). Notably, the double mutants still exhibited the defects on silique development and had reduced seed yield, likely contributed by the mutation in *BIK1* (Supplemental Fig 12) (Veronese et al., 2006). *DET2* is the gene that involved in BR synthesis in Arabidopsis. To further investigate the BR hyper-response phenotypes of *bik1* mutants, I generated *bik1det2* double mutants by crossing *bik1* to *det2* mutants. The *bik1det2-1* double mutants also partially suppressed the dwarf phenotype of *det2* (Fig 3.7A). Consistently, the hypocotyls of dark-grown *bik1bri1-5* and *bik1bri1-119* seedlings were longer than those of corresponding single mutants (Fig 3.7B). Under the constant light, *bik1bri1-5* and *bik1bri1-119* seedlings also partially restored the leave growth and hypocotyl length of single mutants (Fig 3.7C). These results suggest that BIK1 genetically interacts with BRI1 and inhibits BR signaling *in vivo*.

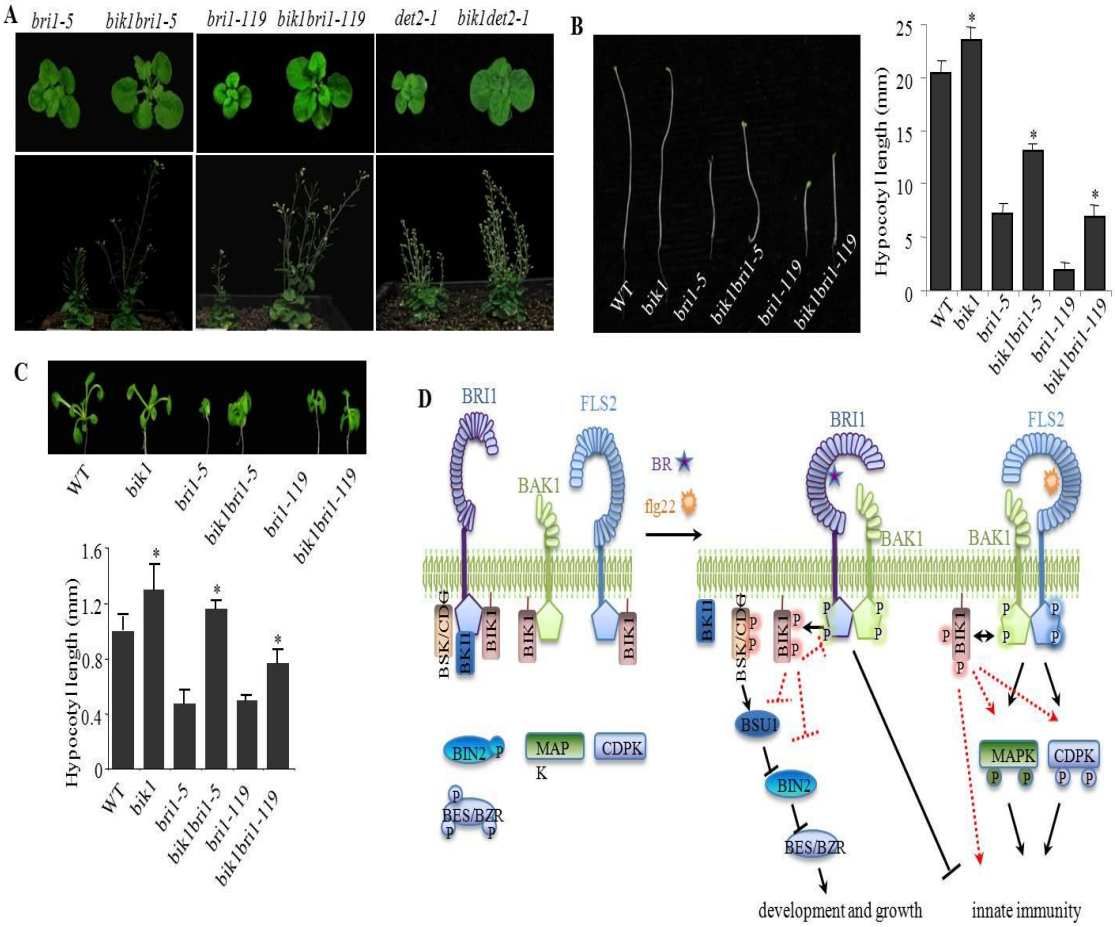

Figure 3. 7 BIK1 acts downstream of BRI1 in BR signaling.
(**A)**The *bik1bri1-5*, *bik1bri1-119* and *bik1det2-1* double mutants partially rescued the growth deficiency of *bri1-5*, *bri1-119* and *det2-1* mutants. The phenotypes of 4-week-old (top panel) and 8-week-old (bottom panel) soil-grown plants are shown. **(B)** The hypocotyls of dark-grown *bik1bri1-5* and *bik1bri1-119* seedlings were longer than those of corresponding single mutants. Representatives of 8-day-old seedlings on ½ MS plates grown in the dark are shown on the left panel and the quantification of hypocotyl length is shown on the right panel. The data are shown as mean ± SE from at least 25 seedlings. Asterisk indicates a significant difference with $P<0.05$ when compared with data from the corresponding single mutant. **(C)** The *bik1bri1-5* and *bik1bri1-119* seedlings partially restored the leave growth and hypocotyl length of single mutants grown under the light. Representatives of 14-day-old seedlings on ½ MS plates under the constant light are shown on the top panel and the quantification of hypocotyl length is shown on the bottom panel. **(D)** A model of BIK1-mediated inverse modulation of flagellin and BR signaling. In the absence of flagellin (flg22) and low level of BR, BIK1 associates with FLS2, BRI1 and BAK1 in an inactive state. BR binding to BRI1 leads to BRI1 activation, which in turn phosphorylates BIK1. The phosphorylated BIK1 is released from BRI1 complex and suppresses BR-mediated plant development and growth. In flagellin signaling, flg22 binding to FLS2 leads to recruitment and activation of BAK1, which phosphorylates BIK1. The phosphorylated BIK1 is able to transphosphorylate FLS2/BAK1 complex and results in the release of BIK1 from the complex to positively regulate flagellin-mediated plant immunity.

Discussion

BIK1, a RLCK from subfamily VII, was originally identified as *Botrytis*-induced kinase and plays critical roles in mediating plant resistance to necrotrophic fungal pathogens *B. cinerea* and *Alternaria brassiccicola* (Veronese et al., 2006). It has been shown previously that BIK1 is rapidly phosphorylated upon bacterial flagellin perception and associates with flagellin receptor complex in transducing plant immune signaling (Lu et al., 2010; Zhang et al., 2010). BIK1 is a direct substrate of BAK1, a shared regulatory component of multiple MAMP receptors and plant hormone BR receptor BRI1. Consistently, BIK1 is involved in immune signaling triggered by multiple MAMPs likely through association with the corresponding receptors. BIK1 is also phosphorylated upon ethylene treatment and required for responses to ethylene (Laluk et al., 2011). Surprisingly, in this study, the phenotypic, genetic and biochemical examination of *bik1* mutants revealed that in contrast to its positive roles in plant immune and ethylene signaling, BIK1 negatively regulates BR-mediated responses and signaling. The *bik1* mutants confer hypersensitivity to BL treatment (Fig 3.1). BIK1 complexes with BRI1 and dissociates from the BRI1 complex upon BL perception likely as a result of BIK1 phosphorylation by BRI1 (Fig 3.4 and 3.5). Intriguingly, BAK1 is required for flagellin-induced BIK1 release from FLS2, but not for BL-induced BIK1 release from BRI1. Consistent with the data that FLS2 is a non-RD kinase with little kinase activity (Schwessinger et al., 2011) whereas BRI1 is a RD kinase with strong kinase activity (Wang et al., 2008a), I observed a direct phosphorylation of BIK1 by BRI1, not by FLS2. Thus, BIK1 relays flagellin signaling via BAK1-mediated

phosphorylation, whereas BIK1 is directly phosphorylated by BRI1 in transducing BR signaling (Fig 3.7D). Differential phosphorylation of BIK1 by BAK1 and BRI1 may determine the substrate specificity and signaling outcomes. Identification of the *in vivo* phosphorylation sites of BIK1 and characterization of their functional requirement in BR- and flagellin-mediated responses will shed light on how BIK1 positively regulates flagellin signaling whereas negatively controls BR signaling.

Several other members of RLCKs, including BSKs (BSK1, BSK2 and BSK3) from subfamily XII and CDG1 from subfamily VIIc have been identified as signaling components in transducing BR signaling via association with BR receptor BRI1 (Kim et al., 2011; Tang et al., 2008). Similar to BIK1, BSKs associate with BRI1 and are released from BRI1 complex upon BR perception. However, unlike BIK1, BSKs and CDG1 play positive roles in BR signaling. CDG1 directly phosphorylates BSU1, a phosphatase that de-phosphorylates the negative regulator BIN2 (Kim et al., 2011). Although BSKs lack apparent kinase activity, phosphorylation of BSK1 by BRI1 promotes BSK1 binding to BSU1 which inactivates BIN2 kinase activity (Kim et al., 2009). Moreover, BSKs and CDG1 differ from BIK1 in that BSKs and CDG1 associate only with BRI1 and are phosphorylated by BRI1, not by BAK1. In contrast, BIK1 associates with both BRI1 and BAK1 and is phosphorylated by BRI1 and BAK1. Apparently, BIK1-BAK1 interaction and phosphorylation are more involved in flagellin signaling than that in BR signaling. Similar with BSKs and CDG1, BR-mediated BIK1 phosphorylation and BRI1-BIK1 dissociation are independent of BAK1. This suggests

the similarity and distinction of individual RLCKs in mediating different plant signaling pathways.

My data indicate that the *bik1* mutants possess enhanced BR signaling. It has been shown that BR homeostasis and signaling antagonize flg22-induced responses (Albrecht et al., 2012; Belkhadir et al., 2012). One question is whether the compromised immune responses in the *bik1* mutants are attributed to the elevated BR signaling. Accumulating evidence argues against this possibility. First, although exogenous application of BL inhibited FLS2- and EFR-mediated certain responses (Albrecht et al., 2012), it has not been reported that BR could promote disease symptom development or bacterial multiplication in *Arabidopsis* (Kemmerling et al., 2007). In contrast, tobacco plants treated with BL exhibited enhanced resistance to multiple pathogens, including *Pseudomonas* bacteria (Nakashita et al., 2003). Besides compromised flg22-induced ROS production and defense gene activation, the *bik1* mutants are also deficient in resistance to nonpathogenic bacterial infection and flg22-mediated restriction of bacterial growth (Lu et al., 2010; Zhang et al., 2010). Second, elevated BR signaling is not directly correlated with compromised immune responses. Although plants overexpressing BRI1 blocked FLS2- and EFR-mediated responses, $BRI1^{sud1}$ plants with normal BRI1 protein level, but increased BRI1 signaling, display enhanced flg22-induced signaling (Belkhadir et al., 2012). It has been proposed that the increased levels of BRI1, not increased BR signaling in BRI1 overexpressing plants, contribute to the antagonistic effects on MAMP signaling. I did not detect the reproducible difference of BRI1 protein level in WT and the *bik1* mutants with an α-BRI1 antibody, suggesting that

enhanced BR signaling in the *bik1* mutants is not caused by over-production of BRI1 receptor. Third, BR treatment did not affect flg22-mediated BIK1 phosphorylation (Albrecht et al., 2012). BIK1 phosphorylation is one of the earliest steps in flagellin signaling. Thus, the antagonistic effects on MAMP signaling by BL treatment are not due to the reduced BIK1 phosphorylation and activity. Together, the functions of BIK1 in flg22 and BR signaling are mechanistically uncoupled and the compromised immune responses in the *bik1* mutants are not simply due to the elevated BR signaling.

It remains elusive how BIK1 positively regulates plant innate immune signaling. The current model suggests that BIK1 functions upstream or independent of MAPK cascade in flagellin signaling although the genetic and biochemical evidence is still lacking. Then, how does BIK1 negatively regulate BR signaling? There are several possibilities. First, BIK1 may regulate GSK3 kinase BIN2 activity. Although GSK3 kinases are considered to be constitutively active to phosphorylate a variety of protein substrates in the absence of biological signals, mammalian GSK3β activity is modulated by phosphorylation, complex formation and priming phosphorylation of its substrates (MacDonald et al., 2009; Peng et al., 2010). Similarly, the activity of plant GSK3 kinase BIN2, a negative regulator in BR signaling, could be possibly modulated by other kinases, such as BIK1. The mutation in BIN2 and its closest homologs, BIN2_Like1 (BIL1) and BIL2 constitutively actives BR signaling and the *bik1* mutants resemble the *bin2bil1bil2* triple mutants with increased accumulation of both phosphorylated and dephosphorylated BES1 and twisted hypocotyls when grown in the dark (Yan et al., 2009). Second, BIK1 may modulate the negative regulator BKI1. BKI1 directly interacts

with BRI1 kinase domain thereby inhibiting BRI1 and BAK1 interaction (Wang and Chory, 2006). Tyrosine phosphorylation of BKI1 by BRI1 releases BKI1 from plasma membrane into the cytosol and enables active BRI1-BAK1 signaling complex formation (Jaillais et al., 2011). It is possible that BIK1 interacts and/or phosphorylates BKI1, thereby blocking its tyrosine phosphorylation by BRI1 and subsequent release from plasma membrane. Alternatively, BIK1-BRI1 interaction may reduce BRI1 tyrosine kinase activity towards BKI1. Third, BIK1 could also directly modulate BRI1 stability and/or activity to fine-tune BR signaling. It has been reported that the C-terminal domain of BRI1 plays a negative role in BR signaling likely through inhibition of BRI1 kinase activity (Wang et al., 2005b). Among several potential phosphorylation sites in the C-terminal domain, S1168 was identified as *in vivo* BR-mediated phosphorylation sites (Wang et al., 2005a). In addition, autophosphorylation of S891 within the glycine-rich loop inhibits BRI1 activity (Oh et al., 2012). Plausibly, BIK1 modulates BRI1 activity through interaction and/or phosphorylation of its C-terminal domain or S891 residue. It also remains possible that BIK1 phosphorylates unknown components that play novel roles in BR signaling. Identification of BIK1 phosphorylation targets will further elucidate the differential functions of BIK1 in BR signaling and flagellin signaling.

CHAPTER IV

A RECEPTOR-LIKE CYTOPLASMIC KINASE, BIK1, RELAYS PLANT IMMUNE SIGNALING FROM THE RECEPTOR COMPLEX TO MAPK CASCADES

Summary

The Arabidopsis FLS2-BAK1 receptor complex initiates immune signaling upon recognition of bacterial flagellin. BAK1 directly phosphorylates BIK1, and the phosphorylated BIK1 was released from receptor complex to relay immune signaling. The flagellin immune signaling was relayed from FLS2-BAK1 complex to downstream through the activation of MAPK cascades and CDPK pathway. However, the underlying mechanism remains elusive. In this study, my work revealed that BIK1 together with the closest homologs PBL1 and NAK1 are required for MEKK1-mediated MAPK activation. The PAMPs-induced MPK3/4/6 activations in Arabidopsis were impaired in *bik1pbl1nak1* mutant, suggesting that BIK1 and its closest homologs function upstream of MAPK cascades in PTI signaling. Genetic assays revealed that the *mekk1/2/3* deletion mutant and *mekk1/summ2* mutant, but not *mekk2* or *summ2* mutants, largely restore various growth defects of *bik1*, suggesting that the alleviated growth defects mainly attribute to the *mekk1* mutation. I also found that BIK1 associates with MEKK1 predominantly on the plasma membrane. My results indicate that BIK1 likely bridges between receptor complexes and MAPK cascades by association of both receptor complexes and MAPK1 cascades to relay PAMP signaling.

Introduction

The first layer of immune response is triggered by the recognition of pathogen/microbe-associated molecular patterns (PAMPs/MAMPs) (Boller and He, 2009; Chisholm et al., 2006a; Jones and Dangl, 2006a). In plants, a myriad of PAMPs are detected by plasma membrane-resident pattern-recognition receptors (PRRs), which act to launch PAMP-triggered immunity (PTI). Different PAMPs trigger largely convergent immune signaling events, including calcium flux, activation of MAPK cascades, production of reactive oxygen species (ROS), production of nitric oxide, induction of defense-related genes, induction of ethylene biosynthesis, deposition of callose and closure of stomata (Boller and Felix, 2009; Boller and He, 2009; Chisholm et al., 2006a; Jones and Dangl, 2006a). PTI contributes plants to fend off a broad spectrum of microbial infections.

One of the best-characterized PRRs in plants is flagellin sensing 2 (FLS2), an leucine-rich repeat receptor-like kinase (LRR-RLK), which recognizes a conserved 22-amino-acid peptide (flg22) derived from bacterial flagellin (Gomez-Gomez and Boller, 2000a). The recognition of flg22 triggers protein hetero-dimerization and phosphorylation between FLS2 and another LRR-RLK BAK1 (brassinosteroid insensitive 1-associated kinase 1) (Chinchilla et al., 2007b; Heese et al., 2007b). BIK1 (*Botrytis*-induced kinase 1), a plasma membrane-resident receptor-like cytoplasmic kinase (RLCK), associates with FLS2 and BAK1 in an flg22-independent manner (Lu et al., 2010; Veronese et al., 2006). Upon flg22 perception, BIK1 is rapidly phosphorylated

by BAK1 and released from the FLS2 and BAK1 complex (Lu et al., 2010; Zhang et al., 2010).

MAPK activation is one of the earliest immune responses upon the recognition of PAMPs (Chisholm et al., 2006a; Dodds and Rathjen, 2010; Tena et al., 2011). In plants, a MAPK cascade is generally consists of a MAP kinase kinase kinase (MAPKKK or MEKK), a MAP kinase kinase (MAPKK or MKK), and a MAP kinase (MAPK or MPK). In *Arabidopsis*, the MEKK1-MKK4/MKK5-MPK3/MPK6 cascade has been proposed to function downstream of FLS2 signaling and activates transcription factors WRKY22 and WRKY29 (Asai et al., 2002). There may be functional redundancy of MEKK1 homolog(s) to regulate the flg22-induced MKK4/MKK5-MPK3/MPK6 cascade activation as activation of MPK3 and MPK6 in *mekk1* mutants was similar as that in WT plants (Ichimura et al., 2006; Nakagami et al., 2006; Suarez-Rodriguez et al., 2007). The MPK3/6 positively regulates PTI signaling to induce defense response in plants. Another flg22-activated MAPK cascade consists of MEKK1, MKK1/MKK2 (two functional redundant MAPKKs), and MPK4 (Gao et al., 2008; Ichimura et al., 2006; Qiu et al., 2008; Suarez-Rodriguez et al., 2007). Previously, the MPK4 cascade was considered to be a negative regulator of PTI signaling as *mekk1*, *mkk1mkk2* and *mpk4* mutants all displayed a constitutive defense responses characterized by elevated salicylic acid (SA) accumulation and *PR* (pathogenesis-related) genes expression. Consequently, *mekk1*, *mkk1mkk2*, and *mpk4* mutants all showed severe dwarf morphologies and enhanced resistance to pathogens (Gao et al., 2008; Petersen et al., 2000; Qiu et al., 2008). However, recent study has revealed that the MPK4 cascade positively regulates basal

defense and this cascade is guarded by a disease resistance (R) protein consisting of nucleotide-binding leucine-rich repeat (NBS-LRR), SUMM2 in a MEKK2 dependent manner. Disruption of the MPK4 cascade led to the up-regulated of *MEKK2*, which then triggers SUMM2-mediated defense responses (Kong et al., 2012; Su et al., 2013; Zhang et al., 2012). Therefore, the emerging model suggests that flg22-induced MPK3/MPK6 and MPK4 cascades positively regulate PTI signaling transduction (Fig 4.1). Nonetheless, the components and mechanisms connecting the upstream FLS2/BAK1/BIK1 signaling receptor complex to the downstream MAPK cascades remain enigmatic.

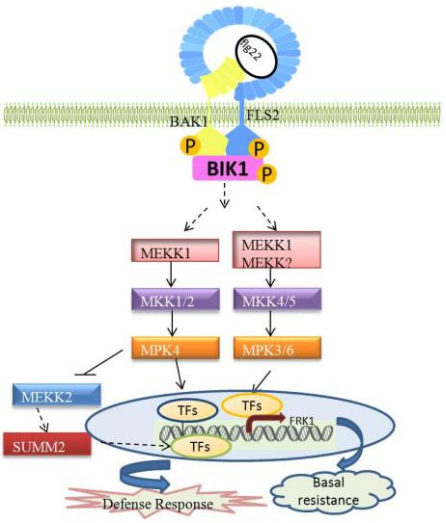

Figure 4. 1 Model of PAMP signaling pathway in plant.
Flagellin signaling relays from the FLS2-BAK1 receptor complex, through the MEKK1-MKK1/2-MPK4 and the MEKK1/MEKK?--MKK4/5-MPK3/6 cascades to downstream defense responses. The MPK4 cascade is guarded by R protein SUMM2 in a MEKK2 dependent manner. Disruption of the MPK4 cascade triggers SUMM2 mediates defense responses.

Method and materials

Plant growth condition

Arabidopsis wild-type (*Col-0*), *bik1, mekk1/2/3, bik1mekk1/summ2, bik1mekk2* and *bik1summ2* plants were grown in pots containing soil (Metro Mix 366) in a growth room at 23°C, 60% relative humidity and 75 μE m^{-2} s^{-1} light with a 12 hr photoperiod for approximately 4 weeks before protoplast isolation or bacterial inoculation.

Plasmid constructs and generation of transgenic plants

Arabidopsis MEKK1 full length genomic DNA was introduced in to a HBT vector for protoplast transient assays. The primer sequences for all these study are listed in the primer table I. Protoplast transient assay was carried out as described previously.

Bimolecular fluorescence complementation assay

The full-length MEKK1 or BIK1- was sub-cloned into the modified bimolecular fluorescence complementation (BiFC) vectors (a kind gift from F. Rolland, Leuven, Belgium) with BamHI and StuI digestion. Two hundred microliters of protoplasts at a density of 2×10^5/mL were transfected with 40 μg of plasmid DNA. Fluorescent signals in the protoplasts were examined with confocal microscope (Leica Microsystems) 18 h after transfection. The filter sets used for excitation (Ex) and emission (Em) are as follows: GFP, 488 nm (Ex)/BP505 to 530 nm (Em); chlorophyll, 543 nm (Ex)/LP650 nm (Em); brightfield, 633 nm. Signals were captured in multichannel mode, and images were analyzed and processed with Leica LAS AF Life and Adobe Photoshop.

ROS production assay

Four to five leaves from each five-week old plant were excised into leaf discs of 0.25 cm^2, following an overnight incubation in 96-well plate with 100 μL of ddH_2O to eliminate the wounding effect. H_2O was replaced by 100 μL of reaction solution containing 50 μM of luminol and 10 μg/mL of horseradish peroxidase (Sigma) supplemented with 100 nM of flg22. The measurement was conducted immediately after adding the solution with a luminometer (Perkin Elmer, 2030 Multilabel Reader, Victor X3), with a 1 min of reading interval for a period of 30 min. The measured value for ROS production from 36 leaf discs per treatment was indicated as means of RLU (Relative Light Units).

RNA isolation and RT-PCR

Total RNA was isolated from 10-day-old seedlings grown on 1/2MS plates, which were treated with 100 nm flg22 for 30 or 60 min. RNA extracted using TRIzol reagent (Life Technologies, USA) was quantified with NanoDrop, treated with RQ1 RNase-free DNase I (Promega, USA) for 30 min at 37℃, and then reverse transcribed with M-MuLV Reverse Transcriptase (NEB, USA). Real-time RT-PCR was carried out using iTaq Universal SYBR Green Supermix (Bio-Rad, USA) on 7900HT Fast Real-Time PCR System (Applied Biosystems, USA). The primers used to detect specific transcript by real-time RT-PCR are listed in Table1.

Result

BIK1 functions upstream of the MAPK cascades

Recognition of PAMPs by PRRs trigger downstream signaling networks controlled by MAPK signaling cascades and CDPK (Ca^{2+}-dependent protein kinases) signaling. These two signaling networks play specific and overlapping roles in programming the defense response genes. *FRK1*, one of the MAPK-specific target genes, is controlled by MAPK signaling cascades but not by CDPK signaling (Boudsocq et al., 2010a). Thus, *FRK1* serves as a PAMP responsive marker gene to indicate the activation of MAPK cascades. I tested the induction of *FRK1* by expression of BIK1 in protoplasts. BIK1 was capable of triggering the induction of *FRK1-LUC* when transiently expressed in protoplasts (Fig 4.2 A). To further determine the impact of BIK1 on MAPK cascade activation, I overexpressed BIK1 in protoplasts and determined the activation of MAPK cascades by immunoblotting using a pMAPK antibody to detect the phosphorylation of MPK3, 4 and 6. Consistent with previously reports, flg22 treatment activates MAPK cascades, indicated by phosphorylation of MPK3, 4 and 6 in Arabidopsis protoplasts (Fig 4.2 B). Transient expression of an HA-tagged BIK1 in protoplasts moderately triggered the activation of MPK3 and MPK6 without flg22 treatment (Fig 4.2 B). These data indicate that BIK1 plays a positive role in MAPK activation in Arabidopsis.

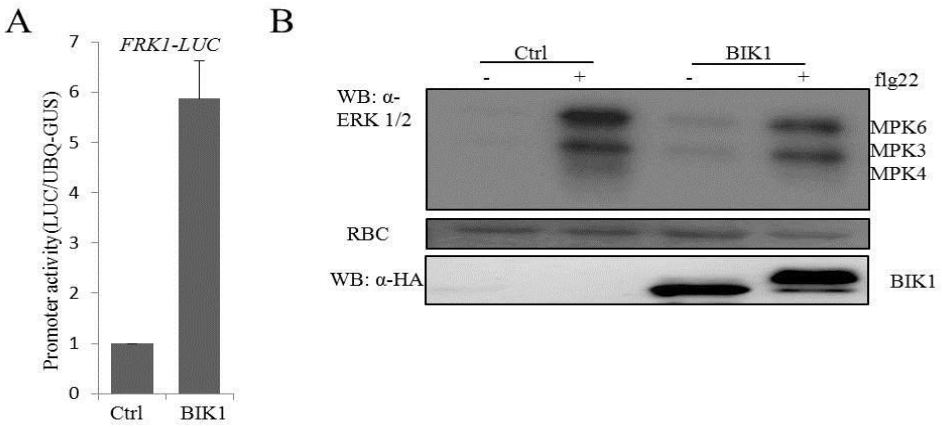

Figure 4. 2 BIK1 functions upstream of MAPK cascade.
(**A**) Expression of BIK1 activates *FRK1-LUC* in protoplast. The reporter *FRK1-LUC* was co-transfected with *BIK1* or a vector control in protoplasts for 6 hr. *UBQ10-GUS* was included as a transfection control and the luciferase activity was normalized with GUS activity. (**B**) BIK1 activates MAPK cascade. BIK1 or control empty vector was transfected in protoplasts. Cells were incubated at room temperature for 8 hours.and treated with or without 200 nM flg22 for 10 minutes. Total proteins were separated by 10% SDS-PAGE gel, and immunoblot with ERK 1/2 antibody (*Upper*) and α-HA-HRP respectively (*Lower*), and the protein loading control was shown by Ponceau S staining for Rubisco proteins (*Middle*).

BIK1 is required for flg22-induced MAPK activation

BIK1 belongs to the RLCK subfamily VII with 48 members. The amino acid sequence alignment, as showed in Fig. 4.3A, indicates that PBL1 is the closest homolog of BIK1 followed by NAK1. It was reported that BIK1 and PBL1 act in an additively manner in PTI (Zhang et al., 2010). To verify the function of BIK1 and its close members in MAPK cascades, I next tested the flg22-induced MAPK activation in *bik1*, *pbl1*, *bik1pbl1* and *bik1pbl1nak1* mutants. The flg22-induced MAPK activation occurred similarly in *bik1, pbl1,* and *nak1* mutants as in WT plants. However, the flg22-induced MAPK activation is compromised in *bik1plb1*and *bik1nak1* double mutants and is further reduced in the *bik1pbl1nak1* triple mutants compared with WT plants (Fig 4.3 *C*). In addition, the flg22-induced *FRK1* induction was significantly reduced when compared

to WT (Fig 4.3D). Therefore, these data indicate that BIK1, as well as PBL1 and NAK1, are required for flg22-induced MAPK activation.

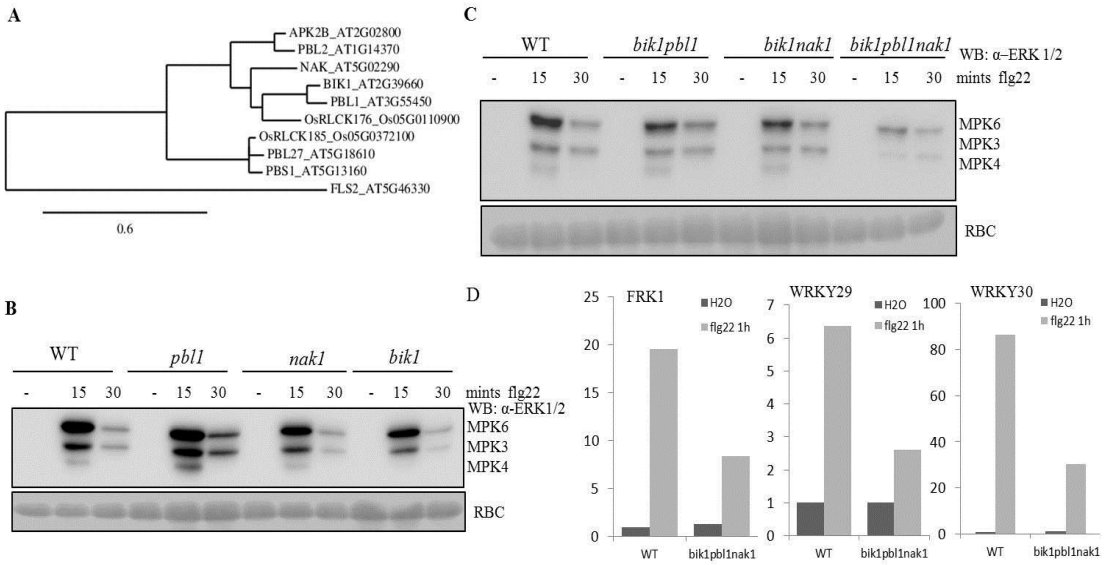

Figure 4. 3 BIK1 is required for flg22-induced MAPK cascade activation.
(**A**)Phylogenetic tree showing the relationship between BIK1 and related homolog kinase proteins in *Arabidopsis*. The full length protein amino acid sequences were aligned and analyzed with ClustalX and tree view algorithms. PBL1 and NAK1 are the closest homolog of BIK1. (**B**) The *bik1*, *pbl1* and *nak1* mutants did not affect flg22-induced MAPK activation. 10-day-old 1/2MS-grown seedlings were treated with 200 nM flg22 or H_2O for indicated time points. Total proteins were separated by 10% SDS-PAGE gel and immunobloted by an α-ERK 1/2 antibody (*Upper)*, and the proteins loading control was shown by Ponceau S staining for RuBisCo (*Lower*) (**C**) The *bik1pbl1nak1* mutants were impaired in flg22-induced MAPK cascade activation. 10-day-old 1/2MS-grown seedlings were treated with 200 nM flg22 or H_2O for indicated time points. Total proteins were separated by 10% SDS-PAGE gel and immunobloted by an α-ERK 1/2 antibody (*Upper)*, and the proteins loading control was shown by Ponceau S staining for RuBisCo (*Lower*). (**D**) The *bik1pbl1nak1* mutants were impaired in flg22-induced PTI genes induction.

BIK1 is required for PAMPs and DAMP-induced MAPK activation

In addition to flagellin, bacterial EF-Tu, PGN, LPS and fungal chitin have been shown to activate MAPK cascades (Boller and He, 2009; Chisholm et al., 2006a; Jones and Dangl, 2006a; Rodriguez et al., 2010). Furthermore, BIK1 was reported as a

convergent component positively regulates PTI and DTI signaling. To determine the requirements of BIK1 for multiple PAMPs and DAMP, I test MAPK activation in *bik1pbl1nak1* seedlings triggered by various PAMPs, including elf18, LPS, PGN and chitin and endogenous DAMP of *Arabidopsis*, ATPEP1. Similar to flg22, elf18, LPS, PGN, chitin as well as ATPEP1 induced activation of MAPK cascades (Fig 4.4 A, B, C and D). Similarly, the MAPK activation was significantly compromised in the *bik1pbl1nak1* mutant, indicating that BIK1, PBL1 and NAK1 function upstream of MAPK cascades in PTI and DTI signaling (Figure 4.4 A, B, C and D).

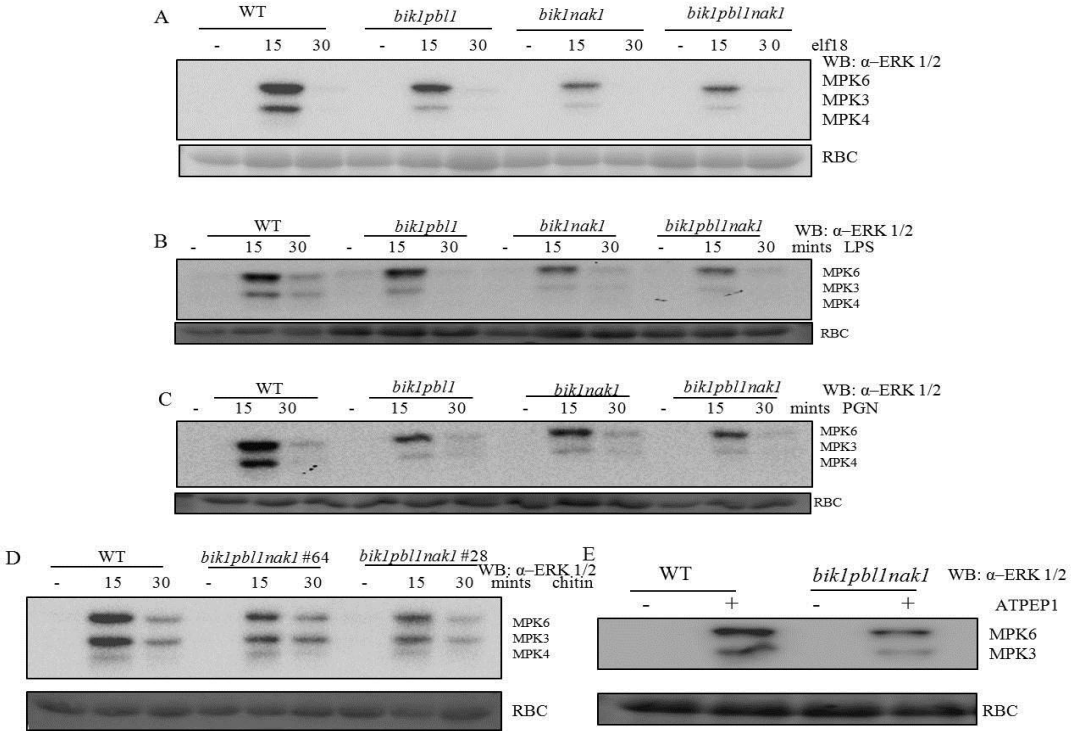

Figure 4. 4 BIK1 functions upstream of PAMP and DAMP-induced MAPK activation.
(**A-E**) *bik1pbl1nak1* mutants were impaired in PAMP/DAMP-induced MAPK cascade activation. 10-day-old 1/2MS-grown seedlings were treated with 100 nM elf18,LPS, PGN, Chitin or ATPEP1 for indicated time points. Total proteins were separated by 10% SDS-PAGE gel and immunobloted with an α-ERK 1/2 antibody (*Upper),* and the proteins loading control was shown by Ponceau S staining for RuBisCo (*Lower*).

BIK1 Y150F has dominant negative effects on the MAPK activation

A tyrosine site Y150, which is located at gatekeeper site of BIK1, required for BIK1 function in PTI signaling, development and growth was previously identified (Lin et al., 2014). Substitution of Y150 to F in BIK1 results in loss-of-function of BIK1, indicated by compromised phosphorylation by BAK1 and BIK1 auto-phosphorylation as well as the inability of $BIK1^{Y150F}$ to complement the defense and growth phenotypes of the *bik1* mutant (Lin, et al., 2014). I further determined whether Y150 is required for BIK1-regulated MAPK activation. Expression of $BIK1^{Y150F}$ in *bik1* resulted in significantly reduced MAPK activation compared to that in transgenic plants carrying empty vector.

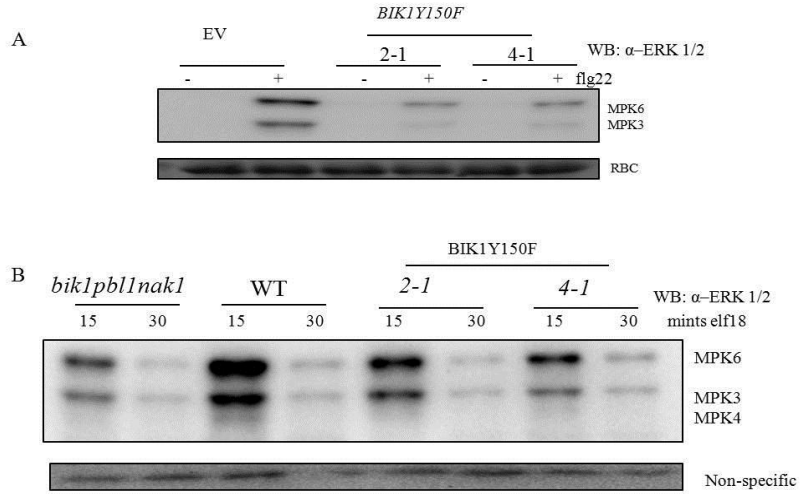

Figure 4. 5 BIK1 Y150F plays a dominant negative role in PAMP-triggered MAPK activation.
(**A**) BIK1Y150F mutant is impaired in flg22-induced MAPK activation. Total proteins from transgenic plant seedlings carrying the empty vector or 35S::BIK1Y150F were subjected to immunoblot with α–ERK1/2 antibody. Total proteins were separated by 10% SDS-PAGE gel and immunobloted with an α-ERK 1/2 antibody (*Upper),* and the proteins loading control was shown by Ponceau S staining for RuBisCo (*Lower*). (**B**) BIK1Y150F mutant is impaired in elf18-induced MAPK activation. 10-day-old seedlings were treated with 100nM elf18 for indicated time. Total proteins were isolated and separated in 10% SDS-PAGE gel, and the phosphorylation of MPK3/4/6 were detected by α–ERK1/2 antibody. Non-specific band serves as loading control.

Furthermore, I observed that BIK1^{Y150F} resulted in compromised elf18-induced MAPK activation to an extent similar to that in *bik1pbl1nak1* (Fig 4.5 B). Taken together, these data indicate that BIK1 Y150F substitution plays as a dominant negative role in PAMP-induced MAPK activation.

The mekk1/2/3 mutant partially restores growth defects of bik1

It was reported that MPK3/6 and MPK4 were activated by MKK4/5 and MKK1/2 respectively (Asai et al., 2002; Gao et al., 2008; Ichimura et al., 2006), and MKK1/2/4/5 were activated by MEKK1 upon flg22 perception (Asai et al., 2002; Gao et al., 2008; Ichimura et al., 2006). When the MEKK1-MKK1/2-MPK4 cascade was disrupted, SUMMER2-mediated autoimmunity will be triggered by increasing abundance of MEKK2 (Fig 4.1) (Kong et al., 2012; Su et al., 2013). The *mekk1* and *mpk4* mutants displayed severe dwarf phenotypes with constitutive high expression of *PR1* and *PR2* genes (Ichimura et al., 2006; Petersen et al., 2000; Suarez-Rodriguez et al., 2007). To determine whether the growth defects of *bik1* were caused by disruption of the MEKK1-mediated cascade, I determined the expression level of *MEKK2* in the *bik1* mutant by using qRT-PCR. I found that *MEKK2* was moderately elevated in the *bik1* mutant compared with wild type (Fig 4.6 B). Consistent with high SA accumulation and growth defects (Veronese et al., 2006), *bik1* also show constitutive expression of *PR1* (Fig 4.6 B). In addition, the *bik1* mutant possesses enhanced resistance to *P.st* DC3000 in an SA-dependent manner (Veronese et al., 2006). These data indicates that *bik1* displays constitutive defense responses. *MEKK1*, together with *MEKK2* and *MEKK3* constitute a

tandemly duplicated gene family. The *mekk1/2/3* deletion mutant, which was caused by a T-DNA insertion that disrupts this gene family, restored *mekk1* growth deficient phenotypes to wild type. The morphologies of *bik1mekk1/2/3* quadruple mutant were shown in fig 4.6 C, the semi-dwarfed and early flowering phenotypes of *bik1* were largely restored by *mekk1/2/3* mutations (Fig 4.6 C). Collectively, these data suggest that the MEKK1-MKK1/2-MPK4 cascade may function down stream of BIK1, and the constitutive defense responses in *bik1* in part attributes from the disruption of this MAPK cascade.

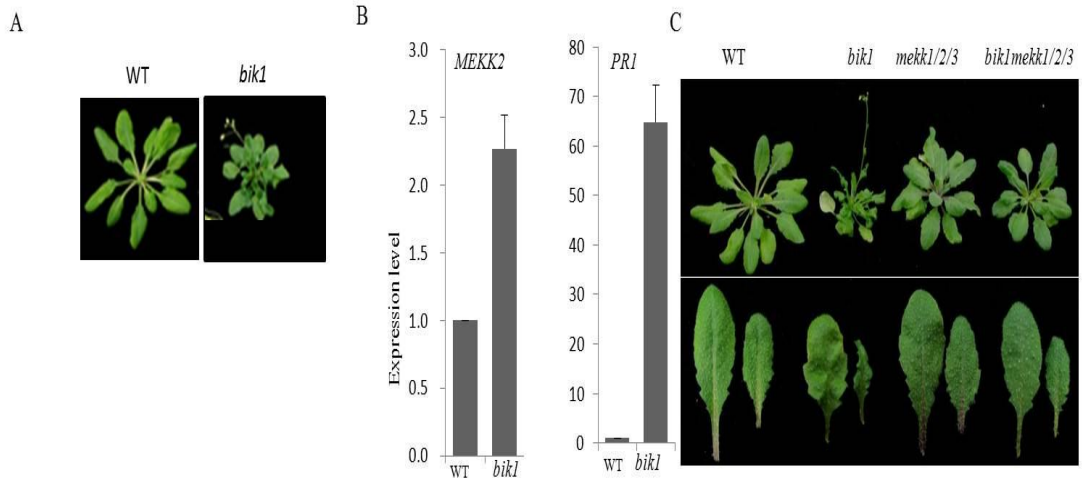

Figure 4. 6 The *mekk1/2/3* mutant partially restores growth defects of *bik1*.
(A) The *bik1* mutant exhibits semi-dwarf phenotypes. 4-week-old adult plants exhibit semi-dwarf phenotypes with smaller rosette, curling wrinkle leaves and early flowering compared to WT. (**B**) Elevated *MEKK2* and *PR1* expression level in *bik1*. Detection of the expression levels of *MEKK2* and *PR1* in 4-week-old WT and *bik1* plants. (**C**) The mekk1/2/3 deletion mutant partially restored bik1 growth deficient phenotypes. *mekk1/2/3* deletion partially restored plant size of (*Up panel*) and leaves morphology of *bik1* (*Bottom panel*).

Suppression of growth and defense response defect of bik1 by mekk1

To determine the genetic mechanism that result in the suppression of *bik1* phenotypes by *mekk1/2/3*, The *bik1mekk2*, *bik1summ2* and *bik1mekk1/summ2* mutants were generated by crossing. The *mekk1* mutant is seedling lethal, which could be suppressed by the *summ2* mutation (Zhang et al., 2012). To determine the genetic relationship between *bik1* and *mekk1*, the *bik1mekk1summ2 triple* mutant was generated. Neither *summ2* nor *mekk2* is capable of suppressing *bik1* growth phenotypes (Fig 4.6 A), whereas, *mekk1/summ2* restored *bik1* growth defect to *bik1mekk1/2/3* level, including the rosette leaf size and morphology (Fig 4.6 B and C). The *mekk1/summ2*, *mekk1/2/3* and *sid2* mutations rescued the wrinkle and curing leaves of *bik1* back to WT level (Fig 4.6 C), whereas *bik1summ2* or *bik1mekk2* exhibited similar leaf morphology as *bik1* (Fig 4.6 C). BIK1 was previously shown to be required for flg22-induced ROS production by directly phosphorylating RobhD (Li et al., 2014b; Lin et al., 2014), and the *bik1* mutant is significantly compromised in the flg22-induced ROS production compared to WT. To determine whether the *mekk1* mutation could affect the defect of ROS production in the *bik1* mutant, I detected the flg22-induced ROS production in the *bik1mekk1/summ2* mutant. The *bik1* mutant largely suppressed flg22-induced ROS production, whereas *mekk1/2/3* and *mekk1/summ2* relieved this suppression in *bik1*, but not *mekk2* or *summ2* mutation, indicating that MEKK1 functions genetically downstream of BIK1, and negatively regulated by BIK1 in growth and flg22-induced ROS production.

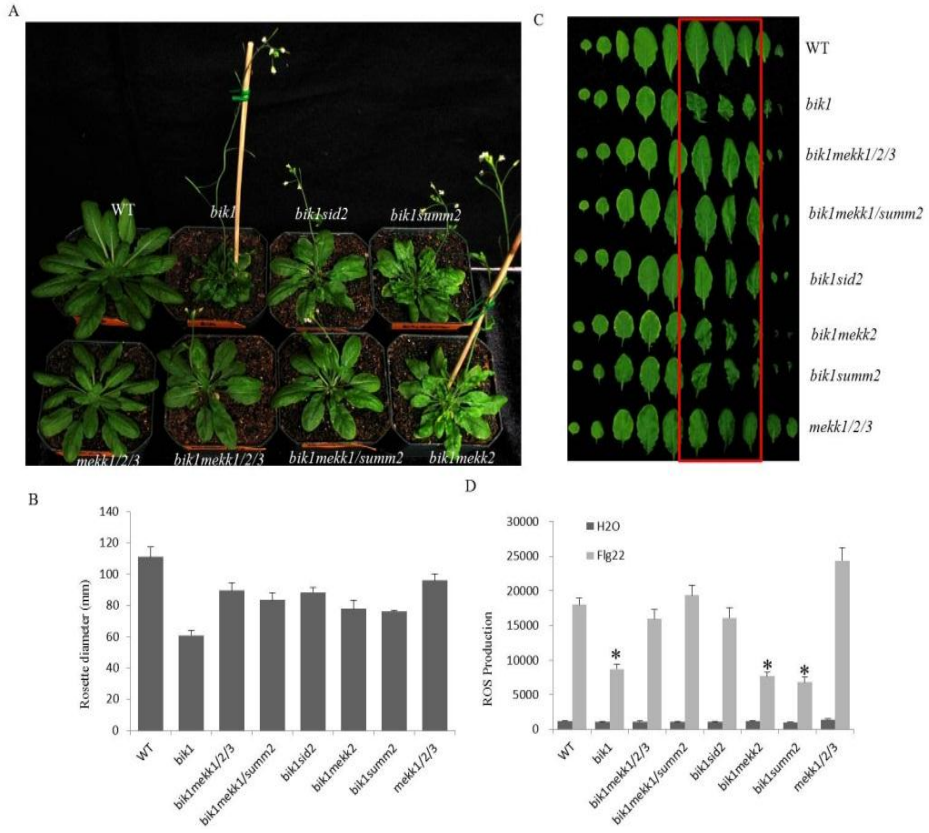

Figure 4. 7 Partial suppression of *bik1* mutant phenotypes by *mekk1*.
(**A**) Morphologies of the WT, *bik1, bik1sid2, bik1summ2, bik1mekk2, bik1mekk1/2/3 and mekk1/2/3.* The photograph shows 5-week-old soil-grown plants. (**B**) The diameter of rosette leaf of WT, *bik1, bik1sid2, bik1summ2, bik1mekk2, bik1mekk1/2/3 and mekk1/2/3.* The leaf diameters of 5-week-old soil-grown plants were measured. Mean values of diameter are presented ±SE for at least 15 replicates. (**C**) The leaf morphology of WT, *bik1, bik1sid2, bik1summ2, bik1mekk2, bik1mekk1/2/3 and mekk1/2/3.* Red box indicated the central matured leaves in different genotypes. (D) flg22-induced oxidative burst in WT, *bik1, bik1sid2, bik1summ2, bik1mekk2, bik1mekk1/2/3 and mekk1/2/3.* ROS production in response to 100 nM flg22 from leaf discs of 5-week-old plants was measured and presented as total photon counts during 30 min of treatment. Values presented are mean ± SE (n=36) and * indicates a significant difference with $p<0.05$ established by a one-way ANOVA when compare with data from WT Col-0 plants.

BIK1 associates with MEKK1

Next we examined whether BIK1 could associate with MEKK1. I performed a co-immunoprecipitation (Co-IP) assay with co-expressing HA-tagged MEKK1 and FLAG-tagged BIK1 in *Arabidopsis* protoplasts. Clearly, BIK1 co-immunoprecipitated MEKK1

in vivo, and the association of BIK1 and MEKK1 was not affected by flg22 treatment (Fig. 4.7 A). To confirm this association, I further performed a bimolecular fluorescence complementation (BiFC) assay with co-expression of MEKK1 fused to the carboxyl-terminal half of YFP (yellow fluorescence protein) (MEKKK1-cYFP) and BIK1 fused to the amino-terminal half of YFP (BIK1-nYFP) in protoplasts. The BiFC indicated that BIK1 associated with MEKK1 on the plasma membrane (Fig 4.7 B). Taken together, these data indicate that BIK1 likely associates with MEKK1 on the plasma membrane.

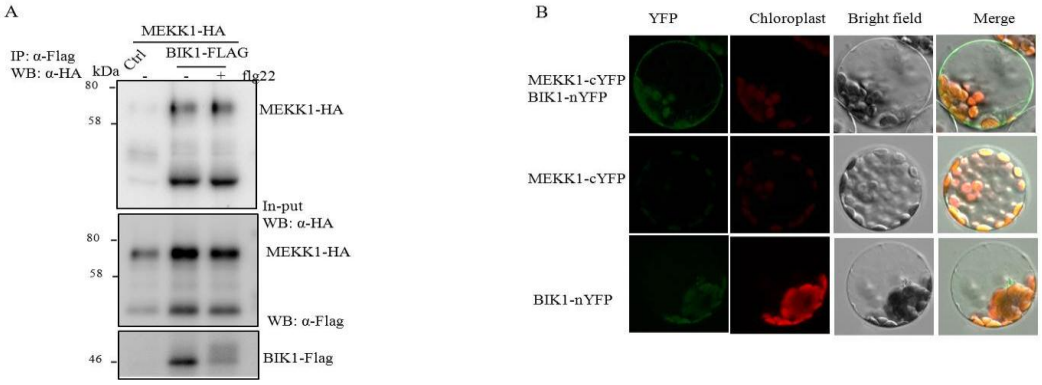

Figure 4. 8 BIK1 associates with MEKK1.
(A) BIK1 associates with MEKK1 in protoplasts. BIK1-FLAG was co-expressed with MEKK1-HA in Arabidopsis protoplasts. Co-IP was carried out with an α-FLAG affinity gel (IP:α-FLAG), and the proteins were analyzed by using Western blot with α-HA antibody. Top shows that BIK1-FLAG co-immunoprecipitate with MEKK1-HA (IP:α-FLAG, WB:α-HA). Middle and bottom show the expression of MEKK1-HA and BIK1-FLAG proteins (WB:α-HA or WB:α-FLAG for input control). Protoplasts were treated with 100nM flg22 for 15 mints. (B) BIK1 associates with MEKK1 in BiFC assay in *Arabidopsis* protoplasts. Various combination of BiFC constructs were transfected into protoplasts, and reconstituted YFP signals were observed under a confocal microscope.

Discussion

The molecular mechanisms underlying how the immune signaling from PRR complexes is relayed to downstream MAPK cascades remain enigmatic. BIK1 associates

with and is phosphorylated by the FLS2-BAK1 complex. Phosphorylated BIK1 is required for flg22-induced PTI responses, including ROS production and calcium flux (Lu et al., 2010; Zhang et al., 2010). It remains unknown whether and how BIK1 phosphorylation is connected to MAPK activation. I have previously shown that constitutive activation of MEKK1 and MKK5 could not induce the phosphorylation of BIK1, indicating that BIK1 functions in either upstream MAPK cascades or independently of MAPK signaling (Lu et al., 2010). It has been reported that, *Xanthomonas* effector AvrAC, a uridine 5'-monophosphate transferase, inhibits plant innate immunity by adding uridine 5'-monophosphate to BIK1 and PBL1, thus blocking conserved phosphorylation sites in the activation loop of BIK1 and PBL1, thereby reducing kinase activity of BIK1 and subsequent inhibition of downstream signaling, including activation of MPK3/MPK6 and MPK4 cascades (Feng et al., 2012). The data indicate that BIK1 may function redundantly with other PBL upstream MAPK cascade. Moreover, recent studies showed that OsRLCK185 and OsRLCK176, the PBL27 and BIK1 orthologs in rice, are involved in OsCERK1-mediated PTI signaling upstream of MAPK cascades (Ao et al., 2014; Yamaguchi et al., 2013). OsCERK1 is required for PGN- and chitin-triggered immune responses. OsRLCK185 and OsRLCK176 belong to the RLCK VII subfamily. OsRLCK185 and OsRLCK176 associate with OsCERK1, and are released from the complex upon chitin or PGN perception, similar to BIK1 releasement from the FLS2 complex upon flg22 perception (Ao et al., 2014; Yamaguchi et al., 2013). Knock down of *OsRLCK176* and *OsRLCK185* led to attenuation of chitin- and PGN-triggered MAPK activation, indicating their requirement for MAPK activation

in chitin- and PGN-induced immune signaling. PBL27 is an ortholog of OsRLCK185 in *Arabidopsis*, which has been shown to exhibit similar function with that of OsRLCK185, and is involved in chitin-induced CERK1-dependent signaling (Shinya et al., 2014; Yamaguchi et al., 2013). Knockout of PBL27 resulted in suppression of CERK-mediated immune responses, including the activation of MPK3/6 and callose deposition. In contrast, PBL27 has very limit contribution to FLS2-mediated immune signaling, suggesting that PBL27 selectively relays immune signaling downstream of CERK1 complexes. Despite the fact that the ortholog of BIK1 in rice, OsRLCK176 has been shown to be required for chitin-induced MAPK activation in rice (Shinya et al., 2014), *bik1* mutant has no obvious effect on flg22-induced MAPK activation in *Arabidopsis*. However, in line with previous findings, I found transient expression of BIK1 is capable of inducing the expression of MAPK specific regulated gene, *FRK1* (Fig 4.2A). Moreover, transient expression of BIK1 induced MAPK activation as well in Arabidopsis protoplasts (Fig 4.2B), indicating that BIK1 is likely to function of upstream MAPK cascades. In fact, knockout of BIK1 along with the homologs, PBL1 and NAK1 result in significant impairment of multiple PAMP-induced MAPK activation, indicating that BIK1, PBL1 and NAK1 function redundantly to relay the signal from PRR complexes to downstream MAPK cascades. I have previously shown that Y150F substitution of BIK1 result in loss of function of BIK1, which led to kinase inactive form of BIK1 (Lin et al., 2014). In this study, I found that Y150F mutation of BIK1 dominantly inhibits flg22/elf18-induced MAPK activation, indicating that the activated

BIK1 kinase positively regulated the PTI signaling from receptor complexes to MAPK cascades.

MEKK1-MKK1/2-MPK4 and MEKK1/?-MKK4/5-MPK3/6 cascades play an important role in relaying PTI signaling to intracellular. The MPK4 cascade was surveilled by R protein SUMM2, therefore disruption of the cascades results in the activation of defense responses, including PR1 induction and accumulation of SA. Loss-of-function of MEKK1, MKK1/2 or MPK4 all results in auto immune responses in plants, which exhibited seedling lethality with high *PR1* expression and SA accumulation. However, mutation on SUMM2 or MEKK2 suppresses the seedling lethality as well as *PR1* expression in *mekk1*, *mkk1/2* and *mpk4* mutants. I therefore cross *bik1* to *mekk1/2/3* mutant to further investigate the genetic relationship between BIK1 and MAPK cascades. The *mekk1/2/3* mutation is capable of suppressing *bik1* semi-dwarfed phenotypes. However, further genetic study revealed that this suppression is contributed by the *mekk1* mutation, but not *mekk2* or *summ2*. This is different from the MEKK1-MKK1/2-MPK4-MEKK2-SUMM2 pathway study, indicating that loss-of-function of BIK1 did not disrupt the MEKK2-SUMM2 surveillance pathway. The *MEKK2* expression level was about 2-fold higher in *bik1* mutant when compared to WT. However, this may not confer to the semi-dwarfed morphology of *bik1* as it was reported that the *mekk2* mutant, which has a T-DNA insertion in the promoter region, is capable of suppressing the elevated *MEKK2* in *mekk1* and *mpk4* therefore restoring growth defects, but the *mekk2* mutant processes about 2-folds higher *MEKK2* transcript level with normal growth phenotypes (Su et al., 2013). Thus, it is likely that the elevated

MEKK2 is not sufficient to trigger SUMM2-mediated immune responses leading to semi-dwarfed phenotypes of the *bik1* mutant.

There are two flg22-induced MAPK cascades in Arabidopsis. MEKK1 was reported to mediate the MKK4/5-MPK3/6 cascade upon stimulation of flg22. There are redundant homologs of MEKK1 in the flg22-induced MPK3/6 activation, and MEKK1 may function as a scaffold in MAPK cascades, similar as Ste11 function in yeast signaling pathway (Kim et al., 1998; Kwan et al., 2004). Recently, RACK1 (receptor for activated C kinase 1) was proposed to function as a scaffold that binds to the G β subunit as well as to all three tiers of the MAPK cascade, including MEKK1, MKK4/5 and MPK3/6 (Zhenyu Cheng, et al., 2015). My co-immunoprecipitation and BiFC assays indicated that BIK1 likely associates with MEKK1.

This work has demonstrated that BIK1 together with the closest homologs PBL1 and NAK1 are involved in MEKK1-mediated MAPK cascades and BIK1 is required for PAMP-induced MPK3/4/6 activation in Arabidopsis. BIK1 functions upstream MEKK1 and associates with MEKK1. These finding demonstrate that BIK1 likely bridges between PRRs and MAPK cascades by associating with both the PRRs complex and MEKK, to relay PAMP signaling from the receptor complex into intercellular signaling networks.

CHAPTER V

CONCLUSION

The dimerization and phosphorylation of receptor-like cytoplasmic kinases (RLCKs) in the receptor complex constitute essential steps to initiate immune signaling. BIK1 was classically defined as a serine/threonine protein kinase and many serine/threonine residues are required for BIK1 functions. Surprisingly, our mass spectrometry analysis revealed that BIK1 also possesses tyrosine kinase activity, suggesting that BIK1 is a dual-specificity kinase. BIK1 is auto-phosphorylated and trans-phosphorylated by BAK1 at multiple tyrosine residues. Mutational and transgenic analyses support the vital role of tyrosine phosphorylation in BIK1-mediated plant innate immunity as certain BIK1 tyrosine mutations were no longer able to complement the *bik1* mutant plant-associated compromised immune responses.

The essential function of tyrosine kinase activity of non-receptor kinase BIK1 in plant immune signaling echoes a parallel signaling pathway mediated by membrane-resident receptor tyrosine kinase (RTK) in metazoans. RTK signaling is typically initiated via dimerization and phosphorylation of downstream non-receptor tyrosine kinases. Recently, *Arabidopsis* RLKs BRI1 and BAK1 were also found to possess tyrosine kinase activity in addition to serine/threonine kinase activity. Thus, although lack of classical tyrosine kinases, tyrosine phosphorylation cascade mediated by plant RLKs and RLCKs is an important regulatory mechanism that controls membrane-resident receptor signaling.

MAPK activation is one of the earliest immune responses upon the recognition of PAMPs. MAPK activation plays a vital role in intercellular signal transduction to regulate the immune related gene expression. However, the molecular mechanisms of how signals transduce from receptor complex to MAPK cascades remains largely unknown. This work has demonstrated that BIK1 together with its closest homologs PBL1 and NAK1 are involved in MEKK1-mediated MAPK cascades and BIK1 is required for PAMP-induced MPK3/4/6 activation in Arabidopsis. BIK1 functions upstream MEKK1 and associates with MEKK1. These findings demonstrate that BIK1 likely bridges between PRRs and MAPK cascades by associating with both the PRRs complex and MEKK, to relay PAMP signaling from the receptor complex into intercellular signaling networks.

Plants have evolved sophisticated mechanisms to deal with diverse and complex environmental conditions via balancing growth and defense. In this study, I showed that in contrast to its positive roles in plant immune signaling, BIK1 negatively regulates BR signaling. The *bik1* mutants are more sensitive to BL treatment and more resistant to the BR synthesis inhibitor BRZ. BIK1 associates with BRI1 on the plasma membrane, and dissociates from the BRI1 complex upon the recognition of BL, likely as a consequence of being phosphorylated by BRI1. In flagellin signaling, BIK1 is phosphorylated by BAK1 in mediating immune signaling. In contrast, in BR signaling, BIK1 is directly phosphorylated by BRI1 to suppress BR signaling. These studies indicated that BIK1 plays distinct and complex roles in plant development and immunity via differential phosphorylation and dynamic association with distinct receptor complexes. Future

studies on the identification of specific phosphorylation sites of BIK1 and characterization of their biological function in BR- and flagellin-mediated signaling will provide insights on how this small kinase plays complex roles in diverse cellular and physiological responses.

REFERENCES

Albrecht, C., Boutrot, F., Segonzac, C., Schwessinger, B., Gimenez-Ibanez, S., Chinchilla, D., Rathjen, J.P., de Vries, S.C., and Zipfel, C. (2012). Brassinosteroids inhibit pathogen-associated molecular pattern-triggered immune signaling independent of the receptor kinase BAK1. Proc Natl Acad Sci U S A *109*, 303-308.

Andreasson, E., Jenkins, T., Brodersen, P., Thorgrimsen, S., Petersen, N.H., Zhu, S., Qiu, J.L., Micheelsen, P., Rocher, A., Petersen, M., *et al.* (2005). The MAP kinase substrate MKS1 is a regulator of plant defense responses. The EMBO Journal *24*, 2579-2589.

Antolin-Llovera, M., Ried, M.K., Binder, A., and Parniske, M. (2012). Receptor kinase signaling pathways in plant-microbe interactions. Annu Rev Phytopathol *50*, 451-473.

Ao, Y., Li, Z., Feng, D., Xiong, F., Liu, J., Li, J.F., Wang, M., Wang, J., Liu, B., and Wang, H.B. (2014). OsCERK1 and OsRLCK176 play important roles in peptidoglycan and chitin signaling in rice innate immunity. The Plant Journal : for cell and molecular biology *80*, 1072-1084.

Asai, T., Tena, G., Plotnikova, J., Willmann, M.R., Chiu, W.L., Gomez-Gomez, L., Boller, T., Ausubel, F.M., and Sheen, J. (2002). MAP kinase signalling cascade in Arabidopsis innate immunity. Nature *415*, 977-983.

Belkhadir, Y., Jaillais, Y., Epple, P., Balsemao-Pires, E., Dangl, J.L., and Chory, J. (2012). Brassinosteroids modulate the efficiency of plant immune responses to microbe-associated molecular patterns. Proc Natl Acad Sci U S A *109*, 297-302.

Boller, T., and Felix, G. (2009). A renaissance of elicitors: perception of microbe-associated molecular patterns and danger signals by pattern-recognition receptors. Annu Rev Plant Biol *60*, 379-406.

Boller, T., and He, S.Y. (2009). Innate immunity in plants: an arms race between pattern recognition receptors in plants and effectors in microbial pathogens. Science *324*, 742-744.

Boudsocq, M., Willmann, M.R., McCormack, M., Lee, H., Shan, L., He, P., Bush, J., Cheng, S.H., and Sheen, J. (2010). Differential innate immune signalling via Ca(2+) sensor protein kinases. Nature *464*, 418-422.

Chaudhary, A., Fresquez, T.M., and Naranjo, M.J. (2007). Tyrosine kinase Syk associates with toll-like receptor 4 and regulates signaling in human monocytic cells. Immunology and Cell Biology *85*, 249-256.

Chinchilla, D., Shan, L., He, P., de Vries, S., and Kemmerling, B. (2009). One for all: the receptor-associated kinase BAK1. Trends Plant Sci *14*, 535-541.

Chinchilla, D., Zipfel, C., Robatzek, S., Kemmerling, B., Nurnberger, T., Jones, J.D., Felix, G., and Boller, T. (2007). A flagellin-induced complex of the receptor FLS2 and BAK1 initiates plant defence. Nature *448*, 497-500.

Chisholm, S.T., Coaker, G., Day, B., and Staskawicz, B.J. (2006a). Host-microbe interactions: shaping the evolution of the plant immune response. Cell *124*, 803-814.

Collier, S.M., and Moffett, P. (2009). NB-LRRs work a "bait and switch" on pathogens. Trends in Plant Science *14*, 521-529.

Demmel, L., Beck, M., Klose, C., Schlaitz, A.L., Gloor, Y., Hsu, P.P., Havlis, J., Shevchenko, A., Krause, E., Kalaidzidis, Y., *et al.* (2008). Nucleocytoplasmic shuttling of the Golgi phosphatidylinositol 4-kinase Pik1 is regulated by 14-3-3 proteins and coordinates Golgi function with cell growth. Mol Biol Cell *19*, 1046-1061.

DeYoung, B.J., and Innes, R.W. (2006). Plant NBS-LRR proteins in pathogen sensing and host defense. Nature Immunology *7*, 1243-1249.

Dodds, P.N., and Rathjen, J.P. (2010). Plant immunity: towards an integrated view of plant-pathogen interactions. Nature Reviews Genetics *11*, 539-548.

Eitas, T.K., and Dangl, J.L. (2010). NB-LRR proteins: pairs, pieces, perception, partners, and pathways. Current Opinion in Plant Biology *13*, 472-477.

Elmore, J.M., Lin, Z.J., and Coaker, G. (2011). Plant NB-LRR signaling: upstreams and downstreams. Current Opinion in Plant Biology *14*, 365-371.

Feng, F., Yang, F., Rong, W., Wu, X., Zhang, J., Chen, S., He, C., and Zhou, J.M. (2012). A Xanthomonas uridine 5'-monophosphate transferase inhibits plant immune kinases. Nature *485*, 114-118.

Gao, M., Liu, J., Bi, D., Zhang, Z., Cheng, F., Chen, S., and Zhang, Y. (2008). MEKK1, MKK1/MKK2 and MPK4 function together in a mitogen-activated protein kinase cascade to regulate innate immunity in plants. Cell Research *18*, 1190-1198.

Gao, X., Chen, X., Lin, W., Chen, S., Lu, D., Niu, Y., Li, L., Cheng, C., McCormack, M., Sheen, J., *et al.* (2013). Bifurcation of Arabidopsis NLR immune signaling via Ca(2)(+)-dependent protein kinases. Plos Pathog *9*, e1003127.

Gomez-Gomez, L., and Boller, T. (2000). FLS2: an LRR receptor-like kinase involved in the perception of the bacterial elicitor flagellin in Arabidopsis. Mol Cell *5*, 1003-1011.

Gou, X., Yin, H., He, K., Du, J., Yi, J., Xu, S., Lin, H., Clouse, S.D., and Li, J. (2012). Genetic evidence for an indispensable role of somatic embryogenesis receptor kinases in brassinosteroid signaling. PLoS Genet *8*, e1002452.

He, K., Gou, X., Yuan, T., Lin, H., Asami, T., Yoshida, S., Russell, S.D., and Li, J. (2007). BAK1 and BKK1 regulate brassinosteroid-dependent growth and brassinosteroid-independent cell-death pathways. Curr Biol *17*, 1109-1115.

Heese, A., Hann, D.R., Gimenez-Ibanez, S., Jones, A.M., He, K., Li, J., Schroeder, J.I., Peck, S.C., and Rathjen, J.P. (2007a). The receptor-like kinase SERK3/BAK1 is a central regulator of innate immunity in plants. Proc Natl Acad Sci U S A *104*, 12217-12222.

Hothorn, M., Belkhadir, Y., Dreux, M., Dabi, T., Noel, J.P., Wilson, I.A., and Chory, J. (2011). Structural basis of steroid hormone perception by the receptor kinase BRI1. Nature *474*, 467-471.

Ichimura, K., Casais, C., Peck, S.C., Shinozaki, K., and Shirasu, K. (2006). MEKK1 is required for MPK4 activation and regulates tissue-specific and temperature-dependent cell death in Arabidopsis. The Journal of Biological Chemistry *281*, 36969-36976.

Jaillais, Y., Hothorn, M., Belkhadir, Y., Dabi, T., Nimchuk, Z.L., Meyerowitz, E.M., and Chory, J. (2011). Tyrosine phosphorylation controls brassinosteroid receptor activation by triggering membrane release of its kinase inhibitor. Genes Dev *25*, 232-237.

Jones, J.D., and Dangl, J.L. (2006a). The plant immune system. Nature *444*, 323-329.

Kadota, Y., Sklenar, J., Derbyshire, P., Stransfeld, L., Asai, S., Ntoukakis, V., Jones, J.D., Shirasu, K., Menke, F., Jones, A., *et al.* (2014). Direct regulation of the NADPH oxidase RBOHD by the PRR-associated kinase BIK1 during plant immunity. Molecular Cell *54*, 43-55.

Karlova, R., Boeren, S., Russinova, E., Aker, J., Vervoort, J., and de Vries, S. (2006). The Arabidopsis somatic embryogenesis receptor KINASE1 protein complex includes BRASSINOSTEROID-INSENSITIVE1. Plant Cell *18*, 626-638.

Kemmerling, B., Schwedt, A., Rodriguez, P., Mazzotta, S., Frank, M., Qamar, S.A., Mengiste, T., Betsuyaku, S., Parker, J.E., Mussig, C., *et al.* (2007). The BRI1-associated kinase 1, BAK1, has a brassinolide-independent role in plant cell-death control. Curr Biol *17*, 1116-1122.

Kim, M.G., da Cunha, L., McFall, A.J., Belkhadir, Y., DebRoy, S., Dangl, J.L., and Mackey, D. (2005). Two Pseudomonas syringae type III effectors inhibit RIN4-regulated basal defense in Arabidopsis. Cell *121*, 749-759.

Kim, S.H., Lee, S.K., and Choi, K.Y. (1998). *Saccharomyces cerevisiae* STE11 may contribute to the stabilities of a scaffold protein, STE5, in the pheromone signaling pathway. Molecules and Cells *8*, 130-137.

Kim, T.W., Guan, S., Burlingame, A.L., and Wang, Z.Y. (2011). The CDG1 kinase mediates brassinosteroid signal transduction from BRI1 receptor kinase to BSU1 phosphatase and GSK3-like kinase BIN2. Mol Cell *43*, 561-571.

Kim, T.W., Guan, S., Sun, Y., Deng, Z., Tang, W., Shang, J.X., Burlingame, A.L., and Wang, Z.Y. (2009). Brassinosteroid signal transduction from cell-surface receptor kinases to nuclear transcription factors. Nat Cell Biol *11*, 1254-1260.

Kong, Q., Qu, N., Gao, M., Zhang, Z., Ding, X., Yang, F., Li, Y., Dong, O.X., Chen, S., Li, X., *et al.* (2012). The MEKK1-MKK1/MKK2-MPK4 kinase cascade negatively regulates immunity mediated by a mitogen-activated protein kinase kinase kinase in Arabidopsis. The Plant cell *24*, 2225-2236.

Korasick, D.A., McMichael, C., Walker, K.A., Anderson, J.C., Bednarek, S.Y., and Heese, A. (2010). Novel Functions of Stomatal Cytokinesis-Defective 1 (SCD1) in Innate Immune Responses against Bacteria. J Biol Chem *285*, 23340-23348.

Kwan, J.J., Warner, N., Pawson, T., and Donaldson, L.W. (2004). The solution structure of the S.cerevisiae Ste11 MAPKKK SAM domain and its partnership with Ste50. Journal of Molecular Biology *342*, 681-693.

Laluk, K., Luo, H., Chai, M., Dhawan, R., Lai, Z., and Mengiste, T. (2011). Biochemical and genetic requirements for function of the immune response regulator BOTRYTIS-INDUCED KINASE1 in plant growth, ethylene signaling, and PAMP-triggered immunity in Arabidopsis. Plant Cell *23*, 2831-2849.

Lee, J.S., Kuroha, T., Hnilova, M., Khatayevich, D., Kanaoka, M.M., McAbee, J.M., Sarikaya, M., Tamerler, C., and Torii, K.U. (2012). Direct interaction of ligand-receptor pairs specifying stomatal patterning. Genes Dev *26*, 126-136.

Lemmon, M.A., and Schlessinger, J. (2010). Cell signaling by receptor tyrosine kinases. Cell *141*, 1117-1134.

Li, B., Jiang, S., Yu, X., Cheng, C., Chen, S., Cheng, Y., Yuan, J.S., Jiang, D., He, P., and Shan, L. (2015). Phosphorylation of trihelix transcriptional repressor ASR3 by MAP KINASE4 negatively regulates Arabidopsis immunity. The Plant Cell *27*, 839-856.

Li, F., Cheng, C., Cui, F., de Oliveira, M.V., Yu, X., Meng, X., Intorne, A.C., Babilonia, K., Li, M., Li, B., *et al.* (2014a). Modulation of RNA polymerase II phosphorylation downstream of pathogen perception orchestrates plant immunity. Cell host & microbe *16*, 748-758.

Li, J., and Chory, J. (1997). A putative leucine-rich repeat receptor kinase involved in brassinosteroid signal transduction. Cell *90*, 929-938.

Li, J., and Nam, K.H. (2002). Regulation of brassinosteroid signaling by a GSK3/SHAGGY-like kinase. Science *295*, 1299-1301.

Li, J., Wen, J., Lease, K.A., Doke, J.T., Tax, F.E., and Walker, J.C. (2002). BAK1, an Arabidopsis LRR receptor-like protein kinase, interacts with BRI1 and modulates brassinosteroid signaling. Cell *110*, 213-222.

Li, L., Li, M., Yu, L., Zhou, Z., Liang, X., Liu, Z., Cai, G., Gao, L., Zhang, X., Wang, Y., *et al.* (2014b). The FLS2-associated kinase BIK1 directly phosphorylates the NADPH oxidase RbohD to control plant immunity. Cell host & microbe *15*, 329-338.

Li, M., Ma, X., Chiang, Y.H., Yadeta, K.A., Ding, P., Dong, L., Zhao, Y., Li, X., Yu, Y., Zhang, L., *et al.* (2014c). Proline isomerization of the immune receptor-interacting protein RIN4 by a cyclophilin inhibits effector-triggered immunity in Arabidopsis. Cell host & microbe *16*, 473-483.

Lin, W., Li, B., Lu, D., Chen, S., Zhu, N., He, P., and Shan, L. (2014). Tyrosine phosphorylation of protein kinase complex BAK1/BIK1 mediates Arabidopsis innate immunity. Proceedings of the National Academy of Sciences of the United States of America *111*, 3632-3637.

Lin, W., Lu, D., Gao, X., Jiang, S., Ma, X., Wang, Z., Mengiste, T., He, P., and Shan, L. (2013a). Inverse modulation of plant immune and brassinosteroid signaling pathways by the receptor-like cytoplasmic kinase BIK1. Proceedings of the National Academy of Sciences of the United States of America *110*, 12114-12119.

Lin, Y.C., Huang, D.Y., Chu, C.L., Lin, Y.L., and Lin, W.W. (2013b). The tyrosine kinase Syk differentially regulates toll-like receptor signaling downstream of the adaptor molecules TRAF6 and TRAF3. Sci Signal *6*, ra71.

Liu, Z., Wu, Y., Yang, F., Zhang, Y., Chen, S., Xie, Q., Tian, X., and Zhou, J.M. (2013). BIK1 interacts with PEPRs to mediate ethylene-induced immunity. Proc Natl Acad Sci U S A *110*, 6205-6210.

Lu, D., Lin, W., Gao, X., Wu, S., Cheng, C., Avila, J., Heese, A., Devarenne, T.P., He, P., and Shan, L. (2011). Direct ubiquitination of pattern recognition receptor FLS2 attenuates plant innate immunity. Science *332*, 1439-1442.

Lu, D., Wu, S., Gao, X., Zhang, Y., Shan, L., and He, P. (2010). A receptor-like cytoplasmic kinase, BIK1, associates with a flagellin receptor complex to initiate plant innate immunity. Proc Natl Acad Sci U S A *107*, 496-501.

MacDonald, B.T., Tamai, K., and He, X. (2009). Wnt/beta-catenin signaling: components, mechanisms, and diseases. Dev Cell *17*, 9-26.

Maekawa, T., Kufer, T.A., and Schulze-Lefert, P. (2011). NLR functions in plant and animal immune systems: so far and yet so close. Nature immunology *12*, 817-826.

Monaghan, J., and Zipfel, C. (2012). Plant pattern recognition receptor complexes at the plasma membrane. Curr Opin Plant Biol *15*, 349-357.

Nakagami, H., Soukupova, H., Schikora, A., Zarsky, V., and Hirt, H. (2006). A Mitogen-activated protein kinase kinase kinase mediates reactive oxygen species homeostasis in Arabidopsis. The Journal of Biological Chemistry *281*, 38697-38704.

Nakashita, H., Yasuda, M., Nitta, T., Asami, T., Fujioka, S., Arai, Y., Sekimata, K., Takatsuto, S., Yamaguchi, I., and Yoshida, S. (2003). Brassinosteroid functions in a broad range of disease resistance in tobacco and rice. Plant J *33*, 887-898.

Nam, K.H., and Li, J. (2002). BRI1/BAK1, a receptor kinase pair mediating brassinosteroid signaling. Cell *110*, 203-212.

Ntoukakis, V., Saur, I.M., Conlan, B., and Rathjen, J.P. (2014). The changing of the guard: the Pto/Prf receptor complex of tomato and pathogen recognition. Current Opinion in Plant Biology *20*, 69-74.

Oh, M.H., Wang, X., Clouse, S.D., and Huber, S.C. (2012). Deactivation of the Arabidopsis BRASSINOSTEROID INSENSITIVE 1 (BRI1) receptor kinase by autophosphorylation within the glycine-rich loop. Proc Natl Acad Sci U S A *109*, 327-332.

Oh, M.H., Wang, X., Kota, U., Goshe, M.B., Clouse, S.D., and Huber, S.C. (2009). Tyrosine phosphorylation of the BRI1 receptor kinase emerges as a component of brassinosteroid signaling in Arabidopsis. Proc Natl Acad Sci U S A *106*, 658-663.

Oh, M.H., Wang, X., Wu, X., Zhao, Y., Clouse, S.D., and Huber, S.C. (2010). Autophosphorylation of Tyr-610 in the receptor kinase BAK1 plays a role in brassinosteroid signaling and basal defense gene expression. Proc Natl Acad Sci U S A *107*, 17827-17832.

Peng, P., Zhao, J., Zhu, Y., Asami, T., and Li, J. (2010). A direct docking mechanism for a plant GSK3-like kinase to phosphorylate its substrates. J Biol Chem *285*, 24646-24653.

Petersen, M., Brodersen, P., Naested, H., Andreasson, E., Lindhart, U., Johansen, B., Nielsen, H.B., Lacy, M., Austin, M.J., Parker, J.E., *et al.* (2000). Arabidopsis map kinase 4 negatively regulates systemic acquired resistance. Cell *103*, 1111-1120.

Postel, S., Kufner, I., Beuter, C., Mazzotta, S., Schwedt, A., Borlotti, A., Halter, T., Kemmerling, B., and Nurnberger, T. (2010). The multifunctional leucine-rich

repeat receptor kinase BAK1 is implicated in Arabidopsis development and immunity. Eur J Cell Biol *89*, 169-174.

Qiu, J.L., Zhou, L., Yun, B.W., Nielsen, H.B., Fiil, B.K., Petersen, K., Mackinlay, J., Loake, G.J., Mundy, J., and Morris, P.C. (2008). Arabidopsis mitogen-activated protein kinase kinases MKK1 and MKK2 have overlapping functions in defense signaling mediated by MEKK1, MPK4, and MKS1. Plant Physiology *148*, 212-222.

Rodriguez, M.C., Petersen, M., and Mundy, J. (2010). Mitogen-activated protein kinase signaling in plants. Annual Review of Plant Biology *61*, 621-649.

Roux, M., Schwessinger, B., Albrecht, C., Chinchilla, D., Jones, A., Holton, N., Malinovsky, F.G., Tor, M., de Vries, S., and Zipfel, C. (2011a). The Arabidopsis leucine-rich repeat receptor-like kinases BAK1/SERK3 and BKK1/SERK4 are required for innate immunity to hemibiotrophic and biotrophic pathogens. Plant Cell *23*, 2440-2455.

Roux, M., Schwessinger, B., Albrecht, C., Chinchilla, D., Jones, A., Holton, N., Malinovsky, F.G., Tor, M., de Vries, S., and Zipfel, C. (2011b). The Arabidopsis Leucine-Rich Repeat Receptor-Like Kinases BAK1/SERK3 and BKK1/SERK4 Are Required for Innate Immunity to Hemibiotrophic and Biotrophic Pathogens. Plant Cell *23*, 2440-2455.

Rushton, P.J., Somssich, I.E., Ringler, P., and Shen, Q.J. (2010). WRKY transcription factors. Trends Plant Sci *15*, 247-258.

Schulze, B., Mentzel, T., Jehle, A.K., Mueller, K., Beeler, S., Boller, T., Felix, G., and Chinchilla, D. (2010). Rapid heteromerization and phosphorylation of ligand-activated plant transmembrane receptors and their associated kinase BAK1. J Biol Chem *285*, 9444-9451.

Schwessinger, B., and Ronald, P.C. (2012). Plant innate immunity: perception of conserved microbial signatures. Annu Rev Plant Biol *63*, 451-482.

Schwessinger, B., Roux, M., Kadota, Y., Ntoukakis, V., Sklenar, J., Jones, A., and Zipfel, C. (2011). Phosphorylation-dependent differential regulation of plant growth, cell

death, and innate immunity by the regulatory receptor-like kinase BAK1. PLoS Genet *7*, e1002046.

Segonzac, C., Macho, A.P., Sanmartin, M., Ntoukakis, V., Sanchez-Serrano, J.J., and Zipfel, C. (2014). Negative control of BAK1 by protein phosphatase 2A during plant innate immunity. The EMBO Journal *33*, 2069-2079.

Shan, L., He, P., Li, J., Heese, A., Peck, S.C., Nurnberger, T., Martin, G.B., and Sheen, J. (2008). Bacterial effectors target the common signaling partner BAK1 to disrupt multiple MAMP receptor-signaling complexes and impede plant immunity. Cell Host & Microbe *4*, 17-27.

She, J., Han, Z., Kim, T.W., Wang, J., Cheng, W., Chang, J., Shi, S., Yang, M., Wang, Z.Y., and Chai, J. (2011). Structural insight into brassinosteroid perception by BRI1. Nature *474*, 472-476.

Shi, H., Shen, Q.J., Qi, Y.P., Yan, H.J., Nie, H.Z., Chen, Y.F., Zhao, T., Katagiri, F., and Tang, D.Z. (2013). BR-SIGNALING KINASE1 Physically Associates with FLAGELLIN SENSING2 and Regulates Plant Innate Immunity in Arabidopsis. Plant Cell *25*, 1143-1157.

Shinya, T., Yamaguchi, K., Desaki, Y., Yamada, K., Narisawa, T., Kobayashi, Y., Maeda, K., Suzuki, M., Tanimoto, T., Takeda, J., *et al.* (2014). Selective regulation of the chitin-induced defense response by the Arabidopsis receptor-like cytoplasmic kinase PBL27. The Plant Journal : for Cell and Molecular Biology *79*, 56-66.

Shiu, S.H., and Bleecker, A.B. (2001). Receptor-like kinases from Arabidopsis form a monophyletic gene family related to animal receptor kinases. Proc Natl Acad Sci U S A *98*, 10763-10768.

Shiu, S.H., and Bleecker, A.B. (2003). Expansion of the receptor-like kinase/Pelle gene family and receptor-like proteins in Arabidopsis. Plant Physiol *132*, 530-543.

Spoel, S.H., and Dong, X. (2012). How do plants achieve immunity? Defence without specialized immune cells. Nature Reviews Immunology *12*, 89-100.

Su, S.H., Bush, S.M., Zaman, N., Stecker, K., Sussman, M.R., and Krysan, P. (2013). Deletion of a tandem gene family in Arabidopsis: increased MEKK2 abundance triggers autoimmunity when the MEKK1-MKK1/2-MPK4 signaling cascade is disrupted. The Plant Cell *25*, 1895-1910.

Suarez-Rodriguez, M.C., Adams-Phillips, L., Liu, Y., Wang, H., Su, S.H., Jester, P.J., Zhang, S., Bent, A.F., and Krysan, P.J. (2007). MEKK1 is required for flg22-induced MPK4 activation in Arabidopsis plants. Plant Physiology *143*, 661-669.

Sun, Y., Fan, X.Y., Cao, D.M., Tang, W., He, K., Zhu, J.Y., He, J.X., Bai, M.Y., Zhu, S., Oh, E., *et al.* (2010). Integration of brassinosteroid signal transduction with the transcription network for plant growth regulation in Arabidopsis. Dev Cell *19*, 765-777.

Takeuchi, O., and Akira, S. (2010). Pattern recognition receptors and inflammation. Cell *140*, 805-820.

Tang, W., Kim, T.W., Oses-Prieto, J.A., Sun, Y., Deng, Z., Zhu, S., Wang, R., Burlingame, A.L., and Wang, Z.Y. (2008). BSKs mediate signal transduction from the receptor kinase BRI1 in Arabidopsis. Science *321*, 557-560.

Tena, G., Boudsocq, M., and Sheen, J. (2011). Protein kinase signaling networks in plant innate immunity. Current Opinion in Plant Biology *14*, 519-529.

Veronese, P., Nakagami, H., Bluhm, B., Abuqamar, S., Chen, X., Salmeron, J., Dietrich, R.A., Hirt, H., and Mengiste, T. (2006). The membrane-anchored BOTRYTIS-INDUCED KINASE1 plays distinct roles in Arabidopsis resistance to necrotrophic and biotrophic pathogens. The Plant Cell *18*, 257-273.

Wang, X., and Chory, J. (2006). Brassinosteroids regulate dissociation of BKI1, a negative regulator of BRI1 signaling, from the plasma membrane. Science *313*, 1118-1122.

Wang, X., Goshe, M.B., Soderblom, E.J., Phinney, B.S., Kuchar, J.A., Li, J., Asami, T., Yoshida, S., Huber, S.C., and Clouse, S.D. (2005a). Identification and functional

analysis of in vivo phosphorylation sites of the Arabidopsis BRASSINOSTEROID-INSENSITIVE1 receptor kinase. Plant Cell *17*, 1685-1703.

Wang, X., Kota, U., He, K., Blackburn, K., Li, J., Goshe, M.B., Huber, S.C., and Clouse, S.D. (2008a). Sequential transphosphorylation of the BRI1/BAK1 receptor kinase complex impacts early events in brassinosteroid signaling. Dev Cell *15*, 220-235.

Wang, X., Li, X., Meisenhelder, J., Hunter, T., Yoshida, S., Asami, T., and Chory, J. (2005b). Autoregulation and homodimerization are involved in the activation of the plant steroid receptor BRI1. Dev Cell *8*, 855-865.

Wang, X.F., Kota, U., He, K., Blackburn, K., Li, J., Goshe, M.B., Huber, S.C., and Clouse, S.D. (2008b). Sequential transphosphorylation of the BRI1/BAK1 receptor kinase complex impacts early events in brassinosteroid signaling. Dev Cell *15*, 220-235.

Wang, Z.Y., Nakano, T., Gendron, J., He, J., Chen, M., Vafeados, D., Yang, Y., Fujioka, S., Yoshida, S., Asami, T., *et al.* (2002). Nuclear-localized BZR1 mediates brassinosteroid-induced growth and feedback suppression of brassinosteroid biosynthesis. Dev Cell *2*, 505-513.

Wolf, S., Mravec, J., Greiner, S., Mouille, G., and Hofte, H. (2012). Plant cell wall homeostasis is mediated by brassinosteroid feedback signaling. Curr Biol *22*, 1732-1737.

Yamaguchi, K., Yamada, K., Ishikawa, K., Yoshimura, S., Hayashi, N., Uchihashi, K., Ishihama, N., Kishi-Kaboshi, M., Takahashi, A., Tsuge, S., *et al.* (2013). A receptor-like cytoplasmic kinase targeted by a plant pathogen effector is directly phosphorylated by the chitin receptor and mediates rice immunity. Cell Host & Microbe *13*, 347-357.

Yan, Z., Zhao, J., Peng, P., Chihara, R.K., and Li, J. (2009). BIN2 functions redundantly with other Arabidopsis GSK3-like kinases to regulate brassinosteroid signaling. Plant Physiol *150*, 710-721.

Yeatman, T.J. (2004). A renaissance for SRC. Nature Reviews Cancer *4*, 470-480.

Yin, Y., Wang, Z.Y., Mora-Garcia, S., Li, J., Yoshida, S., Asami, T., and Chory, J. (2002). BES1 accumulates in the nucleus in response to brassinosteroids to regulate gene expression and promote stem elongation. Cell *109*, 181-191.

Yu, X., Li, L., Zola, J., Aluru, M., Ye, H., Foudree, A., Guo, H., Anderson, S., Aluru, S., Liu, P., *et al.* (2011). A brassinosteroid transcriptional network revealed by genome-wide identification of BESI target genes in Arabidopsis thaliana. Plant J *65*, 634-646.

Zhang, J., Li, W., Xiang, T., Liu, Z., Laluk, K., Ding, X., Zou, Y., Gao, M., Zhang, X., Chen, S., *et al.* (2010). Receptor-like cytoplasmic kinases integrate signaling from multiple plant immune receptors and are targeted by a *Pseudomonas syringae* effector. Cell Host Microbe *7*, 290-301.

Zhang, Z., Wu, Y., Gao, M., Zhang, J., Kong, Q., Liu, Y., Ba, H., Zhou, J., and Zhang, Y. (2012). Disruption of PAMP-induced MAP kinase cascade by a *Pseudomonas syringae* effector activates plant immunity mediated by the NB-LRR protein SUMM2. Cell Host & Microbe *11*, 253-263.

Zipfel, C., Kunze, G., Chinchilla, D., Caniard, A., Jones, J.D., Boller, T., and Felix, G. (2006). Perception of the bacterial PAMP EF-Tu by the receptor EFR restricts Agrobacterium-mediated transformation. Cell *125*, 749-760.

APPENDIX

SUPPLEMENTAL DATA

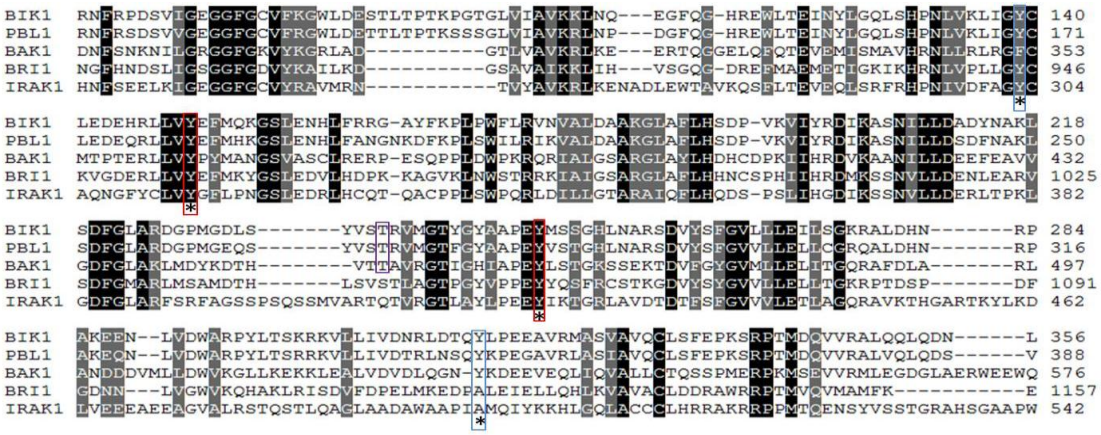

Supplemental Figure 1. Alignment of BIK1 kinase domain with related kinases. Red box indicates that Y150 and Y250 in BIK1 are highly conserved , blue box indicates that Y316 in BIK1 is conserved in PBL1 and BAK1, and purple box indicates that T237 in BIK1 corresponds to T450 in BAK1.

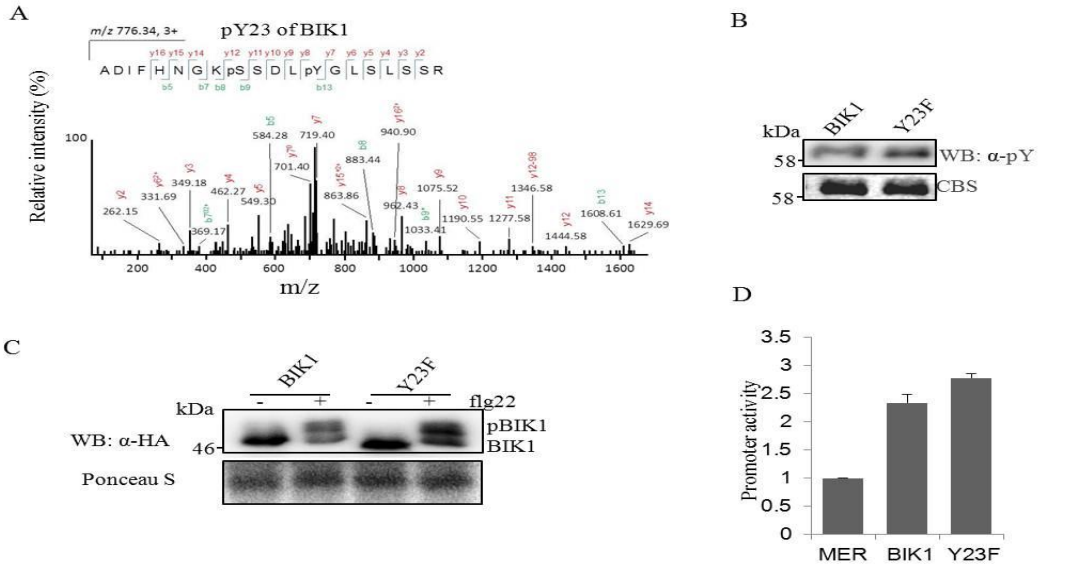

Supplemental Figure 2. Y23 is autophosphorylated but Y23 mutation does not affect the function in flg22 signaling. (**A**) BIK1 Y23 is auto-phosphorylated with MS analysis. (**B**) Y23F does not affect BIK1 auto-phosphorylation on tyrosine residues *in vitro*. The fusion proteins of GST-BIK1 and GST-BIK1Y23F were used in the *in vitro* phosphorylation assay and tyrosine phosphorylation was detected by immunoblotting

with an α-pY antibody (top panel). The protein loading was shown by CBS (bottom panel). (C) Y23F does not affect flg22-induced BIK1 phosphorylation. BIK1 or BIK1Y23Fwere expressed in WT protoplasts for 8 hr followed by 1μM flg22 treatment for 10 min, and subjected with immunoblotting with an α-HA antibody. The flg22-mediated BIK1 phosphorylation is indicated by the mobility shift (top panel) and the protein loading is shown by Ponceau S staining of the membrane (bottom panel). (D) Y23F does not affect *pFRK1::LUC* activation by BIK1. The *pFRK1::LUC* was co-expressed with BIK1, BIK1Y23F or a vector control (MER) in protoplasts for 6 hr. UBQ10-GUS was included as a transfection control and the luciferase activity was normalized with GUS activity.
The above experiments were repeated three times with similar results.

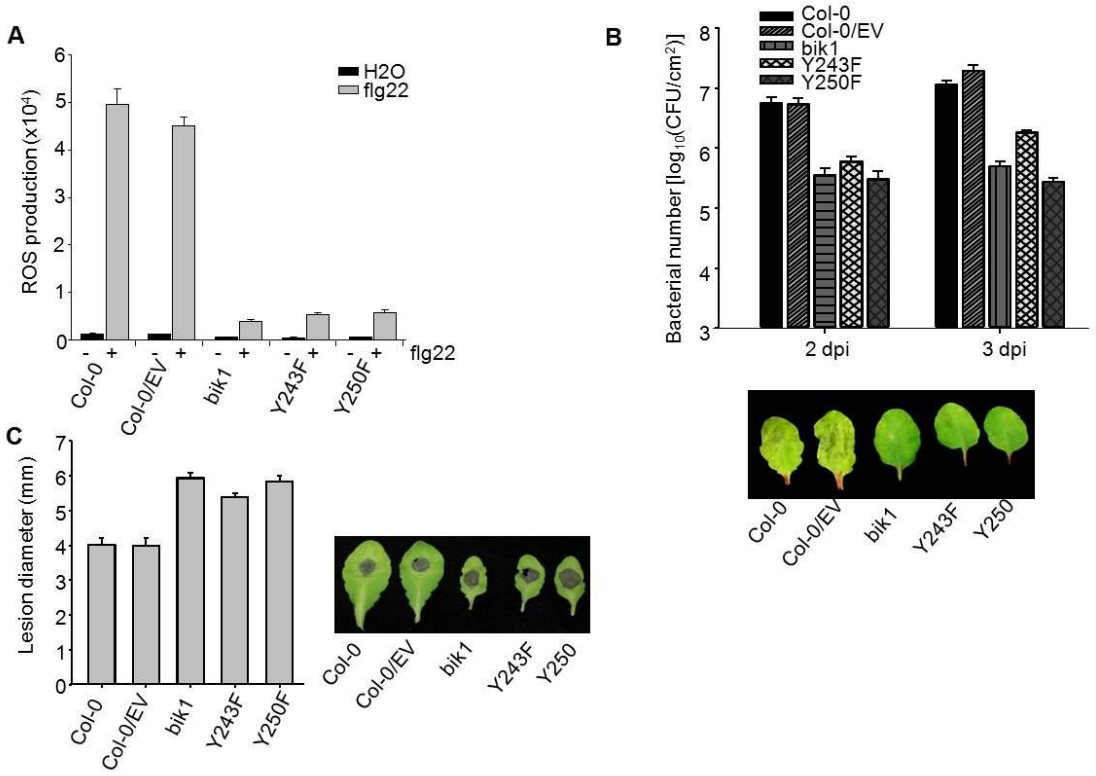

Supplemental Figure 3. BIK1 tyrosine residues are important for its function in plant immunity. (**A**) flg22-triggered ROS production in Col-0, *bik1* mutant and complementation transgenic plants (*pBIK1::BIK1*^{Y243F}-HA line D-2, *pBIK1::BIK1*^{Y250F}-HA line A2). ROS production in response to 100 nM flg22 from leaf discs of 5-week old plants was measured and presented as total photon counts during 30 min of treatment. Values presented are mean ±SE (n=36). (**B**) Bacterial growth of *Psm* infection. Leaves from 4-week old Col-0, *bik1* mutant and complementation transgenic plants (*pBIK1::BIK1*^{Y243F}-HA line D-2, *pBIK1::BIK1*^{Y250F}-HA line A2) were hand-inoculated with *Psm* at $5x10^5$ cfu/ml and the bacterial growth was measured at 2 and 3 dpi. The data are shown as mean±SE of three repeats. The picture was taken at 3 dpi. (**C**) Disease assay of *B.cinerea* infection. Leaves from 4-week old plants (Col-0, *pBIK1::BIK1*^{Y243F}-HA lineD-2, *pBIK1::BIK1*^{Y250F}-HA line A2) were deposited with *B.cinerea* strain BO5 at a concentration of $2.5x10^5$ spores/mL. Disease symptom was recorded 3 dpi. The lesion diameter was measured at 2 dpi. The data are shown as mean ±SE of at least 30 leaves.

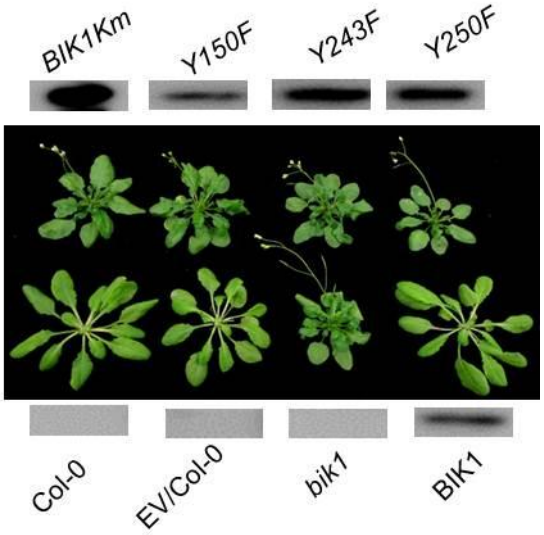

Supplemental Figure 4. Y150, Y234 and Y250 are required for BIK1 functions in growth and development. BIK1^{Y150F}, BIK1^{Y243F} and BIK1^{Y250F} complementation plants fail to rescue *bik1* growth defects and early flowering phenotypes. The protein expression of transgene is shown by Western blot.

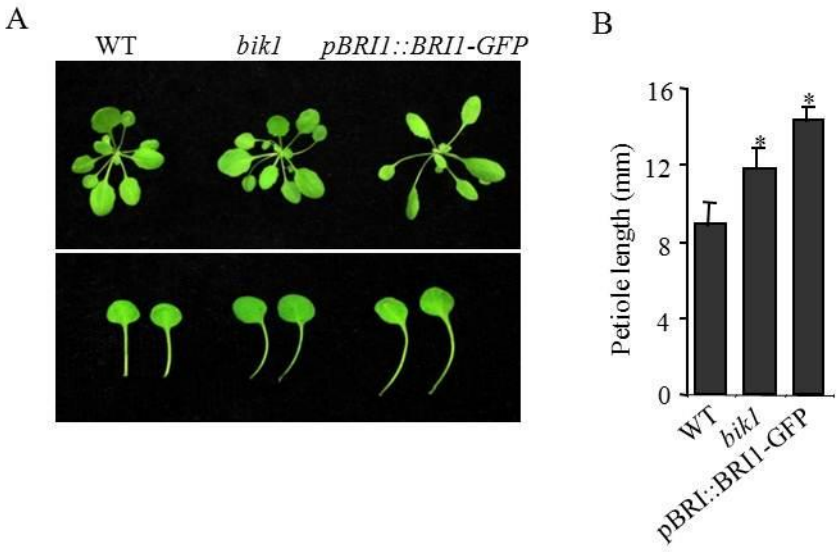

Supplemental Figure 5. The *bik1* mutant plants have moderately elongated and curling petioles, reminiscent of *pBRI1::BRI1-GFP* plants. (**A**) The aerial parts (Upper) and detached second pair of leaves (Lower) of 4-wk-old WT, *bik1* mutant, and *pBRI1::BRI1-GFP* transgenic plants. (**B**) The average petiole length of second pair of leaves of WT, *bik1* mutant, and *pBRI1::BRI1-GFP* transgenic plants. The data are shown as mean ±SE from at least 20 4-wk-old plants. Asterisk indicates a significant difference with$P<0.05$ compared with data from WT plants.

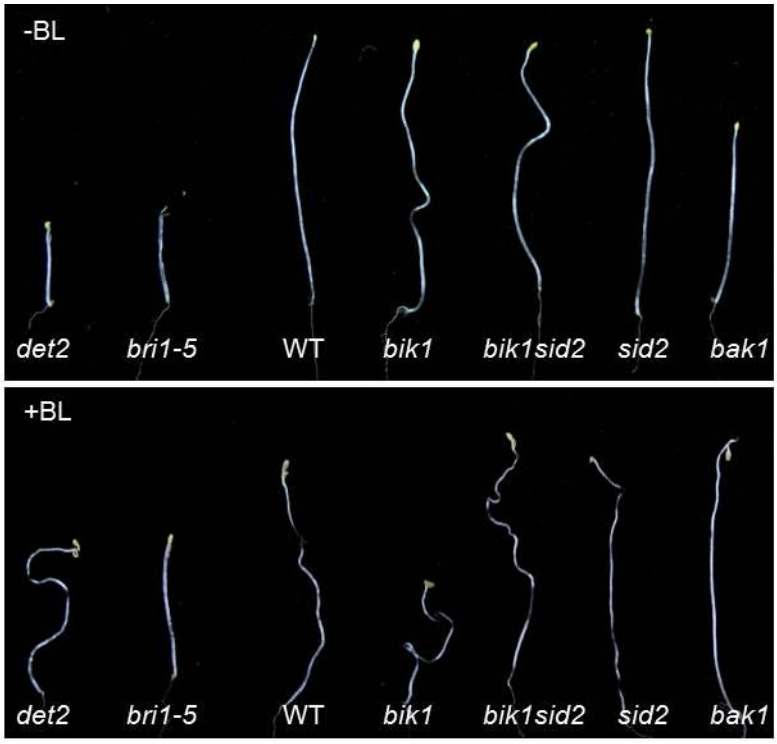

Supplemental Figure 6. The dark grown *bik1* mutant exhibited twisted hypocotyls. The Arabidopsis seedlings of the indicated genotypes were grown in the dark for 7 d in the absence (*Upper*) or presence of 50 nM BL (*Lower*).

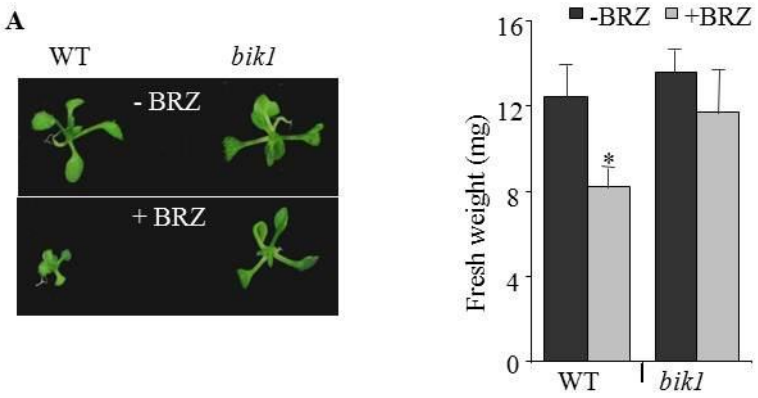

Supplemental Figure 7. Insensitivity of *bik1* mutant to Brassinazole-Resistant (BRZ) treatment. (A) The phenotype of WT and *bik1* mutant grown in 2μM BRZ for 14 d. (**B**)The fresh weight of WT and bik1 mutant in the absence or presence of BRZ. The data are shown as mean±SE from at least 25 seedlings. Asterisk indicates a significant difference with$P<0.05$ compared with data without BRZ treatment.

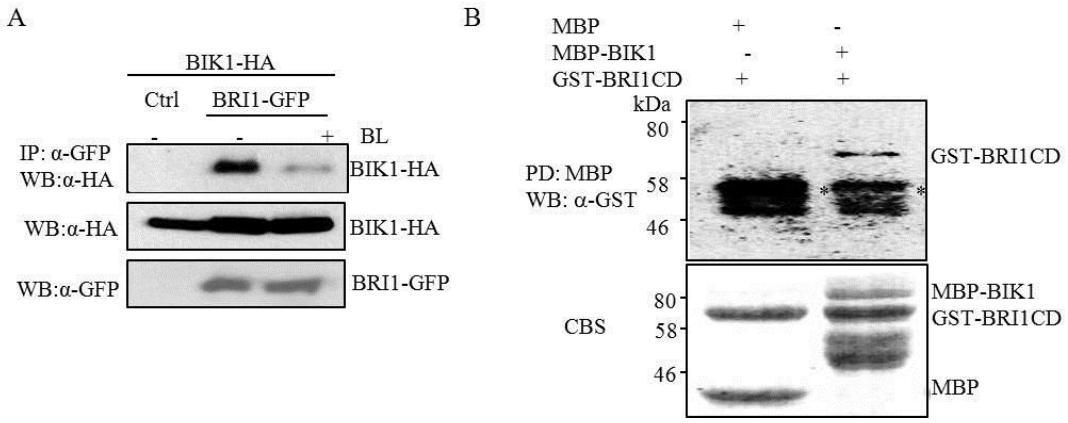

Supplemental Figure 8. BIK1 and BRI1 interaction. (**A**) BIK1-BRI1 association and BL-induced dissociation in *Nicotiana benthamiana.* Two-week-old *N. benthamiana* was inoculated with Agrobacteria carry *35S::BIK1-HA* and *pBRI1::BRI1-GFP*. Two days after inoculation, the leaves were treated with 2μM BL for 3 h. Leaves (1.1 mg) for each example were collected for Co-IP and immunoblot. (**B**) MBP-BIK1 pulls down GST-BRI1CD. An in vitro pull-down assay was performed with MBP or MBP-BIK1 immobilized on amylose-agarose beads as bait (PD:MBP) against GST-BRI1CD fusion proteins. BRI1CD was detected by Western blot with anα-GST antibody, and the protein loading control was shown by CBS. Asterisk indicates nonspecific bands with
α-GST antibody.

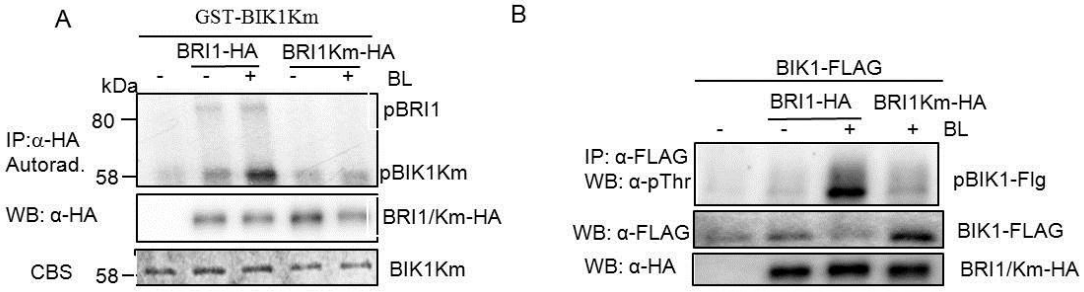

Supplemental Figure 9. BIK1 phosphorylated by BRI1. (**A**) BL treatment enhances BRI1, but not BRI1Km-mediated phosphorylation on BIK1. BRI1-HA or BRI1Km-HA was expressed in WT protoplasts for 10 h followed by 2μM BL treatment for 2 h. BRI1-HA or BRI1Km-HA proteins were immunoprecipitated with an α-HA antibody and subjected to an in vitro kinase assay with GST-BIK1Km proteins as substrates (*Top*).Middle shows the BRI1-HA and BRIKm-HA expression, and Bottom shows GST-BIK1Km proteins. (**B**) BL-induced BIK1 phosphorylation by BRI1. BIK1-FLAG was coexpressed with BRI1-HA or BRI1Km-HA in protoplasts, and incubated for 12 h before treated with 2μM BL for 3 h. BIK1 proteins were immunoprecipitated with an α-FLAG–agarose beads, separated by 10% SDS/PAGE, and immunoblotted with an α-pThr–HRP antibody.

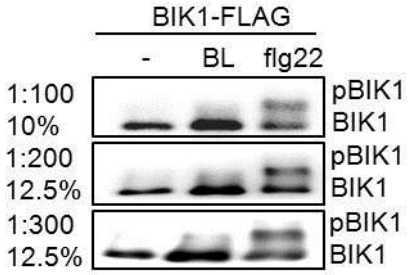

Supplemental Figure 10. BL and flg22 induce BIK1 phosphorylation. The protoplasts were transfected with BIK1-FLAG and incubated for 6 h before 2μM BL treatment for 2 h or 1μMflg22 treatment for 15 min. The samples were collected for SDS/PAGE with indicated acrylamide concentration at different ratio of bisacrylamide to acrylamide.

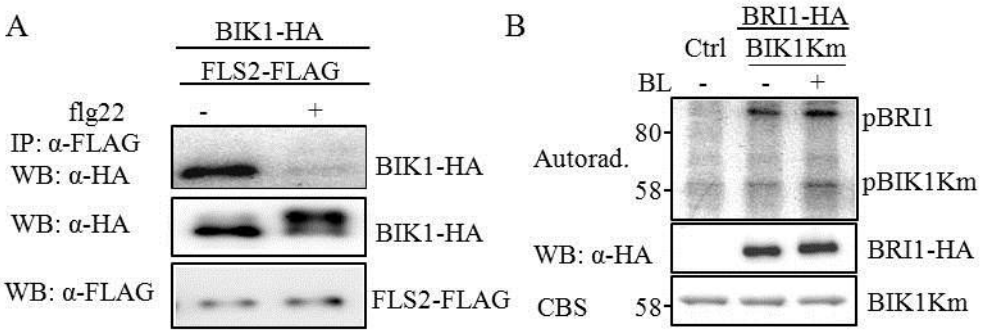

Supplemental Figure 11. Differential dissociation and phosphorylation of BIK1 by FLS2 and BRI1. (**A**) flg22-induced Flagellin Sensing 2 (FLS2)-BIK1 dissociation in WT protoplasts. The protoplasts were coexpressed with BIK1-HA and FLS2-FLAG and incubated for 6 h before1μMflg22 treatment for 15 min. Co-IP was carried out with an α-FLAG antibody (IP: α-FLAG), and the proteins were analyzed by using Western blot with α-HA antibody. (**B**) BRI1-associated kinase 1 (BAK1)-independent BL-induced BRI1 phosphorylation on BIK1. BRI1-HA was expressed in bak1-4protoplasts for 10 h followed by 2μM BL treatment for 2 h. BRI1-HA proteins were immunoprecipitated with α-HA antibody and subjected to an in vitro kinase assay with GST-BIK1Km proteins as substrates.

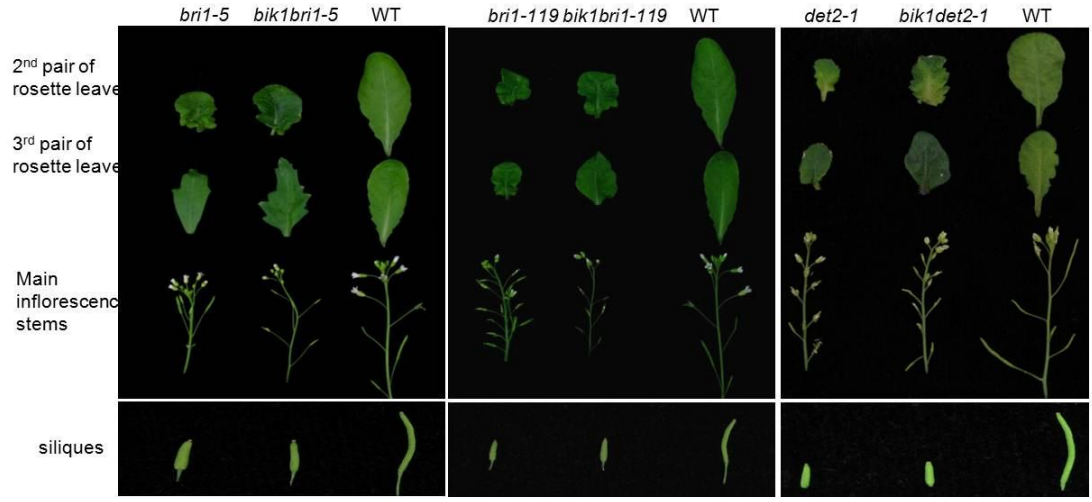

Supplemental Figure 12. Leaves, stems and siliques of 8-wk-old *bik1bri1-5*, *bik1bri1-119*, and *bik1det2* mutants. The second and third pairs of rosette leaves of *bik1bri1-5*, *bik1bri1-119*, and *bik1det2* double mutants are bigger than the corresponding single mutants. The inflorescence and siliques of *bik1bri1-5*, *bik1bri1-119*, and *bik1det2* double mutants still resemble *bik1* mutant.

Supplemental Data Table 1. Primers Used in This Study.

1) Cloning and point mutation primers

Gene	Forward primer	Reverse primer
BRI1 full length	CGGGATCC*ATG*AAGACTTTTTCAAGC TTC	GAAGGCCTTAATTTTCCTTCAGGA AC
BRI1CD	CGGGATCC*ATG*AGAGAGATGAGGAA GAGACG	GAAGGCCTTAATTTTCCTTCAGGA AC
BIK1 promoter	CCGCTCGAGCTCGAGATAGCGATGAG AGAGACAG	CGGGATCCCAAAGCTAAGAACAG ATTC
BRI1CDKm	GCGCGGTGGCTATCGAGAAACTGATT CATG	CATGAATCAGTTTCTCGATAGCCA CCGCGC
BIK1S236A	GAGTTATGTTGCTACAAGGGTCATGG	CCATGACCCTTGTAGCAACATAAC TC
BIK1T237A	GAGTTATGTTAGTGCAAGGGTCATGG	CCATGACCCTTGCACTAACATAAC TC
BIK1S236A/T237A	GAGTTATGTTGCTGCAAGGGTCATGG	CCATGACCCTTGCAGCAACATAAC TC
BIK1Y150F	CGTCTTCTAGTCTTCGAGTTTATGCAA AAAGG	CCTTTTTGCATAAACTCGAAGACT AGAAGACG
BIK1Y234F	GGTGATTTGAGTTTTGTTAGTACAAG G	CCTTGTACTAACAAAACTCAAATC ACC
BIK1Y243F	CATGGGTACTTTTGGGTACGCCG	CGGCGTACCCAAAAGTACCCATG
BIK1Y245F	CATGGGTACTTATGGGTTCGCCGCGC CTGAG	CTCAGGCGCGGCGAACCCATAAGT ACCCATG
BIK1Y250	CGCGCCTGAGTTCATGTCATCAGG	CCTGATGACATGAACTCAGGCGCG

F		
BIK1Y316F	GCTAGACACACAGTTCCTACCTGAAGAAGC	GCTTCTTCAGGTAGGAACTGTGTGTCTAGC
BIK1Km	GTCATCGCCGTTGCAGCGCTTAACCAAGAA	TTCTTGGTTAAGCGCTGCAACGGCGATGAC
BAK1CDT450A	ACACACATGTGACAGCCGCAGTGCGT	ACGCACTGCGGCTGTCACATGTGTGT
BAK1CDT455N	GCAGTGCGTGGGAACATTGGTCATATA	TATATGACCAATGTTCCCACGCACTGC
BAK1CDKm	CTTTAGTGGCCGTTATGAGGCTAAAAGAG	CTCTTTTAGCCTCATAACGGCCACTAAAG

2) qRT-PCR primers

UBQ10	AGATCCAGGACAAGGAAGGTATTC	CGCAGGACCAAGTGAAGAGTAG
CPD	TTGCTCAACTCAAGGAAGAG	TGATGTTAGCCACTCGTAGC
DWF4	CATAAAGCTCTTCAGTCACGA	CGTCTGTTCTTTGTTTCCTAA
BR6OX	AAACCAAAGACTAAGATATGGGG	GAATATCAAGCATAGATTGCGG
FRK1	ATCTTCGCTTGGAGCTTCTC	TGCAGCGCAAGGACTAGAG
WRK29	CTCCATACCCAAGGAGTTATTACAG	CGGGTTGGTAGTTCATGATTG
WRKY30	GCAGCTTGAGAGCAAGAATG	AGCCAAATTTCCAAGAGGAT
PR1	ACACGTGCAATGGAGTTTGTGG	TTGGCACATCCGAGTCTCACTG
MEKK2	ACAACTTGAGGGGGAAATTG	ATTTGACCCGTCCTTGTCTG

Note: For cloning primers, the restriction enzyme sites are underlined and start codon was italicized; for point mutation primers, the mutated sites were underlined.